BIOLOGICAL AGEING OF SKELETAL MUSCLE ENDOTHELIAL CELLS & RESPONSIVENESS TO VEGF-A: ROLE OF EPIGENETIC WRITER EZH2

DAYNA OLIVIA ESSUE

A THESIS SUBMITTED TO THE FACULTY OF GRADUATE STUDIES IN PARTIAL FULFILLMENT OF THE REQUIREMENTS FOR THE DEGREE OF

MASTER OF SCIENCE

GRADUATE PROGRAM IN KINESIOLOGY AND HEALTH SCIENCE

YORK UNIVERSITY

TORONTO, ONTARIO

December 2024

Abstract

In the older population, the loss of small blood vessels (capillaries), known as rarefaction, precedes muscle atrophy. Aging alters the capacity of endothelial cells, the main constituents of capillaries, to form new blood vessels through angiogenesis. Epigenetics has emerged as a new research area to uncover how an ageing phenotype is acquired. Through this project we investigate how the epigenetic writer Enhancer of Zeste Homologue 2 (EZH2) regulates the pro-angiogenic pathway downstream of vascular endothelial growth factor-A (VEGF-A) and its receptor 2 (VEGFR-2) in skeletal muscle microvascular endothelial cells (SMECs) using an *in-vitro* model of aging. Our results suggest that EZH2 activity might restrain angiogenesis by impairing the expression of genes downstream of the VEGF-A pathway, such as *Nr4a3* and *Egr3*. Our findings indicate that EZH2 potentially supports vascular aging. Yet, caution is required as *in-vitro* models, such as passaging, fails to reproduce all aspects of aging, more particularly senescence in primary cells.

Acknowledgments

I want to thank my past and present lab mates Sokaina Akhtar, Brian Lam, Alita Gideon and Pierre Lemieux. Thank you all for your help, advice and fun conversations during my time in the lab. Thank you to Sokaina and Brian for teaching me how to run a BCA and western blot. Thank you to Alita for listening to my rants, offering advice and helping me work through issues here and there. A special thank you to Pierre Lemieux, for your kindness and patience in introducing me to several wet lab and cell culture techniques; for your constant support and helping hand. The lab was a wonderful experience because of all of you.

Thank you to Dr. Carol Bucking for being part of my defense committee and Dr. Olasunkanmi Adegoke for your support as my committee member during my proposal and thesis writing.

Thank you to Dr. Birot, your constructive criticism and probing questions during lab meetings truly helped me to grow and stretch my thinking.

Thank you Dr. Roudier, for your constant support and belief in me and my capabilities. Thank you for helping me learn new techniques, reflecting on data with me and pushing me just a little bit to challenge myself more and more. I cannot thank you enough for taking a chance on me.

Thank you to my one and only KINE buddy Olivia Ramraj. I could not have made it this far without you as my best-friend, confidante and stress-walk partner.

Thank you to my family; Mom, Dad, Grandma Joyce, Grandma Lilieth, Niki, Allison and my late baby-boi Milo. Thank you all for your love, support and prayers. I love you all very much.

Lastly, but most important of all, I want to thank Yahweh. God has given me strength beyond what I thought I was capable and has blessed me with abundant life and favour, day after day through His son Jesus, my loving saviour and faithful friend. Yahweh will be my God until my last breath. ALL glory to Him alone.

Table of Contents

List of Tables

Methods

List of Figures

Literature Review

Methods

Primary Data Figures

Supplemental Figures

List of Abbreviations

Akt	Protein kinase B
ANOVA	Analysis of variance
β-gal	Beta- galactosidase
BCA	Bicinchoninic acid assay
C:F	Capillary-to-fibre ratio
CD	Capillary density
ChIP-seq	Chromatin immunoprecipitation with high-throughput sequencing
COD	Change of direction
CVD	Cardiovascular disease
DALYs	Disability-adjusted life years
DEG	Differentially expressed genes
Dll-4	Delta like-4
DMSO	Dimethyl sulfoxide
DNA	Deoxyribonucleic Acid
EC	Endothelial cell
ECM	Extracellular matrix
EGR3	Early growth response 3
ERRα	Estrogen-related receptor-alpha
ESCs	Embryonic stem cells
EZH2	Enahancer of zeste homologue 2
H3	Histone 3
HATs	Histone acetyltransferases
HBMECs	Human brain micro-endothelial cells
HCNEs	Highly conserved noncoding elements
HDAC	Histone deacetylases
HIF-1α	Hypoxia inducible factor-1-alpha
HMTs	Histone methyltransferases
HPRT	Hypoxanthine-guanine phosphoribosyltransferase
HSCs	hematopoietic stem cells
HUVECs	Human umbilical vein endothelial cells
IFN-γ	Interferon gamma
iNOS	Inducible nitric oxide synthase
JMJD-1.2	JumonjiC (JmjC)-domain-containing protein 1.2
KDR	Kinase domain receptor-2
KO	Knock-out
MAPK	Mitogen activated protein kinase
Mdm2	Murine double minute-2
DMTs	Histone demethylases
MEFs	Mouse embyronic fibroblasts
miRNAs	MicroRNAs

mRNA	Messenger ribonucleic acid
mSMECs	Mouse skeletal muscle endothelial cells
NAD+	Nicotinamide adenine dinucleotide positive
NHANES	National health and nutrition examination survey
NO	Nitric oxide
NR4A1	Nuclear receptor subfamily 4 group A member 1
Nr4a3	Nuclear receptor subfamily 4 group A member 3
PAD	Peripheral artery disease
PDK4	Pyruvate dehydrogenase lipoamide kinase isozyme 4
PECAM	Platelet endothelial cell adhesion molecule
PGC-1α/β PPARGC1A	Peroxisome proliferator-activated receptor gamma coactivator-alpha/beta
PI3K	Phosphoinositide-3-kinase
PKC	Protein kinase-C
PLCγ	Phospholipase-C gamma-1
PPAR-δ	peroxisome proliferator-activated receptor-delta
PRC2	Polycomb repressive complex 2
PTMs	Post-translational modifications
RCT	Randomized controlled trial
RIPA	Radioimmunoprecipitation assay
RNA	Ribonucleic acid
RNAII	RNA Polymerase II
RNA-seq	RNA sequencing
ROS	Reactive oxygen species
SASP	Senescence associated secretory phenotype
SiRNA	Small interfering RNA
SIRT1	Sirtuin 1
ST	Straight-line
TF	Transcription factors
TNFα	Tumour necrosis factor-alpha
UTX	Ubiquitously transcribed tetratricopeptide repeat on chromosome X
VEGF-A/B/C	Vascular endothelial growth factor A/B/C
VEGFR-1/2/3	Vascular endothelial growth factor receptor 1/2/3
VO_{2max}/peak VO_2	Maximal oxygen uptake
VSMCs	Vascular smooth muscle cells
VWF	Von willebrand factor
WT	Wild type

Literature review

1. Ageing & disease

World life expectancy has more than doubled in the last two centuries from 25 years of age to 65 years for men, and 70 for women (Oeppen & Vaupel, 2002). Life expectancy in Canada alone has risen from 75 years in 1980 to almost 82 in 2022 (Government of Canada, 2021). With the advancement of technology, life expectancy is predicted to continue increasing. Though individuals on average tend to live longer, most are living with life-long disease/comorbidities. When measuring quality of life, Disability-Adjusted Life Years (DALYs) are generally the measurement of choice. One DALY represents the loss of the equivalent of one year of full health (World Health Organization, 2024). Data collected by the World Health Organization show that Canada overall had an estimated 11,362 DALYs across all ages and all causes. However, when stratified by those below and above the age of 50 we observe that 3431 are experienced by those under 50 and 7930 are experienced by those over 50 (World Health Organization, 2024). That is an increase of 57%. In another study conducted by the Public Health Agency of Canada, data was extracted from the Canadian Community Health Survey 2011/12 on 105 416 Canadians adults. They found that 12.9% of Canadians are living with 2 or more chronic diseases. Of this total, 3.1% are in the 20-34 aged cohort while 31.3% are aged 65 and over (Roberts et al., 2015). The authors concluded that age along with low household income and education were major determinants correlated with multimorbidity prevalence. In Canada, a higher disease rate is experienced by those in higher age brackets with its prevalence consistently increasing as individuals age.

Ageing is seen as major determinant of health and a risk factor for disease (Niccoli & Partridge, 2012). While the process of ageing is highly complex and yet to be fully understood, much of the

effects of ageing are due to biological changes that take place over time. Biological ageing is the culmination of changes over time resulting from the natural accumulation of molecular and cellular damage (World Health Organization, 2024). This damage presents itself most typically as functional decline and increases in degenerative diseases; by reducing the ability of our bodily systems to maintain optimal function and therefore health (Gladyshev et al., 2021).

The most common chronic diseases experienced by the elderly in Canada according to the Public Health Agency of Canada include; cancer, cardiovascular diseases, diabetes, hypertension, mental illness and suicide, musculoskeletal disorders, neurological diseases, oral diseases, respiratory diseases, falls and multimorbidity (P. H. A. of Canada, 2021). While manifestation of disease is often unpredictable and varies from individual to individual, many of the diseases listed above can be controlled and prevented through adequate physical activity.

Due to the relationship observed between age and disease, interests have shifted from prolonging life to instead emphasising the need to reduce morbidity and promote healthy ageing, with physical activity being a key behavioural factor.

1.1 Exercise & disease

Exercise is an important factor to maintaining optimal health and fitness. Regular exercise is known to aid in maintaining better heart, muscle and immune health along with several other areas. As previously mentioned, physical activity or exercise training is known to not only reduce the risk of disease but help to maintain better health for individuals living with several chronic diseases including cardiovascular, metabolic, immune diseases and cancers. A study conducted on 130,000 subjects in 17 countries looked at the effect of physical activity on mortality and cardiovascular disease (CVD). They found that both recreational and non-recreational physical activity was

associated with lower mortality and CVD risk regardless of the income status of the country. They also concluded that higher rates of physical activity showed greater reductions in mortality and CVD risk (Lear et al., 2017).

Hypertension and periodontal disease are two of the most common conditions suffered among older Canadians affecting 65.7% and 52% respectively (S. Canada, 2020) Both hypertension and periodontal disease have been shown to be either associated with physical inactivity or improved upon by increased physical activity. In a Randomized Controlled Trial (RCT) conducted by Cornelissen and colleagues, on healthy sedentary men and woman over the age of 55, diagnosed with high blood pressure; they found that 10 weeks of either high-intensity or low intensity training lowered Systolic Blood Pressure, with an average decrease ranging from 3 to 8 mmHg (Cornelissen et al., 2010). These findings are further supported by several other studies (Georgiades et al., 2000; Krustrup et al., 2013; Tsai et al., 2002).

In a study conducted using a nationally representative data set from the National Health and Nutrition Examination Survey (NHANES) 2011–2012 based in the United States, they examined the association between physical activity and sedentary behaviour with periodontal disease. The authors concluded that individuals with higher total physical activity, higher leisure time physical activity, and lower amount of total sedentary behaviour had lower periodontal disease prevalence (Almohamad et al., 2022).

Even several cancer studies have demonstrated that exercise training whether in early or late stages show significant improvement in quality of life, independence, endurance, cognitive functioning, muscle strength and fatigue (Cormie et al., 2013; Henke et al., 2014; Hwang et al., 2012; Oldervoll et al., 2011).

Along with its many benefits for managing and preventing disease, exercise is highly valuable for its role in maintaining functional capacity in older age. Exercise is also crucial to the maintenance of muscle mass and strength. This is of great concern as low muscle mass is associated with higher mortality in both healthy individuals and those living with comorbidities (Koeppel et al., 2021).

2. Skeletal Muscle

Skeletal muscle is the muscle within the body under voluntary control. It constitutes approximately 40% of the human body and is of vital importance to daily living (Frontera & Ochala, 2015). Skeletal muscle not only allows us to have the strength to move and participate in daily activities, but it contributes largely to energy metabolism and storage, through the storage of amino acids and glycogen. Skeletal muscle also plays a vital role in thermal regulation and oxygen consumption during movement (Frontera & Ochala, 2015).

Greater muscle mass is often associated with better health compared to those with a lower muscle mass. Studies show that increased muscle mass improves glucose utilization aiding in the maintenance of glucose control (Taha et al., 2022). Studies have also shown that decreased muscle mass is associated with hypertension. A study conducted by Park and colleagues in 2013, on 6832 adults who participated in the 2009 Korea National Health and Nutrition Examination Survey looked at the association between sarcopenia (the age-related loss of muscle mass), obesity and hypertension. The authors concluded that sarcopenic obesity is associated with hypertension, while low muscle mass is also correlated with hypertension, independent of abdominal obesity (Park et al., 2013).

Sarcopenia is a common condition observed in the elderly. Sarcopenia leads to increased frailty in the older population which is not only correlated with a higher risk of falls and hospitalisation but

increased risk of chronic diseases (Angulo et al., 2016). Physical activity has been shown to be beneficial for those living with sarcopenia. In a meta-analysis and systematic review conducted by Sánchez-Sánchez et al. in 2024, including over 230,000 older individuals, the authors concluded that higher levels of total physical activity were inversely associated with sarcopenia and there was a protective association identified for moderate-to-vigorous physical activity (Sánchez-Sánchez et al., 2024). These studies further indicate that adequate muscle mass and physical activity is critical for overall health and can be more beneficial in disease states.

Maintaining muscle mass and strength is of great concern to the elderly as it correlates with prolonged autonomy and independence. Skeletal muscle is highly adaptive; therefore, it must undergo cyclic stress to maintain its capacity to do and sustain work. If activity levels decrease, skeletal muscle will begin to lose mass and force-capacity (White et al., 1984). Maintaining healthy muscle, however, is in large part due to the level of capillarization.

2.1 Skeletal muscle microvasculature

The microvasculature is a dense vascular network made up of arterioles, venules and capillaries. Capillaries run along the length of a muscle fibre, where they innervate it. Capillaries supply the muscle with the necessary nutrients it needs, such as oxygen, glucose, and fatty acids, while removing waste products such as carbon dioxide, potassium, lactic acid, reactive oxygen species (ROS) and more (Murrant et al., 2017).

In a study conducted by Prior and colleagues, they compared levels of muscle capillarization in sarcopenic vs non-sarcopenic individuals. They found that participants in the sarcopenic group had significantly lower VO_{2max} compared with nonsarcopenic participants ($p < 0.05$). Vastus lateralis biopsy analyses also showed that sarcopenic participants had 18% fewer capillary contacts per

fiber and 20% lower capillary-to-fiber ratio ($p < .01$) (Prior et al. 2016). The authors believe their findings suggest that capillary rarefaction, which is the loss of capillaries, precedes loss of muscle mass, as seen in sarcopenia (Prior et al., 2016).

In older individuals with chronic diseases, rarefaction of the skeletal muscle capillaries is a determinant of exercise intolerance. Kitzman et al. in 2014 clearly established that in older individuals with heart failure a positive correlation exists between skeletal muscle capillarization, and physical performance measured by peak VO_2 (Kitzman et al., 2014). This was further confirmed by the meta-analysis performed by Schmid et al. in 2024 where the analysis of 27 cross-sectional studies demonstrated a clear positive association between capillary-to-fibre ratio and peak VO_2 (Schmid et al., 2024). While studies have not directly linked level of muscle capillarization to muscle performance alone, it is generally known that trained individuals show levels of muscle capillarization ~2-3 fold greater than in untrained individuals (Hellsten & Gliemann, 2024). These studies further support that the skeletal muscle microvasculature is vital not only to health of skeletal muscle but overall health of the individual.

3. The Vascular System

The vascular system is present in every inch of the body and of vital importance to bodily function. It not only serves to aid in the transport of oxygen and nutrients but also immune cells and waste. The vascular system is made up of arteries and arterioles, which in general carry oxygen rich blood away from the heart, veins and venules which carry oxygen deficient blood toward the heart, and capillaries. Capillaries are the smallest blood vessels present in the body and are the point of gas, nutrients, and waste exchange. Capillaries are composed of a single layer of endothelial cells (EC), structurally strengthened by a basement membrane and pericytes. The thin walls of capillaries allow for optimal diffusion conditions for oxygen and other compounds. The

capillary endothelium also includes small gaps between the endothelial cells, allowing for diffusion of larger, non-permeable compounds (Hellsten & Gliemann, 2024).

While the vascular network is present in all areas of the body and its many systems, over 50% of the total vascular surface of the body is found within the skeletal muscle capillaries (Wagenmakers et al., 2016). The vascular system is vital to the health and performance of all other bodily systems which is why maintaining its health and function, and further study in this area is highly valuable.

The capillary network is highly plastic, constantly adapting to meet the energy demands of the muscle. Capillarization can be maintained, regress (rarefaction) or expand (angiogenesis), with each of these processes starting at the level of the endothelial cell.

3.1 The Endothelial cell

Endothelial cells (ECs) are the most common and widespread cells in the body. ECs are classified as simple squamous epithelial cells; with their luminal surface exposed to contents within the blood and their basal surface anchored by a glycoprotein basement membrane (Krüger-Genge et al., 2019). ECs are the first point of contact to substances found in the bloodstream and regulate passage of these substances into the tissue (Eelen et al., 2020).

ECs which together form the endothelium, play a role in the regulation of many functions, such as protection (hematoencephalic, intestinal, renal, and hepatic barriers), reception, transport (oxygen, nutrients, growth factors), secretion, absorption, and synthesis functions (Kerr et al., 2011).

There are three main structural types of capillaries which are classified by permeability; fenestrated, continuous and sinusoidal. Fenestrated capillaries, have several small pores and are found in organs where quick exchange of materials is necessary, such as the kidneys and intestines.

Continuous capillaries, have a continuous un-interrupted lining, and are found where exchange of materials is tightly controlled such as the brain, heart, lungs and skeletal muscle. Sinusoidal capillaries have large pores creating a discontinuous endothelium and are found where there is exchange of large molecules such as the liver and bone marrow (Gifre-Renom et al., 2022). In the same way, ECs across the endothelium show an incredible level of heterogeneity as they are highly specified to their local organ environment. Their heterogeneity is closely associated with plasticity, the ability of ECs to adapt to environmental cues through the mobilization of genetic, molecular, and structural alterations (Larionov et al., 2024). This ability is best demonstrated through their role in angiogenesis, which will be further expanded on in the following section. As previously mentioned, ECs are important to many regulatory functions and as such, maintaining their health and proper function, and the study of these processes is highly valuable, especially in the context of skeletal muscle and its role in overall health.

3.2 Angiogenesis

Angiogenesis, the process by which the vascular network expands, is the growth of new blood vessels, more specifically new capillaries from preexisting ones.

Angiogenesis occurs through two processes: sprouting and splitting angiogenesis. In splitting angiogenesis, or intussusceptive angiogenesis, the vessel wall extends into the lumen essentially splitting a single vessel into two parallel vascular tubes. This form of angiogenesis is considered faster, more efficient and takes place mainly during embryonic development (Burri & Tarek, 1990). This form of angiogenesis does not expand the vascular tree per se but instead creates more connections within the existing vascular network (Adair & Montani, 2010).

Sprouting angiogenesis is the branching off of the vascular network to an oxygen deficient area. The hypoxic tissue releases growth factors, the most well-known being vascular endothelial

growth factor (VEGF). The VEGF family has three main proteins, VEGF-A, VEGF-B and VEGF-C. VEGF-A is the most potent and studied angiogenic factor and is known to be necessary for both forms of angiogenesis (Gianni-Barrera et al., 2018). VEGF-A has several isoforms, the most common being VEGF-$A_{165.}$ There are multiple receptors to VEGF-A, but most of VEGF-A dependent physiological functions are mediated through its capacity to activate VEGFR-2 (Pérez-Gutiérrez & Ferrara, 2023).

For sprouting angiogenesis several fundamental steps must take place; enzymatic degradation of the capillary basement membrane, EC proliferation, migration, tube formation, vessel fusion, vessel pruning, and pericyte stabilization (Adair & Montani, 2010).

Despite not being stem cells, ECs must retain phenotypic plasticity to perform angiogenesis and there are three main EC phenotypes involved; tip, stalk and phalanx. Tip cells are polarized cells with long filipodia which are sensitive to hypoxia induced growth factors and essentially lead the growth of the vessel to the hypoxic tissue. Stalk cells trail tip cells, proliferate, elongate the sprouts, and form lumens (De Smet et al., 2009), they literally elongate the vessel behind the tip cell as it navigates toward the hypoxic stimulus (Adair & Montani, 2010). These phenotypes are highly interchangeable, with the stalk cells becoming tip cells and vice versa, several times through the angiogenic process (De Smet et al., 2009; Jakobsson et al., 2010) Typically, the cell exposed to the highest levels of growth factors such as VEGF-A become the tip cell (Adair & Montani, 2010). The main pathway which controls these changes is VEGFR-2/Notch signalling. Each of these receptors negatively controls the expression of the other. Phalanx cells are quiescent ECs, which line the vessel once new tubes have been formed, they perform the necessary EC functions, optimizing blood flow and perfusion (De Smet, 2009).

As previously mentioned, one of the strongest drivers of angiogenesis is hypoxia (Adair et al., 1990). Exercise not only greatly increases hypoxic stress in the skeletal muscle but mechanically through shear stress, the frictional force of flowing blood, and passive stretch of the muscle. Muscle contraction and metabolism are both known to have great influence in creating a pro-angiogenic environment as well (Hellsten & Gliemann, 2024). All these factors, which are combined in exercise training, create the perfect environment for angiogenesis to take place.

3.3 Exercise induced skeletal muscle angiogenesis

Per Anderson first observed increases in the level of capillarization after training in 1975. He took biopsies from the lateral portion of the quadriceps femoris muscle of 9 young healthy males, 5 untrained and 4 trained. He took 4 subjects from the untrained group and trained them at 80% of their VO_2 max for 4 x 20 minutes sessions a week, for 7 weeks. This resulted in a 13% increase in VO_2 max. Capillary density increased with training from 289 ± 15 cap./mm^2 to 356 ± 23 cap./mm^2 ($p < 0.05$) and capillary to fibre ratio increased from 1.39 ± 0.18 and 1.95 ± 0.06 ($p < 0.05$) (Andersen, 1975).

This phenomenon, of increased capillarization after training has been proven time and again (Andersen & Henriksson, 1977; Gavin et al., 2007; Jensen et al., 2004). In a meta-analysis conducted by Liu et al. in 2022, they looked at measures of capillary density (CD) and capillary-to-fibre (C:F) ratio, before and after training. They included 57 trials from 38 studies. C:F was measured in 391 subjects from 47 trials, whereas CD was measured in 428 subjects from 50 trials. The authors concluded that in sedentary subjects, continuous moderate-intensity training and interval training with high intensity led to increases in capillarization, whereas low-intensity training has less effect (Y. Liu et al., 2022). Exercise induces angiogenesis within the skeletal

muscle due to the creation of a pro-angiogenic environment due in large part to the release of several pro-angiogenic factors from the muscle fibre.

3.3.1 Contractile activity and the production of angiogenic factors by the muscle fibre

Exercise creates a pro-angiogenic environment in skeletal muscle at multiple levels. The contractile activity of the myofiber not only increases oxygen demand creating a hypoxic environment but the mechanical stress of the working muscle induces the release of potent pro-angiogenic factors, most prominently VEGF-A, as well as adenosine (Høier et al., 2010) and Nitric Oxide (NO) (Stamler & Meissner, 2001).

NO, though not critical to the angiogenic process, inhibition of its production has been observed to attenuate the *VEGF-A* mRNA response to exercise in skeletal muscle (Gavin et al., 2000).

Adenosine infusion has been observed to enhance *VEGF-A* mRNA at baseline, even further when combined with exercise, and when adenosine receptor A_{2B} was blocked, the *VEGF-A* response was almost completely abolished (Høier et al., 2010). The authors state that the *VEGF-A* response was also strongly associated with Mitogen Activated Protein Kinase (MAPK) illustrating its sensitivity to metabolic factors.

VEGF-A is the most potent and well-studied angiogenic factor and is known to be necessary for angiogenesis. Myocyte VEGF-A deletion studies have proven VEGF-A to be vital to angiogenesis and endurance performance. In a study by Olfert and colleagues in 2010, to determine whether VEGF-A expression is required for skeletal muscle capillary adaptation to exercise training, gastrocnemius muscle capillarity was measured in myocyte-specific VEGF-A gene-deleted ($mVEGF^{-/-}$) and wild-type (WT) littermate mice following 6 weeks of treadmill running (1 h/day, 5 days/wk). Post-training capillary density was significantly increased by 59% ($P < 0.05$) in the

gastrocnemius in WT mice but did not change in mVEGF$^{-/-}$ mice. Maximal running speed and time to exhaustion during submaximal running increased by 20% and 13% ($P < 0.05$), respectively, in WT mice after training but were unchanged in mVEGF$^{-/-}$ mice (Olfert et al., 2010).

3.3.1.1 Transcriptional regulation of skeletal muscle angiogenesis

Transcription factors (TF) known to be upregulated due to muscle contraction are Hypoxia Inducible Factor (HIF-1α) and Peroxisome Proliferator-Activated Receptor Gamma Coactivator PGC-1α/β(Ross et al., 2023) either independently or co-actively with Estrogen-Related Receptor-α (ERRα) (Arany et al., 2008).

Studies have shown that in response to exercise, HIF-1 α is activated and aids in changes in gene expression. After a single bout of knee extension exercise with reduced blood flow manipulation in young healthy males, HIF-1 α protein levels increased and remained elevated six hours post exercise, while HIF-1 α mRNA levels did not change (Ameln et al., 2005). *VEGF-A* mRNA increased 3 times more in the restricted blood flow subjects than the control subjects after an acute bout of exercise. *VEGF-A* mRNA remained elevated for 6 hours post-exercise, mimicking the pattern observed in HIF-1 α the protein level (Ameln et al., 2005).

In study conducted by Chinsomboom and colleagues in 2009, looking at comparisons in levels of capillarization in the quadriceps muscle PGC-1α knockout (KO) mice, compared to their wild type (WT) controls in response to 14 days of ad libitum wheel running. After exercise, capillary density increased >2-fold in WT control animals, in their PGC-1α KO counterparts however, there was almost no increase in capillary density (Chinsomboon et al., 2009).

In a study by Arany et al. in 2008, they examined the role of ERR-α in regulating endogenous VEGF-A. Primary skeletal muscle cells were infected with adenovirus expressing ERR-α. They

observed three-fold induction of *VEGF-A* mRNA compared to controls. To verify whether ERR-α is required for the PGC-1α-mediated induction of *VEGF-A*, primary mouse embryonic fibroblasts were prepared from ERR-$\alpha^{-/-}$ and wild-type animals, and the expression of VEGF-A was evaluated after infection with adenovirus expressing PGC1-α. In wild-type mouse embryonic fibroblasts, PGC-1α induced *VEGF-A* expression sevenfold, compared to controls. In sharp contrast, the induction of *VEGF-A* by PGC-1α was completely abrogated in *ERR-*$\alpha^{-/-}$ mouse embryonic fibroblasts (Arany et al., 2008). This illustrated that PGC-1α and ERR-α can independently or co-actively induce transcription of *VEGF-A*. All these studies have one commonality, the primary measure is VEGF-A. Due to its vital role in the angiogenic process its regulation is of great importance.

3.3.2 Impact of muscle fibre generated angiogenic factors on skeletal muscle endothelial cells

ECs express receptors of VEGF-A such as the receptor 1 (VEGFR-1) and the receptor 2 (VEGFR-2) (Melincovici et al., n.d.). While VEGF-A has a higher affinity to VEGFR-1 than VEGFR-2, VEGFR-2 is the active receptor for the angiogenic process (Shibuya, 2011). VEGF-A and VEGFR-2 are central to exercise-driven angiogenesis in the skeletal muscle, supporting both splitting and sprouting angiogenesis.

The VEGF-A/VEGFR-2 interaction causes several signalling cascades leadings to EC survival, proliferation and migration. Briefly, downstream of VEGFR-2; the phosphoinositide-3-kinase (PI3K) and protein kinase B (Akt) pathway promote EC survival (Haas & Nwadozi, 2015). Akt can also enhance EC basal production of NO resulting in increased vascular permeability and migration of ECs. The phospholipase-C Gamma-1, Protein kinase-C and Mitogen Activated Protein Kinase (PLCγ-PKC-MAPK) pathway is highly activated and used as a crucial signal for endothelial proliferation and migration (Shibuya, 2011).

As previously mentioned, ECs known as tip cells express filopodia and lead the migration of ECs to the pro-angiogenic stimulus. As the tip cell migrates toward an angiogenic stimulus, other ECs known as stalk cells proliferate, forming and elongating the new vessel. Tip cells express the highest levels of VEGFR-2 for enhanced sensitivity to VEGF in the extracellular matrix (ECM), to accurately lead vessel formation (Adair & Montani, 2010).

High activity of VEGFR-2 in tip cells activates Delta Like-4 (Dll4-), a Notch ligand, which promotes notch signalling. Activation of the notch pathway reduces VEGFR-2 expression in adjacent cells, lowering sensitivity to VEGF-A, promoting them to phenotypically behave as stalk cells favouring proliferation over migration (Kume, 2009). These studies reveal the crucial role of VEGFR-2 signaling to EC survival, proliferation and migration, processes necessary for angiogenesis.

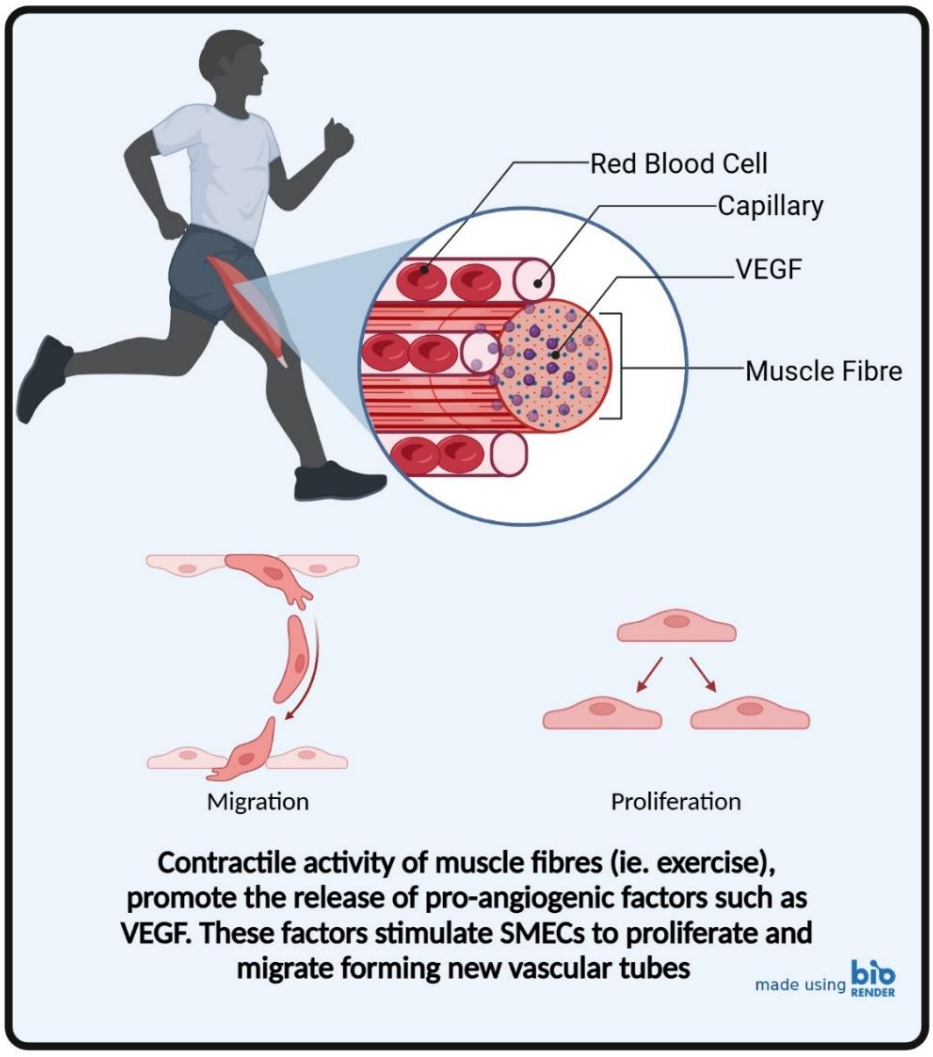

Figure 1. Effect of pro-angiogenic factors on ECs.

Contractile activity of muscle fibres, promote the release of pro-angiogenic factors such as VEGF, which induce several signalling cascades resulting in the proliferation and migration of ECs which assemble into new vascular tubes.

3.3.2.1 VEGFR-2: Vascular Endothelial Growth Factor Receptor 2

VEGFR-2, also known as Kinase domain receptor-2 (Kdr) in humans and Flk-1 in mice, is a tyrosine kinase receptor and the primary receptor for the angiogenic process. Not only is it

necessary for survival of ECs (Paz et al., 2012), VEGFR-2 interacts with its ligand VEGF, creating a signalling cascade to promote the expression of filopodia on the tip cell, to lead EC migration; a process necessary for angiogenesis.

Several studies confirm the necessity of VEGFR-2 to the angiogenic process. In a study by Shalaby and colleagues in 1995, they developed Flk-1 deficient mice using homologous recombination in embryonic stem (ES) cells. This mutation resulted in death in utero between 8.5 and 9.5 days post-conception, as a result of an early defect in the development of haematopoietic and endothelial cells. The authors state that organized blood vessels could not be observed in the embryo or yolk sac at any stage, and haematopoietic progenitors were severely reduced. The authors concluded that Flk-1/VEGFR-2 is absolutely necessary for embryogenesis/angiogenesis (Shalaby et al.,1995). Inhibition of VEGFR-2 has been observed to result in a significantly delayed angiogenesis phenotype (Lu et al., 2023) and a short-term blockage of the VEGF/VEGFR-2 interaction has been shown to result in capillary regression (Kamba et al., 2006). In a study by Kamba and colleagues in 2006, they used a small-molecule VEGFR tyrosine kinase inhibitor, to competitively inhibit the VEGF-VEGFR-2 interaction. Mice were injected twice daily for 7, 14, or 21 days. They observed that when VEGF was prevented from binding with VEGFR-2 for 14 days it resulted in a 21% regression in pancreatic islet capillaries (Kamba et al., 2006).

3.3.2.2 Downstream effectors of VEGFR-2: Early Growth Response 3 (Egr3) & Nuclear Receptor Subfamily 4 Group A Member 3 (Nr4a3)

Early growth response 3 (Egr3) is a zinc-finger transcription factor. Growing research on this transcription factor has demonstrated it to be highly responsive to VEGF-A stimulation and contributes greatly to VEGF-A-mediated angiogenesis (Abe & Sato, 2001). VEGF-mediated induction of *Egr3* regulates EC growth and migration, neo-angiogenesis, hemostatic balance and

leukocyte adhesion (Suehiro et al., 2010). *Egr3* knockdown attenuates VEGF-A-mediated growth, migration and tube formation of human primary ECs (Suehiro et al., 2010). In a study by Suehiro and colleagues in 2010, an *Egr3* knockdown was conducted using transient transfection of HUVECs with 2 independent siRNAs against *Egr3* resulting in significant inhibition of VEGF-A-responsive *Egr3* mRNA expression (90% and 72% reduction, respectively). The HUVECs were treated with 50 ng/mL VEGF-A and cells were then enumerated over time. VEGF-A treatment of cells transfected with control SiRNA resulted in a 2.4-fold increase in cell number after 48 hours, this effect was inhibited 36% to 75% by *Egr3* knockdown (Suehiro et al., 2010).

Nr4a3 also known as neuron-derived orphan receptor 1 is the last of a family of 3 nuclear receptor TFs. The Nr4A family of nuclear receptors are constitutively active orphan receptors, whose transcriptional activity is independent of the binding of a ligand; with transcriptional activity depending more so on their gene expression levels and post-translational regulation (Martínez-González et al., 2021). VEGF-A robustly activates the expression and functional activity of all three NR4A members suggesting their potential influence in VEGF-A-mediated angiogenesis. In a study of NR4A1$^{-/-}$ knockout mice, angiogenesis, and micro-vessel permeability was almost completely inhibited (Zeng et al., 2006).

Decreases in methylation on *Nr4a3* mRNA specifically, induced proliferation of vascular smooth muscle cells (VSMCs) suggesting *Nr4a3* plays a role in vascular remodelling. Huo and colleagues observed that knockdown of fat mass and obesity-associated (FTO) in VSMCs was found to decrease the methylation level of *Nr4a3* mRNA which was associated with AngII induced VSMC proliferation (Huo et al., 2022).

Nr4a3 has also been shown to be necessary for tube formation in human brain micro-endothelial cells (HBMECs) (Goyal & Goyal, 2019). In a study by Goyal & Goyal in 2019, they used CRISPR/Cas9 technology to create knockdowns of several genes in HBMECs, one of which was *Nr4a3*; after which they conducted tube formation and cell migration assays. They observed a significant reduction in capillary tube formation following knockdown of *Nr4a3* ($p< 0.05$) (Goyal & Goyal, 2019).

4. The ageing vasculature

Several changes take place in the vasculature as an individual ages. These changes are often attributed to endothelial dysfunction, which is a major contributor to several diseases such as atherosclerosis; CVD, peripheral artery disease (PAD); hypertension and diabetes (Hadi et al, 2005). These conditions are exacerbated by endothelial dysfunctions such as arterial stiffening, breakdown in EC tissue barrier functioning, and limited EC nitric oxide production (Ting et al, 2021; Ungvari et al, 2018).

4.1 The ageing vasculature: senescence

Cellular senescence is characterized by permanent cell cycle arrest and distinct changes in cell morphology, metabolism, chromatin reorganization, gene profiles and activation of a senescence associated secretory phenotype (SASP) (Ting et al, 2021).Senescence has been highlighted as a hallmark of ageing (Avelar et al., 2020; Valieva et al., 2022) and linked to the progression of age-related diseases such as CVD and renal dysfunction (Ting et al, 2021).

In a study conducted by Minamino et al. in 2002, they compared staining for β-galactosidase (β-gal), a common marker indicative of increased lysosomal activity often observed in senescent cells, in coronary arteries and internal mammary arteries of 4 autopsied individuals diagnosed with

ischemic heart disease. Strong β-gal staining was observed in atherosclerotic lesions of the coronary arteries but not in the internal mammary arteries, they followed this with immunohistochemical staining using anti-factor VIII antibody, which verified that these positive cells were in fact vascular ECs (Minamino et al., 2002). This study highlights the role of senescence in endothelial dysfunction.

Replicative senescence, which is senescence observed by the continuous expansion of cells *in-vitro*, was first observed by Leonard Hayflick (Hayflick, 1965). Replicative senescence in culture through serial passaging has long been observed as a valid model of ageing, in several cell types including endothelial cells, to evaluate potential changes in cellular and molecular processes (Cristofalo & Pignolo, 1993; Jothi & Kulka, 2024; Li et al., 2019; Yi et al., 2020). However, little work has been done on primary skeletal muscle endothelial cells.

4.2 Ageing & the angiogenic response

Angiogenesis is generally accepted to be blunted in the older population (Reed & Edelberg, 2004). Older individuals are at a disadvantage compared to the young as they have a higher incidence of muscle-fibre atrophy, fibre loss and capillary rarefaction (Barnouin et al., 2017). For older individuals, even with training it is more difficult to induce muscular and vascular adaptations. A comparative study of young and aged women found that VEGF-A levels were lower at rest in older individuals, and the exercise-induced increase in VEGF-A was 50% lower than their young counterparts (Croley et al., 2005). It has been observed that, VEGF-A expression is not only decreased with age, but VEGF function is impaired (Sadoun & Reed, 2003), this is supported by studies illustrating that older individuals typically suffer from slower wound healing, indicating poor vascular adaptability (Gosain & DiPietro, 2004).

In humans, studies have consistently shown that baseline measures of capillarization and intermuscular VEGF-A are decreased in aged populations, however measures in response to training are conflicting. Studies tend to support reduced angiogenic capacity in older women compared to young (Gliemann et al., 2021; Olsen et al., 2020), rather than the older population in general, with studies on men showing no differences in vascular adaptations in response to training between young and old men (Gavin et al., 2007)

Age-based studies with observations of reduced angiogenic capacity have been consistently observed, however, in mouse models (Reed et al., 1998; Rivard et al., 1999; Yamaura & Matsuzawa, 1980).

A preclinical study in C57Bl6 mice confirmed that older mice (24-26 weeks old versus 12-14 weeks old) present a decrease in baseline VEGF-A expression before any decrease in capillary-to-fiber ratio was observed. Also, in response to skeletal muscle injury older mice were unable to increase VEGF-A expression impairing muscle regeneration (Endo et al., 2023). Transgenic mice generated to maintain young-like whole body levels of VEGF-A (by forcing VEGF-A expression in hepatocytes) presented massive reduction of age-related sarcopenia and better skeletal muscle structure (reduced central localization of myonuclei, often seen in ageing due to impaired regenerative processes) and more importantly, reverse age-related capillary rarefaction in multiple organs and tissues, including the skeletal muscle through a mechanism that requires the activity of VEGFR-2. This highlights the importance of VEGF-A/VEGFR-2 signaling and its role in aging. Yet, decreases in the availability of tissue VEGF-A might not be the only mechanism that impairs angiogenesis with aging. The intrinsic properties and capacity of endothelial cells to respond to VEGF-A might also explain age-related alterations in angiogenesis.

Indeed, microvascular endothelial cells isolated from F344xBN rats aged 24 months expressed impairment in their intrinsic tube forming ability in response to VEGF-A treatment, compared with that of cells isolated from young F344xBN rats aged 3 months (Ungvari et al., 2013).

A study conducted by Di and colleagues in 2013 indicates that reductions in vascular regeneration with age can also be attributed to reduced ability of endothelial progenitors to activate VEGFR-2 (Di et al., 2013).

Despite the inconsistent observations of reduced capacity for exercise induced angiogenesis observed in humans, the evidence of reduced capillarization and VEGF-A expression is undeniable. Studies have suggested that these characteristics may be attributable to endothelial dysfunction (Jia et al., 2019; Rivard et al., 1999) which has also been observed in mice and therefore additional research on murine models is needed. Further elucidating these issues is vital to aid those in the older population in maintaining capillarization and thereby skeletal muscle and overall health.

5. Epigenetics

Chromatin is comprised of genomic DNA wrapped around a core of four histone proteins that include histone 2A, 2B, 3 and 4 (McGee et al., 2009; Strahl & Allis, 2000). The spatial relationship between DNA and the histone core determines the transcriptional status of surrounding genes. Epigenetics is the study of the overarching process of several mechanisms that modify gene expression while maintaining the integrity of the genome itself. This is possible through the following epigenetic mechanisms; DNA methylation, histone modifications and micro RNAs (miRNAs) (Peixoto et al., 2020). DNA methylation is straightforward as the name states, the addition of a methyl group directly on the gene body, typically occurring at CpG islands. Histone

modifications are modifications that are post-translational in nature (PTMs) such as methylation, acetylation, phosphorylation and ubiquitination found on histone tails. MicroRNAs (miRNAs) are small non-coding RNAs with the capability of modulating gene expression at the post-transcriptional level either by inhibiting messenger RNA (mRNA) translation or by promoting mRNA degradation (Correia de Sousa et al., 2019). Histone modifications and their role in skeletal muscle capillarization as it is an adaptation that is strictly regulated, and histone modifications are known to have to ability to change rapidly in response to environmental stimulus, such as in the context of exercise.

5.1 Histone Modifications

Histone modifications are post-translational modifications (PTM) added to the N-terminus of histone tails that subsequently alter chromatin structure through their influence on nuceolsomal interactions (Bannister & Kouzarides, 2011). These modifications are input or removed by histone modifying enzymes known as histone writers and erasers which can be classified as histone methyltransferases (HMTs), histone demethylases (DMTs), histone deacetylases (HDAC), histone acetyltransferases (HATs) and more. Again, several PTMs can take place such as methylation, acetylation, phosphorylation and ubiquitination.

Histone modifications can aid in the creation and maintenance of three fundamental chromatin states; euchromatin, constitutive heterochromatin and facultative heterochromatin. When activation marks (i.e. $H3K4me^3$, H3K27ac) are placed on the histone, it will yield to a euchromatin formation, wherein histones are organized loosely, allowing for easier access to DNA for transcription, and thereby result in the upregulation of genes. When silencing marks (ie $H3K27me^3$, $H3K9me^3$) are placed on the histone, it will yield a constitutive heterochromatin formation, wherein histones are more tightly packed, making DNA less accessible, and thereby

resulting in downregulation of genes. Constitutive heterochromatin is typically propagated on regions across species and maintained over the lifespan of an individual (Morrison & Thakur, 2021). There is also an in-between state known as facultative chromatin. Facultative heterochromatin allows chromatin to more easily shift to a euchromatin state. Facultative heterochromatin typically exists in regions of developmental genes which are strictly controlled, sometimes transiently, based on developmental or environmental cues (Morrison & Thakur, 2021). A hallmark of facultative heterochromatin could be 'bivalent chromatin' that is marked with both silencing and activation marks, which will be discussed more thoroughly in a later section. Chromatin structure is constantly changing resulting in adjustments in gene expression based on environmental influence, factors such as diet, physical activity, exposure to various toxins and much more (Alegría-Torres et al., 2011).

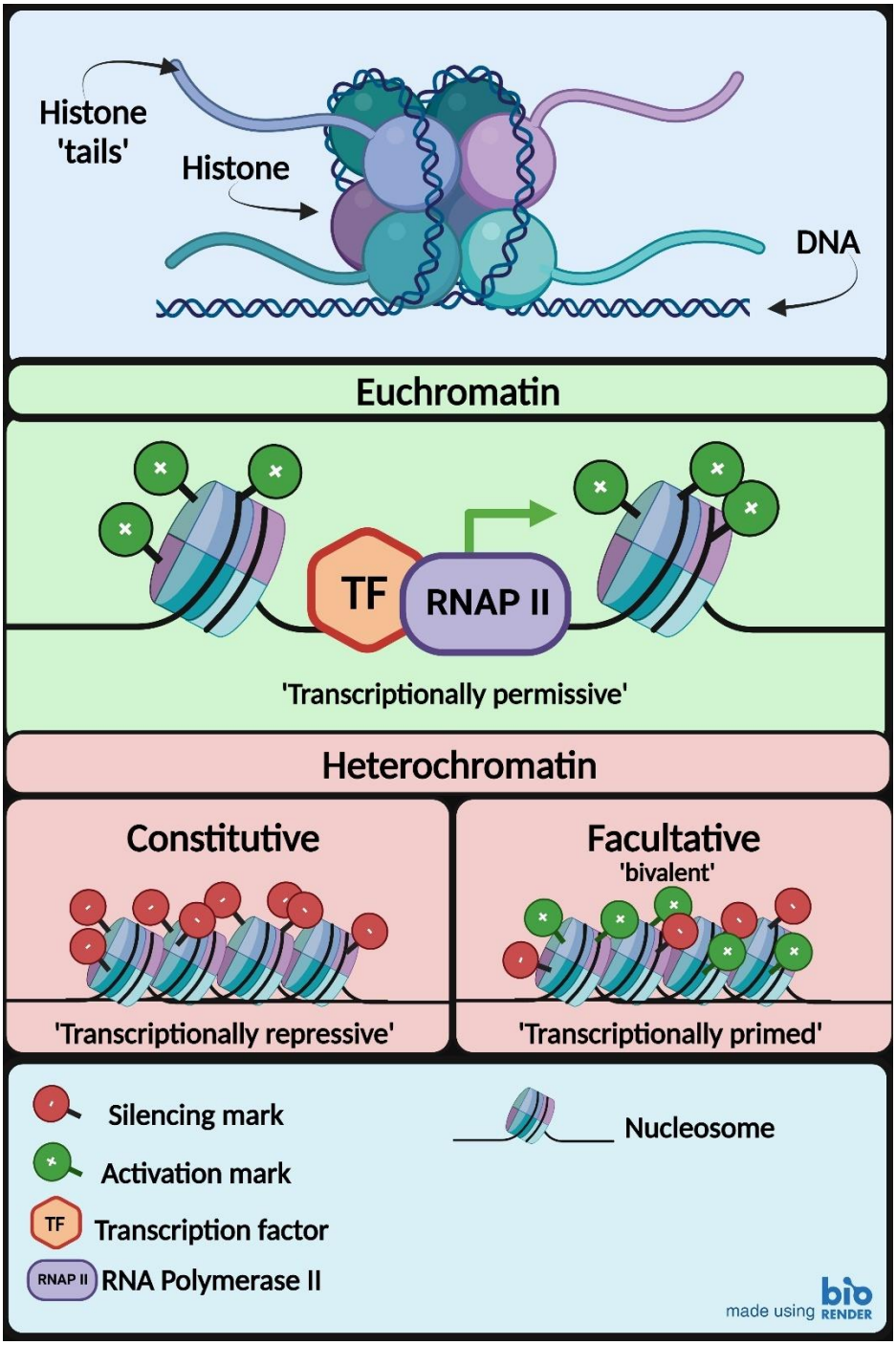
Histone 'tails'
Histone
DNA
Euchromatin
TF
RNAP II
'Transcriptionally permissive'
Heterochromatin
Constitutive
'Transcriptionally repressive'
Facultative
'bivalent'
'Transcriptionally primed'
Silencing mark
Activation mark
TF
Transcription factor
RNAP II
RNA Polymerase II
Nucleosome
made using bio RENDER

Figure 2. Chromatin states and influence of histone modifications

DNA is wrapped around histone proteins. Tails of histones can acquire post-translational modifications that can impact the tri-dimensional shape of DNA. Euchromatin are transcriptionally permissive. Constitutive heterochromatin is condensed and static and therefore in a transcriptionally repressed state. This type of heterochromatin is characterized by a greater abundance of silencing histone modifications. Facultative heterochromatin has the capacity to switch between a transcriptionally primed and transcriptionally repressed state. This heterochromatin often contains both activation and silencing marks.

5.2 Epigenetics & external factors

Several environmental and behavioural factors have been found to influence epigenetic mechanisms resulting in changes in gene expression. There have been studies observing epigenetic changes due to behavioural factors such as diet, exercise, air pollution and even nightshift work, among many others (Alegría-Torres et al., 2011). In a study by Tarantini et al., in 2009, demonstrated that iNOS (inducible Nitric Oxide Synthase) promoter methylation decreased in blood samples of foundry workers with well-characterized exposure to PM10 in samples taken at the end of a four-day work week compared day one (Tarantini et al., 2009). A study of night shift workers showed alterations in blood DNA methylation of inflammatory genes such as Interferon Gamma (IFN-γ) and Tumour Necrosis Factor- alpha (TNFα) (Bollati et al., 2010) In an exercise study, human muscle biopsies show increases in global acetylation of lysine 36 of histone H3 following 60 minutes of cycling exercise (McGee et al., 2009). Together these studies demonstrate the immense influence environmental and behavioural factors have on epigenetic mechanisms.

5.2.1 Epigenetics & exercise: skeletal muscle

In the skeletal muscle, the increase in contractile activity alters the expression of transcription TFs and co-activators, many of which have been found to be strongly associated with or regulated by epigenetic mechanisms (Kawano, 2021).

A study by Barrès et al. in 2012, revealed that whole genome methylation was decreased in skeletal muscle biopsies (vastus lateralis) obtained from healthy sedentary men and women after a single VO_2 peak test, which ceased at volitional fatigue. Exercise also induced dose-dependent expression of PGC-1α, pyruvate dehydrogenase lipoamide kinase isozyme 4 (PDK4), and peroxisome proliferator-activated receptor-delta (PPAR-δ), together with a marked hypomethylation (10% decrease) on each respective promoter (Barrès et al., 2012). In another study by Maasar and colleagues in 2021, looking at the effect of different sprint protocols (Change of direction (COD) or straight-line (ST)) on methylome and transcriptome signatures in the vastus lateralis of young male athletes, found that VEGF-A and its downstream nuclear transcription factor, *NR4A1* had enriched hypomethylation within their promoter regions. *VEGFA* and *NR4A1* were also significantly upregulated. They also confirmed increased gene expression of *VEGF-A*, and considerably larger increases in the expression of canonical metabolic genes *PPARGC1A* (that encodes *PGC1*-α) and *NR4A3* in COD vs. ST exercise (Maasar et al., 2021). Changes due to exercise have also been observed in histone modifications. A study by McGee and colleagues in 2009, found that 60 minutes of cycling exercise brought increases in H3K36 acetylation, which is association with transcriptional elongation, in the vastus lateralis compared to baseline. They also found that HDAC 4 and 5, associated with transcriptional repression due to their ability to remove acetylation marks, were exported from the nucleus during exercise (McGee et al., 2009). Further, Lim and colleagues in 2020, reported that acute resistance

exercise significantly upregulated the distribution of acetylated H3, mono-methylation of lysine 4 on histone H3(H3K4me^1), and the tri-methylation on lysine 27 of histone H3 (H3K27me^3) to the pre-exercise levels. After 10 weeks of resistance exercise training, the expression of these genes was maintained at a higher level than the pretraining level. The distribution of acetylated H3 at these loci was found to be upregulated after resistance exercise training. These results indicated that histone modifications in the skeletal muscles robustly responded to acute exercise, with exercise training maintaining transcriptionally active status of the muscle (Lim et al., 2020). Together these studies support the great ability of exercise to influence histone modifications with continuous training maintaining the alterations to then maintain skeletal muscle adaptations.

5.2.2 Epigenetics & exercise induced skeletal muscle angiogenesis

Few studies in general have shown epigenetic modulation of angiogenic factors. A study by Fu et al. in 2014, demonstrated for the first time that acupuncture can effectively up-regulate *VEGF-A* expression through H3K9 acetylation modification directly at the VEGF-A promoter and hence activate VEGF-A induced angiogenesis in a model of myocardial ischemia (Fu et al., 2014). Ubiquitously transcribed tetratricopeptide repeat on chromosome X (UTX, coding by the gene KDM6A) a H3K27 demethylase and KMT2D a di-methylase and their impact on H3K27 and H3K4 have been implicated for their necessary roles in cardiogenesis (Ang et al., 2016; Lee et al., 2012). However, as previously stated, exercise has a profound effect on the epigenome (the totality of epigenetic marks present in the genome) and it is one of the few contexts in adulthood in which angiogenesis occurs. After a single bout of exercise, almost 2000 genes are upregulated in response to the contractile activity in the skeletal muscle (Kanzleiter et al., 2015). Below, we will shift focus to epigenetic mediators that have been shown to be specifically involved in exercise-induced skeletal muscle angiogenesis.

5.2.2.1 Epigenetic mediator Mdm2: Murine Double Minute-2

Murine double minute-2 (Mdm2) is an E3 ubiquitin ligase most well-known for its role as a negative regulator of tumour suppressor p53. In the context of skeletal muscle, Mdm2 has been shown to stabilize *VEGF* mRNA and protein expression, with overexpression of Mdm2 resulting in enhanced expression of *VEGF* mRNA and protein (Zhou et al., 2011). Research from our lab has shown that Mdm2 is an important regulator of skeletal muscle angiogenesis. Reduction of Mdm2 resulted in lower levels of basal muscle capillarization, lower levels of exercise-induced *VEGF-A* expression and impaired capillarization (Roudier et al., 2012, 2013). Interestingly, Mdm2 might exercise epigenetic function by interactions with histones directly and enzymes catalysing histone modification (Arena et al., 2018; Minsky & Oren, 2004; Wienken et al., 2017). Mdm2 has been implicated in influencing VEGFR-2 expression; when Mdm2 was deleted in Mouse Embryonic Fibroblasts (MEFs) an upregulation in VEGFR-2 protein was observed (Hawkins et al., 2010). Limited evidence suggests that Mdm2 may play a role in regulating *VEGFR-2*, yet, it clearly shows that Mdm2 is a necessary and important regulator of skeletal muscle angiogenesis.

5.2.2.2 Histone writer EZH2: Enhancer of Zeste Homologue 2.

Enhancer of Zeste Homologue 2 (EZH2) is a long-studied histone methyltransferase that acts as the catalytic subunit of the Polycomb Repressor 2 (PRC2) complex. The Polycomb Repressor Group family is known for their role in chromatin compaction which is vital for the regulation of genes in early development. PRC2 is involved in various biological processes, including differentiation, cell identity and proliferation, and stem-cell plasticity (Margueron & Reinberg, 2011). EZH2 implements the histone mark H3K27me^3 which denotes a tri-methylation on lysine 27 of histone H3, a well-known mark of gene repression. While chromatin rich with H3K27me^3 marked promoters were considered functionally repressive, it was later shown that the promoters

remained accessible to TFs (Hawkins et al., 2010) and is therefore now considered as facultative heterochromatin (Brookes et al., 2012).

Mdm2 has been observed to interact with the PRC2 complex and in turn possibly regulate EZH2 activity (Wienken et al., 2016). Bivalent marking, the presence of H3k27me^3 and an activation histone mark (i.e. H3k4me^3) on the same gene can prime genes for easier inactivation or activation in a context dependent manner, such as during hypoxia (Prickaerts et al., 2016) EGR3 has also been observed to be strictly controlled by bivalent marking (J. Chen et al., 2020), suggesting a possible regulatory role of EZH2. Further evidence that EZH2 may regulate EGR3 is; inhibition of EZH2 resulted in the upregulation of EGR3 in neurons in a mouse model (H. Liu et al., 2019). EZH2 has also been observed to directly influence EC function. EZH2's expression and methyltransferase activity were observed to positively regulate endothelial cell proliferation, migration and tube formation (Y.-T. Chen et al., 2016; Maleszewska et al., 2016). This strongly suggests that EZH2 may play a role in regulating skeletal muscle angiogenesis.

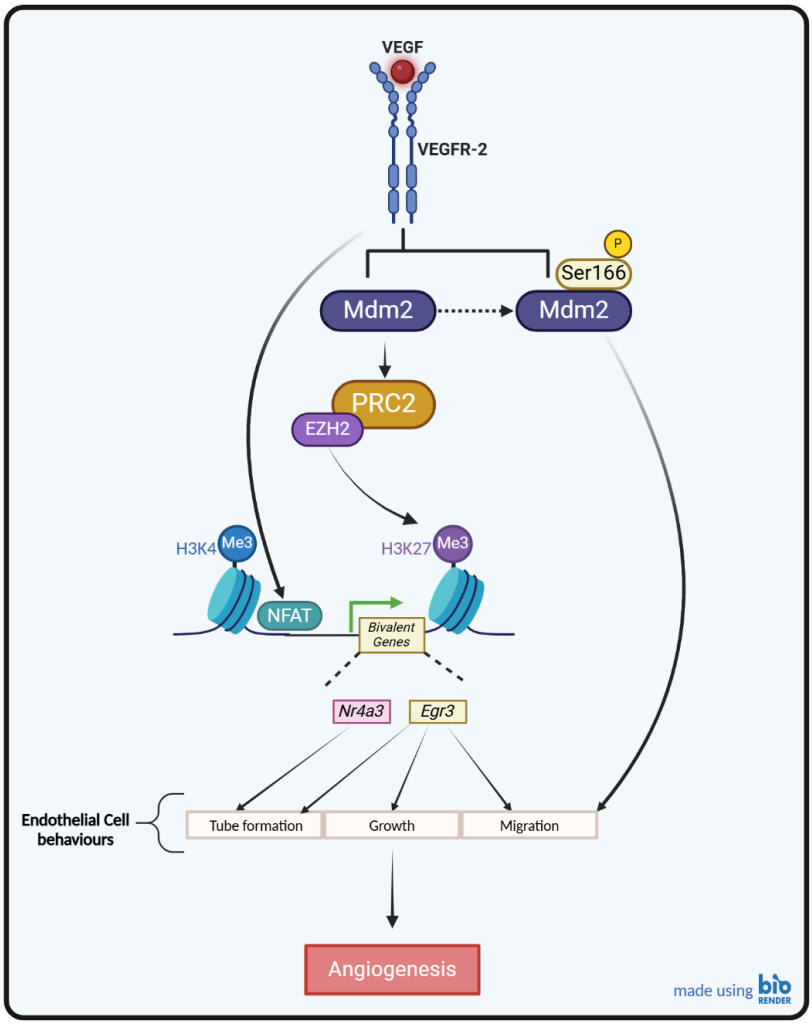

Figure 3. Epigenetic regulation of downstream effectors of VEGFR-2

VEGF-A interacts with VEGFR-2 activating the transcription factor nuclear factor of activated T cells (NFAT) and Mdm2. Activation of NFAT results in the induction of downstream effectors of VEGFR-2 *Egr3* and *Nr4a3,* promoting endothelial cell migration and proliferation. Mdm2 phosphorylation on serine 166 enhances endothelial cell migration. Mdm2 also associates with EZH2 within the PRC2 complex enhancing its activity, potentially increasing H3K27me^3 marking on PRC2 regulated genes resulting in downregulation of these genes.

5.3 Bivalence

'Bivalence' denotes a chromatin state in which both canonically repressive and active marks typically H3K27me^3 and H3K4me^3, respectively mark the histone simultaneously. It was first described in the work by Azuara et al. in 2006, in their study on mapping the epigenetic profile of embryonic stem cells among other stem cell types, and their post-differentiation progeny (Azuara et al., 2006). Their work was quickly followed by Bernstein and colleagues looking at epigenetic regulation of highly conserved noncoding elements (HCNEs) (Bernstein et al., 2006). Bivalence was initially thought to only be important in early development and stem cells, as it is generally observed to exist in regions of developmental genes. Researchers postulated that it was for strict control of these genes that they might quickly become active or repressive in response strong developmental or committal cues. However, a study from Zhao et al in 2021, took a mathematical approach to uncover the necessary conditions for the emergence of bivalent chromatin. In their discussion they state that "by analyzing the transitions among chromatin states in response to external stimulus or noise, we demonstrated that bivalent chromatin could serve as a poised state, which has the potential to switch to multiple states and facilitates a stepwise transition between repressive chromatin state and activating chromatin state, to mediate phenotypical plasticity" (Zhao et al., 2021). While this does not directly implicate bivalence as an important regulatory characteristic in ECs, due to the capacity and necessary phenotypic changes ECs must undergo for the angiogenic process, it is possible that bivalence may be involved in the EC response to environmental stressors and the angiogenic process overall.

5.3.1 Bivalence & VEGF responsiveness

In recent years, two fundamental studies have revealed the role of bivalence in VEGF responsiveness. In a study by Chen and colleagues in 2020, they conducted chromatin immunoprecipitation followed by high-throughput sequencing (ChIP-seq) to profile the genomic occupancy of multiple histone modifications; including $H3K4me^2$ (a mark of both active promoters and enhancers), $H3K4me^3$ (a mark of active promoters), H3K27ac (a mark of active enhancers and promoters), and $H3K27me^3$ (a mark of repressed enhancers and promoters), on human umbilical vein endothelial cells (HUVECs) that were stimulated with VEGF-A for 0 to 12 hours. They also used their previously reported RNA sequencing (RNA-seq) expression profiles identifying 29,722 differentially expressed genes (DEG) (J. Chen et al., 2017). Of these genes they found that 3379 were marked bivalently with both $H3K4me^3$ and $H3K27me^3$. This possibly suggested that bivalence contributed to the responsiveness of VEGF-A. To verify this, they cross referenced the co-occurrence of $H3K27me^3$ and $H3K4me^3$ on the promoters of DEGs; genes previously found to respond significantly to VEGF-A stimulation and observed that 81.79% of their promoters were bivalently marked (J. Chen et al., 2020). These observations suggest that bivalent marking may contribute largely to the regulation of VEGF responsiveness and as a result angiogenesis. The authors also state that some bivalently marked DEGs had key functions in vascular identity and homeostasis, one of which was *Egr3* (J. Chen et al., 2020).

Later in 2022, Kanki and colleagues demonstrated the role of bivalence in the regulation of important angiogenic genes. They developed a comprehensive epigenomic mapping of dynamic transcriptional events in HUVECs, focusing on major histone-code profiles in response to VEGF-A stimulation. They divided all responding genes into classes based on how quickly they responded to VEGF. Immediate-early response genes, which they termed Class-I genes, were upregulated

within the first 15 minutes of VEGF stimulation; these genes were observed to increase only transiently. The expression of these genes quickly returned to basal levels and was unable to be upregulated again upon sequential VEGF-A stimulation for up to 1 hour. These Class-I genes were revealed to all be important regulatory TFs, one of which was *Egr3*. To verify the existence of a bivalent state on the *Egr3* gene loci, they performed sequential ChIP assays using first an antibody targeting H3K4me^3 and then a re-ChIP using an antibody against H3K27me^3. The locus in the first intron of *Egr3* revealed positive marking of both H3K4me^3 and H3K27me^3 at 15 and 60 min after VEGF stimulation, compared to a control region. This reveals the tight regulation that bivalence allows for on angiogenic relevant genes. The authors conclude that the gene loci of indispensable immediate-early angiogenic TFs exclusively acquired bivalent histone marks after VEGF stimulus (Kanki et al., 2022).

5.4 Epigenetics of ageing & role of EZH2

The epigenetics of ageing has emerged as a novel area of interest as gene expression, which it regulates, is necessary for cell identity and more importantly, function. Because of their crucial role in determining cellular function, age-associated changes in transcriptional factors and chromatin states may represent a critical foundation in the creation of the ageing phenotype (Booth & Brunet, 2016). Age-associated dysfunctions in several epigenetic mechanisms such as DNA methylation, histone modifications, transcription factor activity and many more have been observed (Boot & Brunet, 2016). EZH2 has been directly identified in shaping the ageing epigenome (Mozhui & Pandey, 2017), therefore EZH2 and its activity during ageing has garnered further interest. Conflicting evidence of EZH2's age-associated changes in activity, lead to an understanding that these changes may be specie, cell and even gene specific. This, however, makes uncovering its role in ageing an increasingly complex process.

Lu et al. reported that EZH2 may have an inverse relationship with Sirtuin 1 (SIRT1) a Nicotinamide Adenine Dinucleotide (NAD+) dependent deacetylase that has been observed to increase lifespan and glucose tolerance in rodents. They observed with SIRT1 knockdown, EZH2 protein levels were increased with greater nuclear localization (L. Lu et al., 2011). Also, mice with higher JumonjiC (JmjC)-domain-containing protein 1.2 (JMJD-1.2) expression, a demethylase known to remove H3K27me^3, live longer, suggesting decreased H3K27me^3 levels and possibly EZH2 activity, may be associated with longevity (Merkwirth et al., 2016). Similar findings have been observed in mouse liver cells (Yang et al., 2023) and myoblasts (L. Liu et al., 2013), and skeletal muscle of killifish (Cencioni et al., 2019).

In 2014, Sun and colleagues conducted a comprehensive genomic analysis of DNA methylation and histone modifications of hematopoietic stem cells from both young and old mice. H3K27me^3 deposition in young versus old murine hematopoietic stem cells (HSC) revealed that while H3K27me^3 levels increased at most loci, there were also loci with decreased H3K27me^3 levels with age. Indicating that age-associated changes in EZH2 regulation may be gene specific (Sun et al., 2014).

In a study on human progeria, a congenital disease caused by a genetic mutation that results in rapid biological ageing, Shumaker and colleagues examined the inactive X chromosome of female patient fibroblasts and compared to controls. They found that H3K27me^3 marking was almost completely lost (Shumaker et al., 2006). Again, EZH2's change in activity in ageing seems to be specie, cell and gene specific and therefore, more research on its age-associated changes of gene regulation is needed.

Table 1. Current knowledge of age-associated changes in EZH2 activity. Arrows indicate general reported change

Reference	Specie	Tissue/Cell type	Change in EZH2 activity/H3K27me^3 marking
L. Lu et al., 2011	Human	HeLa cells	↗ nuclear localization of EZH2
Yang et al., 2023	Mice	Hepatocytes	↗ H3K27me^3 marking
L. Liu et al., 2013	Mice	Myoblasts	↗ H3K27me^3 marking
Cencioni et al., 2019	Killifish	Whole skeletal muscle	↗ H3K27me^3 marking
Sun et al., 2014	Mice	HSC	↗ H3K27me^3 marking at some loci but ↘ at others
Shumaker et al., 2006	Human Progeria	Fibroblasts	↘ H3K27me^3 marking

Rationale for the study

As highlighted in the literature review, the skeletal muscle microvasculature is at the center of muscle health and whole-body function. Maintaining the function and angiogenic capacity of the muscle microvasculature helps to slow age-related loss of physical functions, supporting better fitness and health. While epigenetics processes, such as the establishment of histone modifications, have emerged as key to angiogenesis, controlling how endothelial cells sense pro-angiogenic factors (e.g. VEGF-A). Evidence cumulates indicating that aging alters these epigenetic processes, including those regulated by the epigenetic writer EZH2. To date, most in-vitro studies aiming to investigate the impact of aging are done using endothelial cell models, such as HUVECs, that are not microvascular. Limited in-vitro studies have utilized microvascular endothelial cells isolated from skeletal muscle.

Here, we utilize a model of skeletal muscle microvascular endothelial cells (SMECs) to investigate the impact of aging on EZH2-related epigenetic process that controls the transcriptional response to VEGF-A.

Gap of Knowledge

Evidence suggests that EZH2 may play a role in ageing, however, minimal observations have been made on the influence of EZH2 on angiogenic capacity in the context of ageing. We hope to further elucidate EZH2's role in age progression to clarify the extent of its influence on VEGF responsiveness and angiogenic factors.

Scientific Questions

- Does enhanced EZH2 activity, such as in the context of ageing, decrease the ability of skeletal muscle microvascular endothelial cells to respond to VEGF-A?
- Is serial passaging a valid model of ageing in the context of primary endothelial cells?

Hypothesis

We hypothesize that when modeling ageing using serial passaging of skeletal muscle microvascular endothelial cells (SMECs), SMECs will lose their capacity to respond to VEGF-A stimulation. We hypothesize if loss of responsiveness is observed, it will be due part due to an increase in EZH2 activity, measured through its canonical histone mark H3K27me^3.

Objectives

- Assessing whether serial passaging of mouse primary skeletal muscle microvascular endothelial cells (mSMECs) impairs the responsiveness to VEGF-A of bivalently marked genes down-stream of VEGFR-2 (i.e. *Egr3* and *NR4a3*)

- Delineating whether serial passaging represents a valid model of aging in primary skeletal muscle endothelial cells by measuring markers of senescence in mSMECs isolated from young adult and old mice (Aged mSMECs)
- Evaluating the impact of EZH2 inhibition on the capacity of mSMECs to increase the expression of bivalently marked genes responsive to VEGF-A.

Methods

Cell Culture

Mouse C57BL/6 primary skeletal muscle microvascular endothelial cells (mSMECs) isolated from adult (Cat. C57-6220) or old mice (Aged mSMECs) (Cat. A57-6220) (Cell Biologics Inc., Cedarlane, Burlington, ON, Canada) were plated on gelatin-coated dishes (1.5% Gelatin Type A (BioShop, Cat. Gel771.500, BioShop Canada Inc, Burlington, ON, Canada)) and cultured at 37° C and 5% CO_2 in complete endothelial cell medium (Cell Biologics Inc., Cat. M1168, Cedarlane, Burlington, ON, Canada) (excluding L-glutamine) and supplemented with 5 mLs of Glutamax (Cat. 35050061, Gibco, Thermofisher, Whitby, ON, Canada). Cells were used between passages P7 and P9 at a density of ~9500-12,000 cells/cm^2.

GSK343 & VEGF-A Treatment

mSMECs were treated with GSK343, an inhibitor of EZH2, at a concentration of 1μM (Cell Signalling Technology, Cat. 6244) or DMSO (Dimethyl Sulfoxide), Thermofisher, Cat. D12345) for either 2 or 48 hours. mSMECs were then treated with or without Recombinant Murine $VEGF_{165}$ (PeproTech, Cat. 450-32), depending on respective group, for 30 minutes at 100 ng/ml. Before treating with VEGF, cells are starved overnight (~16hrs) in OptiMem (Thermofisher, Cat. 31985-070).

Protein Extraction

Proteins were extracted from mSMECs that were plated at a cell density of 9500 cells/cm^2 in a 60mm^2 dish ~48hrs prior to reaching sub-confluency. Proteins were then extracted using Radioimmunoprecipitation assay (RIPA) lysis buffer (50 mM Tris Base, 100mM NaCl, 1% Triton X-100, 1% sodium deoxycholate, 5mM EDTA, pH 8.0) with protease inhibitor 1mM PMSF,

phosphatase inhibitors 1 mM NaF and Na3VO4, a protease inhibitor cocktail (Complete mini, Roche Diagnostics; Cat .049006845001) and a phosphatase inhibitor cocktail (Complete mini, Roche Diagnostics; Cat .11836153001). Briefly, cell cultures were washed 3 times with PBS before performing extraction using 100µl of RIPA buffer. After 20 minutes lysis incubation at 4˚C, (gently vortexing @ T=0 and T=10mins) and sonicating (5 cycles ON, 5 cycles OFF), homogenates were centrifugated at 16,000 g and 4˚C for 15 minutes. Supernatants were collected and used for downstream analysis of protein by western blotting.

RNA extraction

mSMECs were plated in 6-well plates at a density of 9500 or 12,000 cells/ cm^2. After ~48hrs RNAs were extracted with Qiazol lysis reagent (Cat.15596026). Briefly, cell cultures were washed 3 times with PBS before scraping and extracting RNAs with 700µl of Qiazol lysis reagent. Lysate was stored in -80° C until purification.

Determining Protein Concentration

Protein concentration is determined using a Bicinchoninic Acid Assay (BCA). Cell protein extracts are loaded in a standard 96-well plate in triplicates and measured at 562 nm absorbance on a Gen5 plate reader (Biotek). Cell protein lysate is diluted 1:10 in ddH_2O. Standard curve is plotted using Bovine serum albumin (Sigma-Aldrich A7906). BCA reagent used were, Bicinchoninic Acid (Cat. B9643) and Copper II Sulfate (Cat. C2284) and together with diluted samples were incubated for 30 minutes at 37°C.

Western Blotting

20 µg of protein lysate proteins were diluted in a 1/5 vol./vol. ratio in 2.69 mM sucrose, 0.28 M sodium dodecyl sulfate (SDS), 2.84 M b-mercaptoethanol, 14 µM bromophenol blue, 0.5 M Tris-

base pH 6.8, separated by sodium dodecyl sulfate polyacrylamide gel electrophoresis (SDS-PAGE), and then blotted on either a 0.2 μm or 0.45 μm nitrocellulose membrane (Cytiva, 0.2 μm Cat . 45004001, 0.45 μm Cat. 45004003, Marlborough, USA). Inter-gels comparison was done by using inter-gels lane average comparison. Quality of the transfer was controlled by Ponceau S Red staining. After blocking with 5% fat-free milk in 0.1% tween tris-buffered saline buffer, membranes were probed with the following primary antibodies; KDR: Cell signalling (9698S, Whitby, Canada), H3K27me^3: Cell signalling (9733S, Whitby, Canada), H3: Cell Signalling (4499S, Whitby, Canada), α/βTubulin: Cell Signalling (2148S, Whitby, Canada).

RNA Isolation and Quantification

mSMEC RNA isolation and purification was performed using miRNeasy micro kit (Qiagen, Cat. 217084).RNA was purified according to manufacturer's instructions using chloroform-phenol based purification. After purification, RNA is eluted in 20μl of Rnase free water. RNA was quantified using Gen5 plate reader (Biotek) at 1:10 dilution and a 260/280 nm absorbance. RNA was deemed acceptably pure with a 260/280 absorbance ratio reading of ~1.7-2.1.

Reverse Transcription-qPCR

400ng of RNA was reverse-transcribed using the High-Capacity RNA-to-cDNA kit (Applied Biosystems, Cat. 4387406, ThermoFisher Scientific, Burlington, ON, Canada). Semi-quantitative real-time PCR was performed for each sample in triplicate using TaqMan® Gene Expression assay probes (listed below) and TaqMan® Fast Advanced Master Mix (Applied Biosystems, Cat. 4444557, ThermoFisher Scientific, Burlington, ON, Canada) for 40 cycles of denaturation at 95˚C for 3 seconds, followed by annealing and extension at 60˚C for 30 seconds. *EGR3* and *VEGFR-2, p16 and p21* were measured and the ΔΔCt method was used to express the relative changes. mRNA changes were normalized to *HPRT* or *β-actin* gene. Data and expressed as $2^{-\Delta\Delta Ct}$.

Table 2. List of Taqman probes

Assay ID	Target	Sequences
Mm01545399	*Hprt*	GGACTGATTATGGACAGGACTGAAA
Mm01222421	*Kdr*	CATCCTAGAGCGCATGGCACCCATG
Mm00516979	*Egr3*	CAATCAGATGGCTACAGAGAATGTG
Mm00450071	*Nr4a3*	ATGGTTAAGGAAGTTGTGCGTACAG
Mm00494449	*p16*	AGCACGCCCAGGGCCCTGGAACTTC
Mm00432448	*p21*	GACCAGCCTGACAGATTTCTATCAC
Mm02619580	*β-actin*	CGGAGCCTCGGGCTGCCCAAGGTCT

Chromatin Immunoprecipitation-qPCR

Approximately 2 to 4 million mSMECs were washed with PBS, trypsinized and counted. Cells were then centrifugated at 0.5 RCF for 5 minutes and the pellet was resuspended in PBS. Cells were then re-centrifugated at 0.5 RCF for 5 minutes, supernatant was removed, and cells were resuspended in a 1% formaldehyde solution (Sigma-Aldrich, Cat. No. F8775). Cells were fixed for 7 minutes under rotation at room temperature and quenched for 5 minutes with 125 mM glycine (BioShop, Cat. No. GLN001). Pellet was washed 3 times by resuspension in cold PBS and centrifugated at 12, 000 g for 4 minutes before being resuspended in ChIP Lysis Buffer (50mM Tris, 10mM EDTA, 1% SDS, pH 8.0), vortexed for 15 seconds and incubated under rotation for 20 minutes at 4°C. Following lysis, chromatin was sheared to achieve a peak fragment size of ~300 bp (Bioruptor Plus, Diagenode). An aliquot of chromatin was taken for DNA Input and to confirm DNA fragment size. DNA fragment sizes from chromatin extract were assessed by automated electrophoresis on a 4200 TapeStation System (Agilent Technologies) using D1000 ScreenTape (Agilent Technologies, Cat. No. 5067-5582). For immunoprecipitation, roughly 1.5 µg sheared chromatin was diluted 1:10 in ChIP Buffer (50mM Tris, 167mM NaCl, 1.1% Triton X-100, pH

8.0) and 3 µg of antibody for histone target of interest was added overnight at 4°C on rotation: H3K27me^3 (Diagenode, Cat. No. C15410195). The following day, 20 µL of DiaMag protein A-coated ChIP-seq grade beads (Diagenode, Cat. No. C03010020-150) were added to samples and incubated at 4°C on rotation for 4-hours. Samples were then washed four times for 4-minutes with Low Salt wash buffer (50mM Tris, 1mM EDTA, 150mM NaCl, 0.1% SDS, 1% Triton X-100, pH 8.0) followed by two washes for 5-minutes with high salt wash buffer (50mM Tris, 1mM EDTA, 500mM NaCl, 0.1% SDS, 1% Triton X-100, pH 8.0). After washing, sample beads were resuspended in 150 µL of ChIP Elution buffer (10mM Tris, 5mM EDTA, 300mM NaCl, 0.5% SDS, pH 8.0) and incubated at 65°C and 800 rpm for 45-minutes. The eluted supernatant was then collected and treated with 20 µg RNAse A (ThermoFisher Scientific, Cat. No. EN0531) for 30-minutes at 37°C, followed by treatment with Proteinase K (ThermoFisher Scientific, Cat. No. EO0491) at a final concentration of 0.6 mg/ml for 2-hours at 65°C and 800 rpm. ChIP DNA was purified using PureLink PCR Purification Kit according to manufacturer's instructions (ThermoFisher Scientific, Cat. K310001). ChIP DNA was eluted in 50 µl of nuclease free water (Ambion, Cat. No. 9932) and stored at -20°C until analysis.

qPCR probes used to measure abundance of H3K27me3 on promoter regions of Kdr and Egr3

Table 3. List of Taqman probes used for detection H3K27me^3 mark enrichment on TSS regions of *Kdr* and *Egr3*, post ChIP.

TSRs		Sequences	TSS location
KDR	Forward primer	CATGACAAAACCCACCCAGAT	NC_000071.7 – Chr 5 76,093,487-76,139,118 bp, - strand
	Reverse Primer	TGGACCTAAGGATAGGCATTCTGT	
	Probe	CCATGTGGATAAATC	
EGR3	Forward primer	GCAAACTCGCCGAGAAGCT	NC_000080.7 Chr 14 c70314346-70315001
	Reverse Primer	TGTCAGGCAATTGATTTAGCAAA	
	Probe	CGGTGACCATGAGCA	

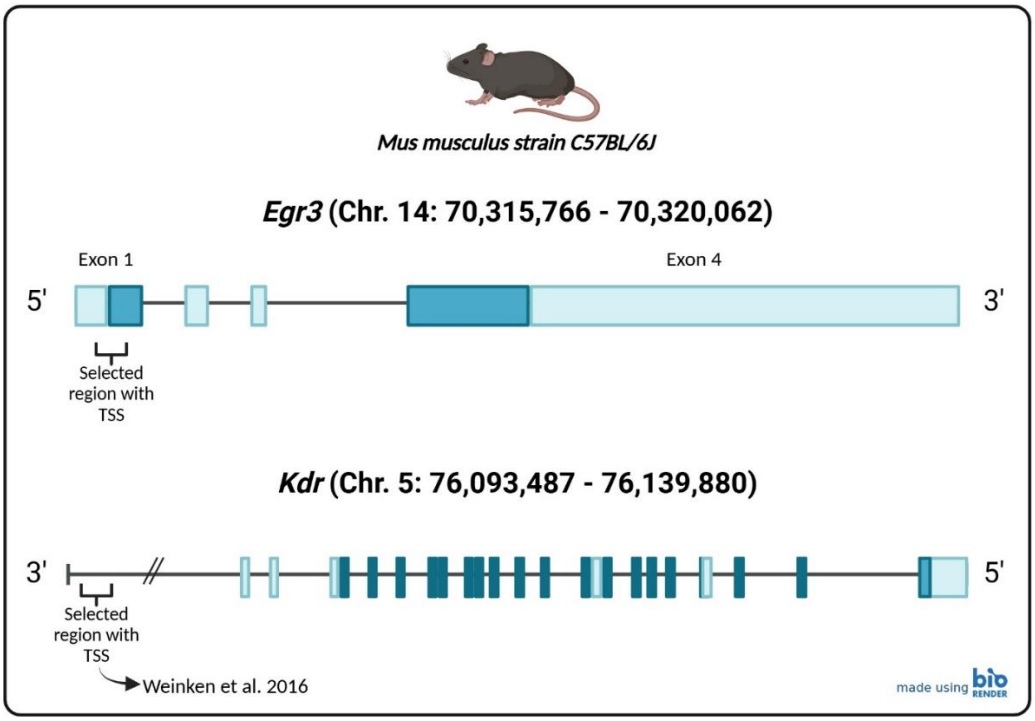

Figure 4. Schematic representation of the TSRs assessed by ChIP on the promoters of Egr3 and Kdr genes

TSS regions (TSRs) on KDR and EGR3 were identified based on a previous publication that reported enrichment of H3K27me3 on KDR promoter (Wienken et al., 2016), obtained from the UCSC Table Browser) and using the Eukaryotic promoter database (EPD) for EGR3. Taqman probes of these TSS regions on the promoters were designed using Primer 3 following the recommendation from ThermoFisher.

***Determination of %* of INPUT**

The enrichment in H3K27me^3 marks was estimated using the percentage of input (% INPUT). The % INPUT can be calculated once the cycle threshold (Ct) of the INPUT (CqIN) and the ChIP product (CqCHIP) are estimated; however, it needs to take into consideration the dilution factor (DF). ChIP protocol was performed at constant volume. Taking in consideration the initial volume of lysate used for the IP (150µl) and for the input (25 µl) and the dilution performed to have an INPUT at 5%, the INPUT was 20 times more diluted than the ChIP product. The dilution factor was then 120. Therefore, the % INPUT was calculated using the following formula: % INPUT = 2 (CqIN – Log2 (DF) – CqCHIP), where DF = 120. CqIN and CqCHIP are determined by qPCR (see above). % of INPUT was calculated for anti-H3K27me^3 ChIP product.

B-Galactosidase Cell Staining

Cell staining was performed using Senescence β-Galactosidase Cell Staining Kit (Cell Signaling Technology, cat .9860). Cells were stained for ~24 hrs at 37° C in a dry incubator and overlaid with 70% glycerol for long term storage. For staining images, four individual fields of view per well were counted under 100X magnification, and results were presented as the average of all fields of view. Image J was used to perform automatic analysis of particles stained. Briefly, RBG images were transformed into a black and white binary image. An image was used to set the

threshold for particles analysis. Once the experiment has determined a threshold that allows efficient detection of particles. Then the threshold was applied for analysing all images. Using the analyse particle tools, the software automatically retrieves the number of particles found in the staining images, the intensity of the staining and the areas covered by the stained particles. These values were then normalized to the number of cells counting per field of images

Statistical Analyses

All statistical analyses were performed on Graph pad Prism, using; welch t- tests, two-way ANOVA, one-way ANOVA and significance of $P \leq 0.05$. All data are presented with mean +/- S.E.M. Tukey testing was used to test multiple comparisons in the ANOVA analyses.

Presentation of Data

Experiments corresponding to β-galactosidase staining, comparisons made to mSMECs isolated from old mice and the ChIP- H3K27me^3, were only repeated once and can be found in the main results section (n=3-6 per group). Experiments for quantification of VEGFR-2 and H3K27me^3 proteins, and mRNA of *Egr3* and *Nr4a3* have been replicated at least 3 times (n=3-6 per group) and can be found in the main results section. Figures within the results show a single representative experiment based on summary data (all experiments pooled together). All repeats of experiments can be found in the supplemental data.

Results

VEGFR-2 expression significantly decreases with the passaging of mSMECs

We first observed with the passaging of mSMECs that VEGFR-2 expression significantly decreases at both the protein and mRNA levels. A preliminary experiment was performed to test whether passaging will change the basal level of VEGFR-2 **(Figure 5)**. VEGFR-2 was detected under the form of 3 mains bands at 150 kDa, 230 kDa and 250 kDa, corresponding roughly the theorical molecular weights previously reported for the mouse protein (150 kDa, 200kDa and 220 kDa) (Lemieux et al. 2022; Takahashi & Shibuya, 1997). The most significant differences were observed between P7 and P9 for the higher molecular form of VEGFR-2. When comparing P9 to P7 passage, a decrease by 86% was observed ($p<0.01$). Therefore, we decided to pursue our analysis measuring differences between P7 and P9, aiming to increase the robustness of this first observation.

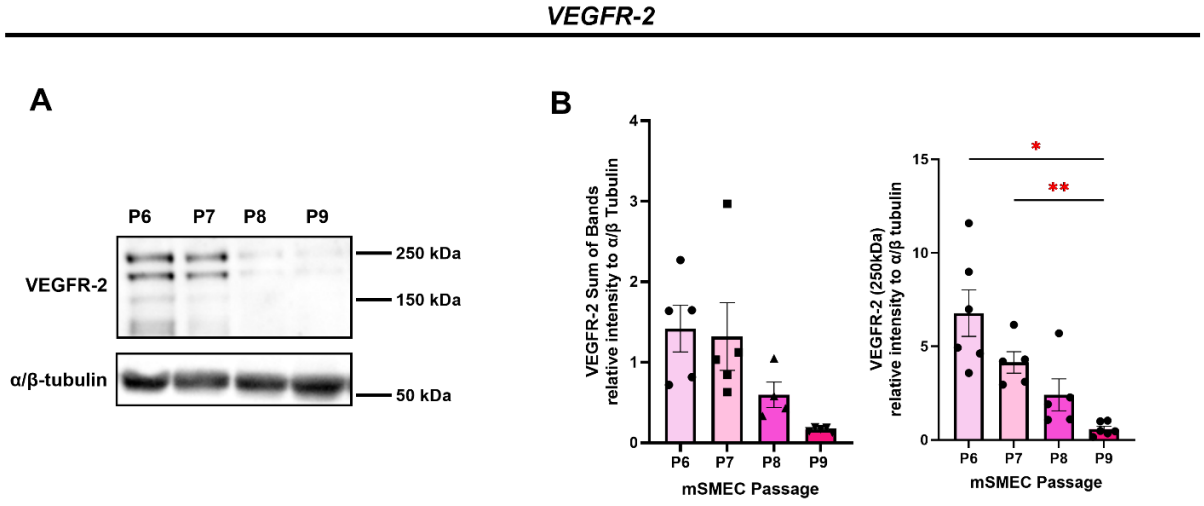

Figure 5. VEGFR-2 protein expression decreases with the passage of mSMECs. **(A)** Representative immunoblot for VEGFR-2 expression over passages 6 to 9 of mSMECs. α/β-Tubulin was used as the loading control. **(B)** One-way ANOVA for quantitative analysis. *, indicates significant differences P≤0.05; **, indicates significant differences P≤0.01. Data represented as means ± SEM (n=5 or 6 per group).

Figure 6 shows a representative experiment of 3 independent experiments performed. Western blot was first used to assess the impact of passaging of VEGFR-2 protein levels (**Figure 6A & B**). At the protein level, when comparing P9 to P7, we observed an 82% decrease when analysing the sum of all bands and 87%, 84% and 55% when analysing the bands detected at 250kDa, 230kDa and 150kDa, respectively. We then measured VEGFR-2 at the mRNA level **(Figure 6C)**, a significant decrease by 52% was observed (p=<0.0001).

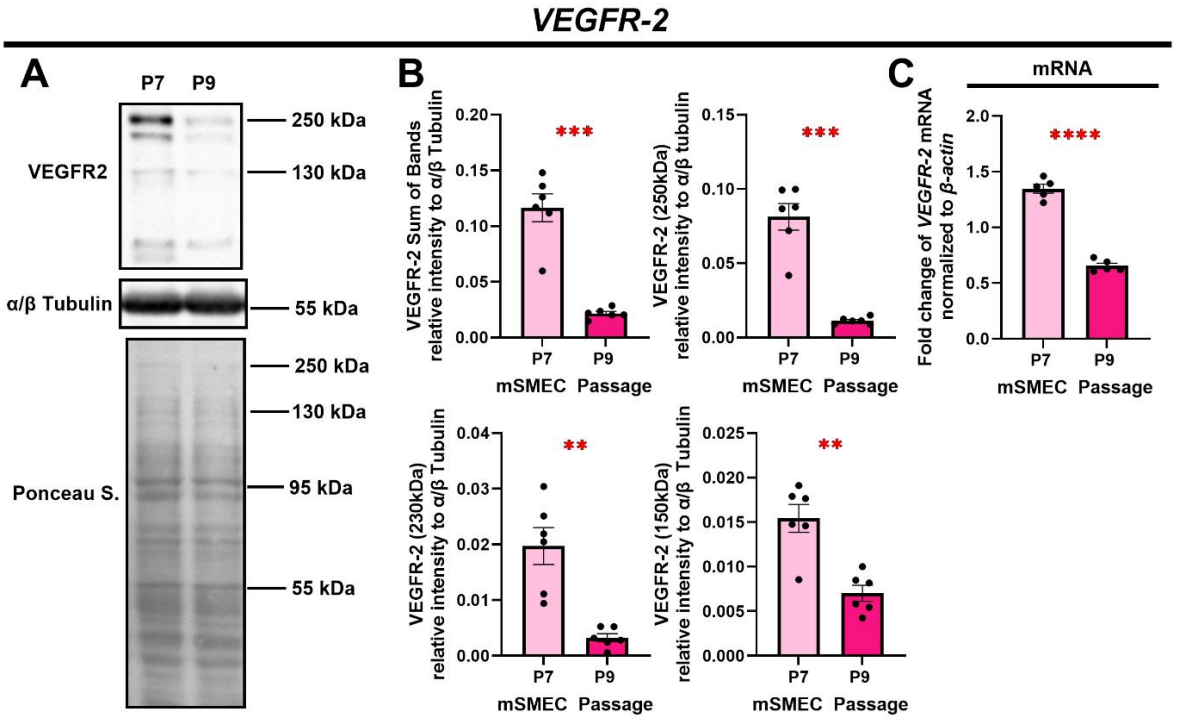
VEGFR-2
A
P7 P9
VEGFR2
250 kDa
130 kDa
α/β Tubulin
55 kDa
Ponceau S.
250 kDa
130 kDa
95 kDa
55 kDa
B
VEGFR-2 Sum of Bands relative intensity to α/β Tubulin
***
VEGFR-2 (250kDa) relative intensity to α/β tubulin
***
VEGFR-2 (230kDa) relative intensity to α/β Tubulin
**
VEGFR-2 (150kDa) relative intensity to α/β Tubulin
**
P7 P9
mSMEC Passage
C
mRNA
Fold change of VEGFR-2 mRNA normalized to β-actin
****
P7 P9
mSMEC Passage

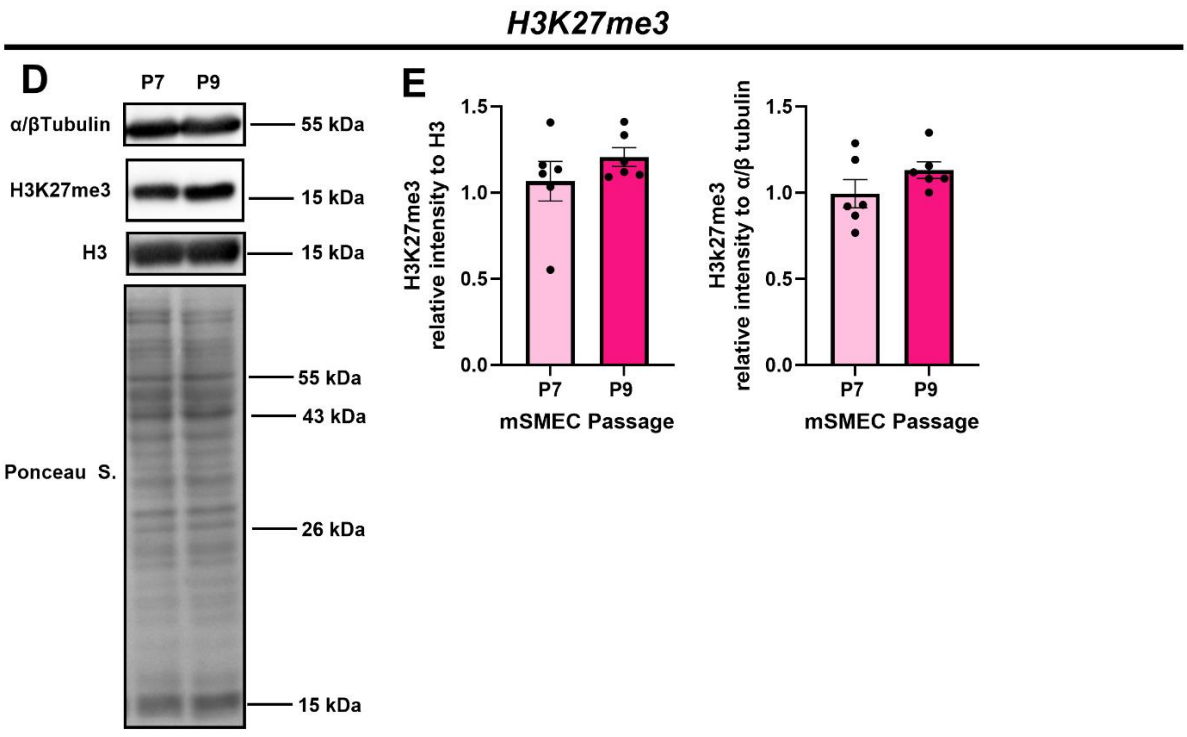
H3K27me3
D
P7 P9
α/βTubulin
55 kDa
H3K27me3
15 kDa
H3
15 kDa
Ponceau S.
55 kDa
43 kDa
26 kDa
15 kDa
E
H3K27me3 relative intensity to H3
H3k27me3 relative intensity to α/β tubulin
P7 P9
mSMEC Passage

Figure 6. Passaging results in a significant decrease in VEGFR-2 protein expression and slight increases in epigenetic mark* H3K27me^3. *mSMECs were cultivated until reaching passage 7 or 9. Protein (A, B, D and E) as well as mRNA (B). **(A)** Representative immunoblot forVEGFR-2 detected in mSMECs protein extracts. α/β-Tubulin was used as the loading control. Ponceau S. staining qualitative analysis confirm equal protein loading and efficient transfer. **(B)** shows quantification of relative intensity of VEGFR-2 relative to α/β-Tubulin, considering all bands detected (150 to 250 kDa) or separately at 250 kDa, 230 kDa and 150kDa **(C)** Level of VEGFR-2 mRNA. Data represented as means ± SEM (n=5/6 per group). **, indicates significant differences P≤0.01; ***indicates significant differences P≤0.001; ****, indicates significant differences P≤0.0001. **(D)** Representative immunoblot for H3K27me^3 global protein expression for passage 7 and passage 9 mSMECs. α/β-Tubulin was used as the loading control. Ponceau S. staining is used qualitatively to visually confirm equal protein loading. Welch's t-test for quantitative analysis was used to detect statistically significant differences. Data represented as means ± SEM (n=5/6 per group).

H3K27me^3 global protein expression increases minimally with the passaging of mSMECs

Next, we wanted to analyse whether passaging primary endothelial cells will change the overall abundance of the H3 silencing mark H3K27me^3. Overall minimal changes were observed when assessing H3K27me^3, as indicated by the ratio of H3K27me^3 to H3 and H3K27me^3 to α/β-Tubulin (**Figure 6D**). We observed a 22% and 23% increase when H3K27me^3 was corrected to H3 and α/β-Tubulin, respectively **(Figure 6E)**.

Senescence markers p16 and p21 are expressed at significantly lower levels in P9 mSMECs compared to P7 mSMECs

Next, we hypothesized that senescence was contributing to the loss of VEGFR-2 in P9 mSMECs compared to P7. We measured the mRNA levels of senescence markers p16 and p21 known as key regulators of the cell cycle promoting cell cycle arrest (Sacco et al., 2021). Contrary to our personal expectations, we observed a significant decrease in p16 **(Figure 7A)** and p21 **(Figure 7B)** in P9 mSMECs compared to P7. We observed a 45.5% ($p<0.0001$) and 44.7% ($p<0.0001$) decrease in p16 and p21 respectively. We went a step further to verify our findings using staining for β-galactosidase (**Figure 7C & D**). β-galactosidase cleaves β-galactose, which is known to accumulate in senescent cells, more particularly in lysosomes. Senescence-associated- β-galactosidase activity (SA-βGal) is one of the most common indicators of senescence (Valieva et al., 2022). We found no significant differences in SA-βGal staining intensity between P7 and P9 mSMECs. However, the staining results further support our mRNA findings of p16 and p21, with slightly lower levels at P9 than P7 **(Figure 7D).**

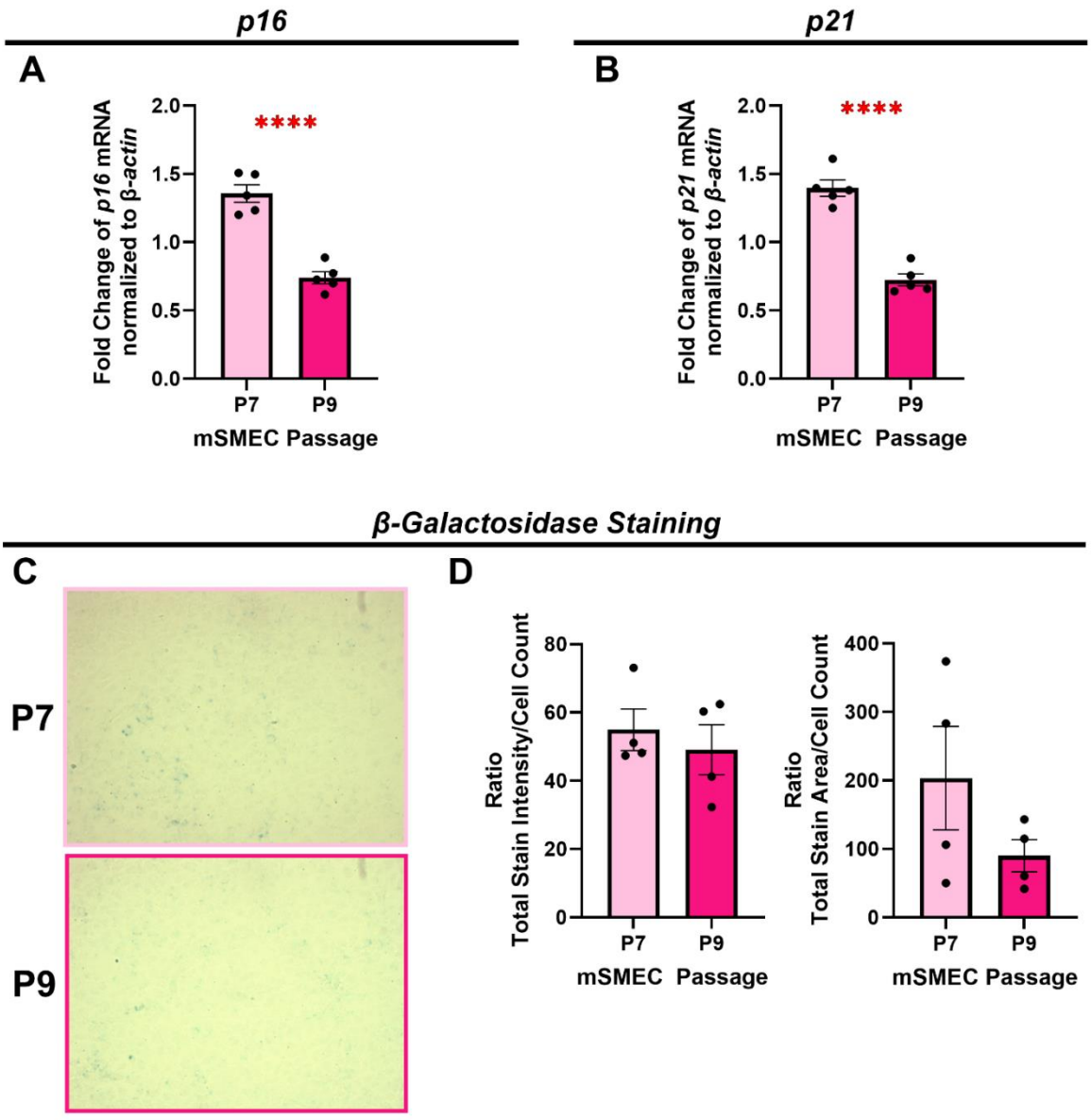

Figure 7. Passaging mSMECs (P7 to P9) does not increase markers of senescence, reduces cell cycle arrest capacity. Welch's t-test analysis of **(A)** p16 **(B)** p21. ****, indicates significant differences P≤0.0001. **(C)** Representative microscope images of β-Galactosidase staining of Passage 7 and 9 mSMECs. **(D)** Quantification of ratio of staining intensity to cell count. Welch's t-test for quantitative analysis was used to detect statistically significant differences. Data represented as means ± SEM (n=4 per group).

Comparing P7 and P8 mSMECs from older mice to P7 and P9 mSMECs from adult mice: Expression of VEGFR-2, H3K27me^3, p16, p21

Next, we wanted to compare how mSMECs isolated from old mice (Aged mSMECs) (representative of true physiological aging, 62 to 78 weeks-old) will respond to passaging compared to mSMECs isolated from normal adult mice. We know that passaging in cell culture has long been used as a model of ageing with some evidence of epigenetic changes observed in vitro closely mimicking in vivo findings in mouse models (Minteer et al., 2021). We observed however, Aged mSMECs at passage 7 and 8 express significantly increased levels of VEGFR-2 at both the protein (**Figure 8A & B**) and mRNA (**Figure 8C**) levels than P7 and P9 mSMECs isolated from adult mice. When comparing analysis of P7 mSMECs from adult versus older mice we observe an 78% increase in the sum of all bands and a 79%, 78% and 93% increase in the 250kDa, 230kDa and 150 kDa bands of VEGFR-2 respectively.

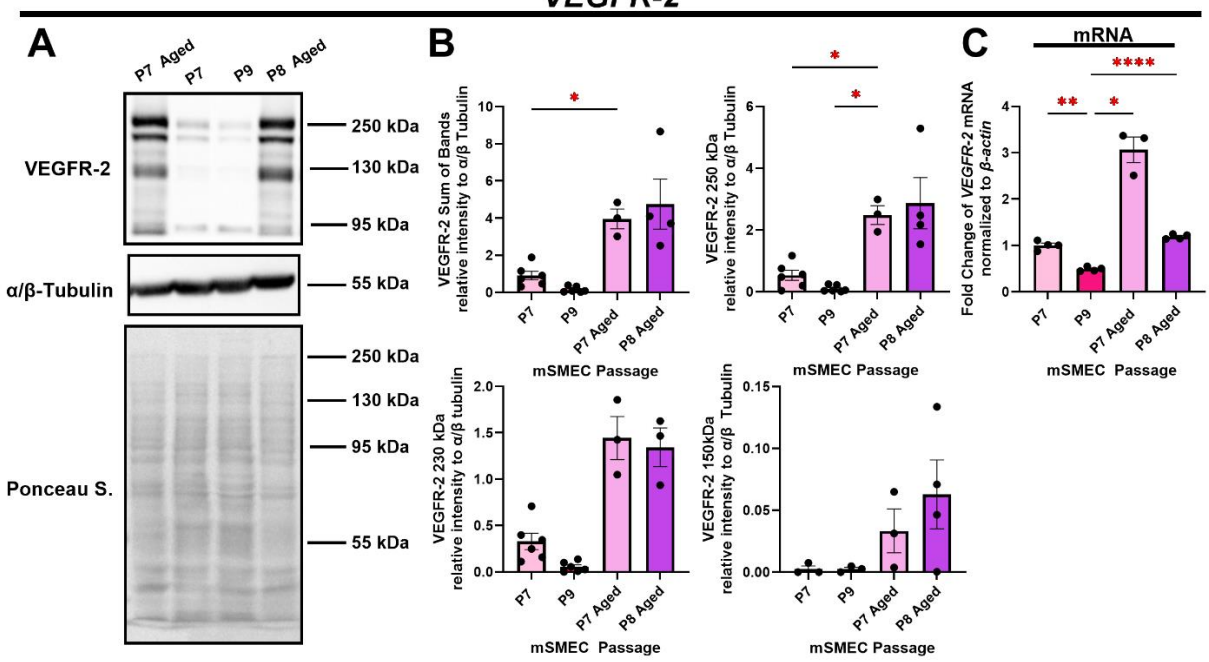
VEGFR-2
A
P7 Aged
P7
P9
P8 Aged
VEGFR-2
α/β-Tubulin
Ponceau S.
250 kDa
130 kDa
95 kDa
55 kDa
B
VEGFR-2 Sum of Bands relative intensity to α/β Tubulin
VEGFR-2 250 kDa relative intensity to α/β Tubulin
VEGFR-2 230 kDa relative intensity to α/β tubulin
VEGFR-2 150kDa relative intensity to α/β Tubulin
mSMEC Passage
C
mRNA
Fold Change of VEGFR-2 mRNA normalized to β-actin
mSMEC Passage

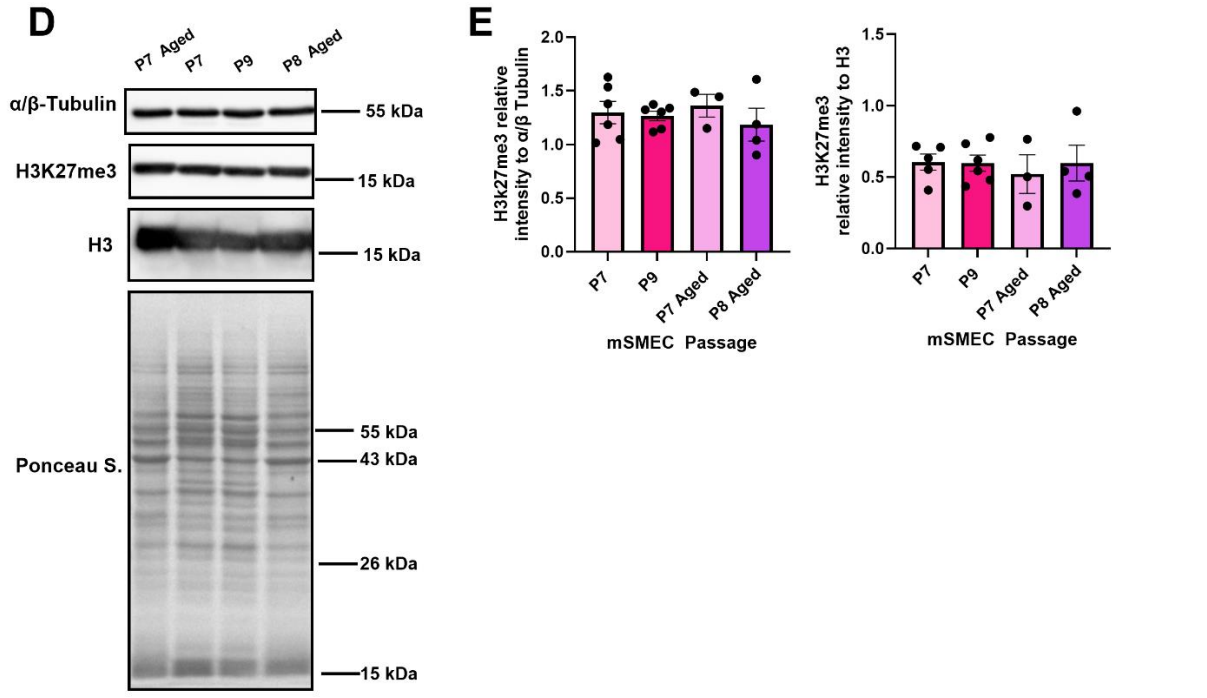
H3K27me3
D
P7 Aged
P7
P9
P8 Aged
α/β-Tubulin
H3K27me3
H3
Ponceau S.
55 kDa
15 kDa
43 kDa
26 kDa
E
H3k27me3 relative intensity to α/β Tubulin
H3K27me3 relative intensity to H3
mSMEC Passage

Figure 8. Changes in protein expression of VEGFR-2 and H3K27me^3 global protein expression observed with passaging not observed in aged mSMECs

A) Representative immunoblot for VEGFR-2 expression in P7 and P9 mSMECs and P7 and P8 aged mSMECs. α/β Tubulin was used as the loading control. Ponceau S. staining is used qualitatively to visually confirm equal protein loading. One-way ANOVA used to quantitative analysis. **B)** VEGFR-2 bands 1-3 (150-250 kDa), **C)** VEGFR-2 mRNA. Data represented as means ± SEM (n =5/6 per group). *, indicates significant differences P≤0.05; ***indicates significant differences P≤0.001; ****, indicates significant differences P≤0.0001. **D)** Representative immunoblot for H3K27me^3 global protein expression of passage 7 and 9 mSMECs and 7 and 8 Aged mSMECs. α/β-Tubulin was used as the loading control. Ponceau S. staining is used qualitatively to visually confirm equal protein loading. **E)** One-way ANOVA for quantitative analysis of H3K27me^3 global protein expression**.** Data represented as means ± SEM (n=5/6 per group).

We observed greater expression of senescence markers in P7 and P8 mSMECs from older mice compared to P7 and P9 mSMECs from adult mice **(Figure 9)**. Comparing P7 mSMECs from adult and older mice we observe a 33% and 54% increase in p16 and p21 respectively. Comparing P7 mSMECs from adult and P8 mSMECs from older mice we observe a 48% and 49% increase in p16 and p21 respectively. We found no significant differences in the global abundance of H3K27me^3 corrected to H3 or α/β-Tubulin **(Figure 8D & E)**.

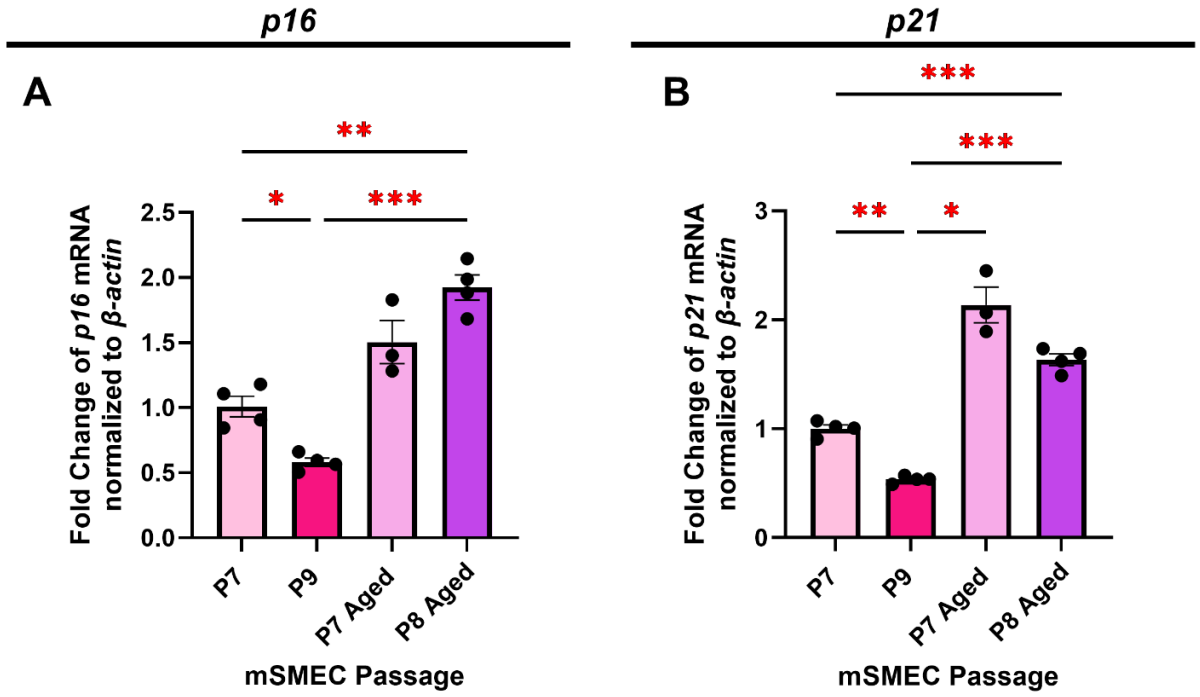

Figure 9. Greater expression of senescence markers p16 & p21 mRNA observed in aged mSMECs compared to mSMECs

One-way ANOVA analysis for **(A)** p16 and **(B)** p21 mRNA in P7 and P9 mSMECs and P7 and P8 Aged mSMECs. Data represented as means ± SEM (n=3/4 per group). *, indicates significant differences P≤0.05; **, indicates significant differences P≤0.01; ***indicates significant differences P≤0.001.

Differences in VEGF-A responsiveness in P7 and P9 mSMECs: Effect of short-term EZH2 inhibition

After concluding that both ageing and senescence are not contributing greatly to the loss of VEGFR-2 in P9 mSMECs, we decided to focus more directly on the role of epigenetic pathways, specifically EZH2. We treated both P7 and P9 mSMECs with EZH2 inhibitor GSK343 for 2 hours followed by VEGF-A stimulation for 30 minutes (**Figure 10A)**. We observed responsiveness to VEGF-A indicated by the fold change of *Egr3* at the mRNA level (**Figure 10B-D**). We found that P7 mSMECs showed a greater response to VEGF-A than P9 mSMECs. P7 mSMECs had an 85% greater fold-change ($P \leq 0.0001$) in *Egr3* than P9 mSMECs **(Figure 10D).** However, when VEGF-A stimulation was combined with short-term EZH2 inhibition P9 mSMECs showed an 48% increase **(Figure 10C)** while P7 mSMECs showed a 57% decrease ($P \leq 0.0001$) **(Figure 10B)** in their *Egr3* response compared to their respective VEGF-A only groups. Our interest was piqued by the difference that short-term EZH2 inhibition (2 hours) made. We know from previous studies that Egr3 is known to be bivalently marked and EZH2 is known to regulate this marking (Kanki et al. 2022; Chen et al. 2020). The study conducted by Chen and colleagues in 2020 showed that EZH2 may be necessary for regulating VEGF-A responsiveness for its role in identifying bivalent regions and causing RNAII pausing. With all this background knowledge in mind, in combination with our findings we decided to probe for Nr4a3, another gene known to be bivalently marked. We observed that again, P7 mSMECs have a greater response to VEGF-A than P9 mSMECs ($P \leq 0.0001$). However, with GSK343 alone we observe a 70% ($P \leq 0.0001$) and 33%($P \leq 0.05$) increase in the Nr4a3 response in both P7 and P9 mSMECs compared to their respective controls **(Figure 10E & F)**. Also, when VEGF-A stimulation was combined with short-term EZH2 inhibition we observe a 32% ($P \leq 0.001$) and 49% ($P \leq 0.001$) increase in the *Nr4a3* response to

VEGF-A stimulation P7 and P9 mSMECs compared to their respective VEGF-A only groups **(Figure 10E-G)**. Therefore, not only do we observe an increased *Nr4a3* response with VEGF-A stimulation alone but with short-term EZH2 inhibition alone as well, and an even greater combination effect.

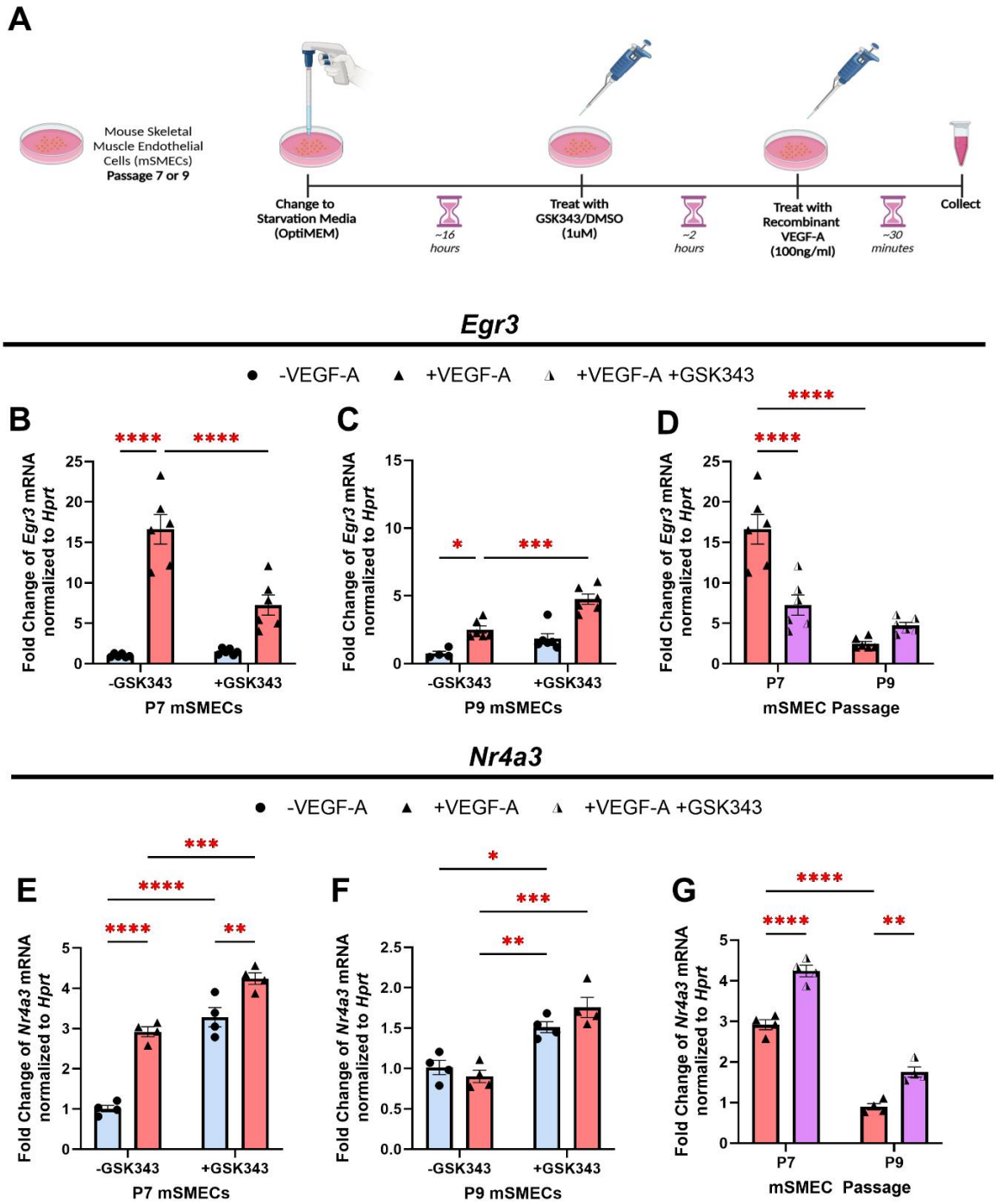
A
Mouse Skeletal Muscle Endothelial Cells (mSMECs) Passage 7 or 9
Change to Starvation Media (OptiMEM)
~16 hours
Treat with GSK343/DMSO (1uM)
~2 hours
Treat with Recombinant VEGF-A (100ng/ml)
~30 minutes
Collect
Egr3
-VEGF-A +VEGF-A +VEGF-A +GSK343
B
C
D
Fold Change of Egr3 mRNA normalized to Hprt
-GSK343 +GSK343
P7 mSMECs
P9 mSMECs
P7 P9
mSMEC Passage
Nr4a3
-VEGF-A +VEGF-A +VEGF-A +GSK343
E
F
G
Fold Change of Nr4a3 mRNA normalized to Hprt
-GSK343 +GSK343
P7 mSMECs
P9 mSMECs
P7 P9
mSMEC Passage

Figure 10. VEGF-A responsiveness of first-responder bivalent genes Egr3 & Nr4a3: Effect of short-term EZH2 inhibition. mSMECs at Passage 7 or 9 were starved for ~16hrs then treated with GSK343 (1μM, pre-treatment) for ~2 hrs followed by VEGF-A stimulation (100 ng/ml for 30 minutes). **A)** Visual representation of experimental plan. **B)** Representative qPCR analysis shows fold change of *Egr3* mRNA induced by VEGF-A stimulation with or without GSK343 inhibition in P7 mSMECs. **C)** Representative qPCR analysis shows fold change of *Egr3* mRNA induced by VEGF-A stimulation with or without GSK343 pre-treatment in P9 mSMECs. **D)** Comparison of the impact of GSK343 pre-treatment on *Egr3* mRNA in P7 and P9 mSMECs all treated with VEGF-A. Data were combined from B and C. **E)** Representative qPCR analysis shows fold change of *Nr4a3* mRNA in response to VEGF-A treatment with or without GSK343 pre-treatment in P7 mSMECs. **F)** Representative qPCR analysis shows fold change of *Nr4a3* mRNA in response to VEGF-A with or without GSG343 pre-treatment in P9 mSMECs. **G)** Comparison of the impact of GSK343 pre-treatment on *Nr4a3* mRNA in P7 and P9 mSMECs all treated with VEGF-A. Data were combined from ***E*** and ***F***. mSMECs were starved overnight (~16hrs) in optiMem. Cells were treated with GSK343 (1μM) or DMSO (1μM) for 2 hours followed by recombinant VEGF-A (100 ng/mL) for 30 minutes. B-G, Hprt was used as a loading control. 2-way ANOVA used for quantitative analyses. Data presented as means ± SEM (n=4/5 per group). *, indicates significant differences $P \leq 0.05$; ***indicates significant differences $P \leq 0.001$; ****, indicates significant differences $P \leq 0.0001$. Graphs show one representative experiment out of the 3 performed.

Effect of long-term (48 hours) EZH2 inhibition on VEGF-A responsiveness of mSMECs at P9

Lastly, our interests were piqued due to the enhancement in *Egr3* responsiveness observed in P9 mSMECs with short-term GSK343 treatment. Therefore, we were curious as to how long-term EZH2 inhibition might affect the EGR3 response. We treated P9 mSMECs with EZH2 inhibitor GSK343 for 48 hours and followed up with VEGF-A stimulation for 30 minutes (**Figure 11**). We found that with 48 hours of EZH2 inhibition we do not observe an increase in the *Egr3* response as with the 2-hour treatment but rather a 43% (P≤0.01) decrease in the *Egr3* response.

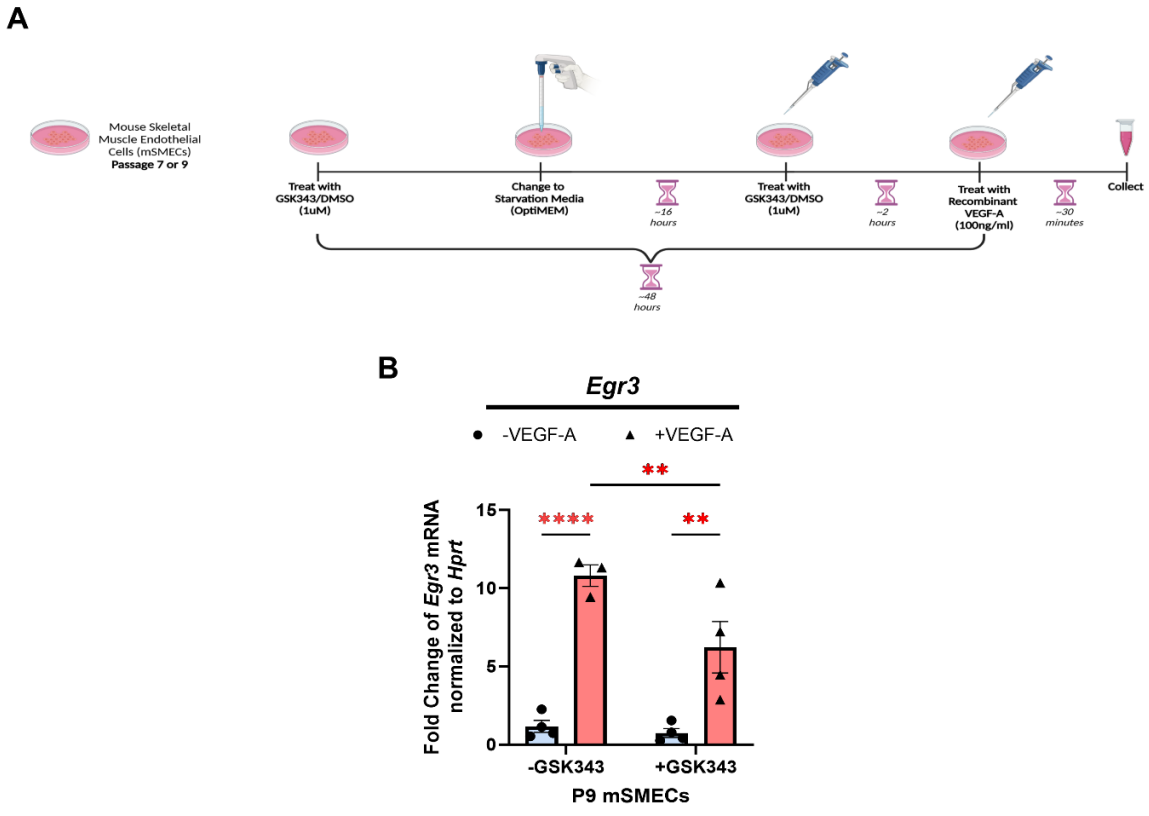

Figure 11. VEGF-A responsiveness of first-responder bivalent gene Egr3: Effect of long-term EZH2 inhibition

Effect of pre-treatment with GSK343 (1μM) for 48 hours followed by VEGF-A (100ng/ml) stimulation for 30 minutes. **A)** mSMECs at Passage 9 were treated with GSK343 (1μM) for ~33 hours, then starved for ~16 hours and treated with GSK343 (1μM) for ~2 hrs for a total treatment duration of 48 hours. GSK343 treatment was followed by VEGF-A stimulation for 30 minutes. **B)** Representative qPCR analysis shows fold change of *Egr3* mRNA in response to pre-stimulation treatment for 48 hours with GSK343 (1μM) followed by VEGF-A (100ng/ml) for 30 minutes of P9 mSMECs. P9 mSMECs were treated with GSK343 (1μM) or DMSO (1μM) for 48hrs followed by stimulation with recombinant VEGF-A (100ng/ml). P9 mSMECs were starved overnight (~16hrs) in optiMem (inclusive in the 48hrs). Cells were then treated with GSK343 (1μM) or DMSO (1μM) for 2 hours (inclusive of the 48hrs) followed by recombinant VEGF-A (100 ng/mL) for 30 minutes. Hprt was used as a loading control. 2-way ANOVA used for quantitative analyses. Data presented as means ± SEM (n=2 to 4 per group). **, indicates significant differences $P \leq 0.01$.

GSK343 treatment: Effect on global abundance of H3K27me^3

Because we observed the differences on the effect of GSK343 treatment on *Egr3* responsiveness to VEGF-A we decided verify for differences in the global abundance of H3K27me^3 after each GSK343 treatment duration. The H3K27me^3 protein data were conducted on 2 separate experiments and therefore to maintain the integrity of the data the 2 treatments cannot be compared directly but rather to the control of their respective experiments. We observed that after 48 hours of GSK343 treatment we observed a 90% decrease in the global abundance of H3K27me^3 compared to control (P≤0.05) **(Figure 12A & B)**. After 2 hours of GSK343 treatment we observed a 22% increase **(Figure 12D & E)** compared to control, which was not found to be statistically significant.

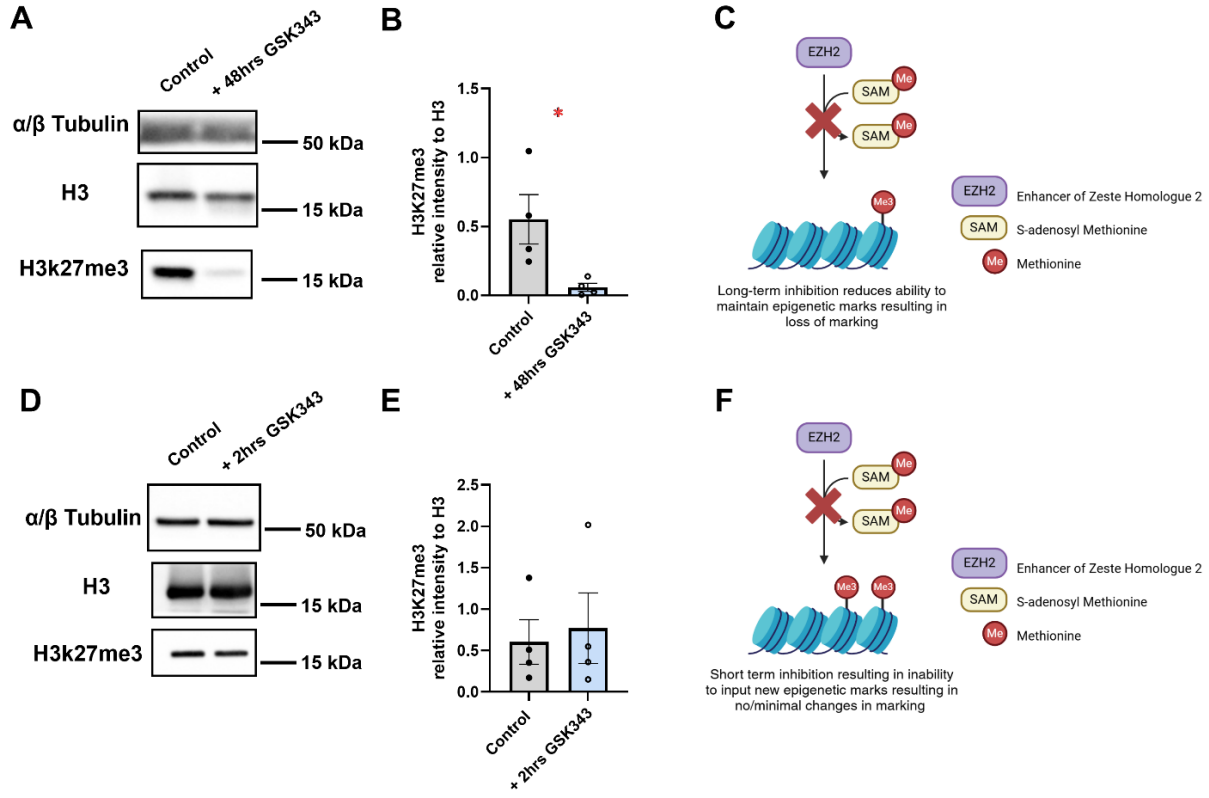

Figure 12: Impact of short-term (2 hours) and long-term (48 hours) EZH2 inhibition by GSK343 on global level of H3K27me³. **A)** Representative immunoblot for mSMECs treated with GSK343 (1μM) or DMSO (1μM) for 48 hours. **B)** Welch's t-test for quantitative analysis. Data represented at means ± SEM (n= 4 per group). *, indicates significant differences P≤0.05. **C)** Schematic representation of the impact of long-term GSK343 treatment on the global abundance of H3K27me³ marks (depletion of H3K27me³, loss of marking on facultative chromatin) **D)** Representative immunoblot for mSMECs were treated with GSK343 (1μM) for 2 hours. **E)** Welch's t-test for quantitative analysis. Data represented at means ± SEM (n= 4 per group). **F)** Schematic representation of the impact of 2 hours of GSK343 treatment on the global abundance of H3K27me³ marks (no change in H3K27me³ marks abundance not capable of gaining new marks).

Chromatin Immunoprecipitation: qPCR analysis of H3K27me3 bound to promoters of Egr3 and Kdr

We conducted chromatin immunoprecipitation for H3K27me³ on P7 and P9 mSMECs at the basal level, followed by qPCR of *Egr3* and *Kdr* (**Figure 13 B & C**). We observe that while there are slight elevations in fold-change relative to % input at P9, 36% for *Egr3* and 48% for *Kdr*, indicating that H3K27me³ was present more abundantly on the promoters of our genes of interest at P9, neither show any significant differences (Figure **13**).

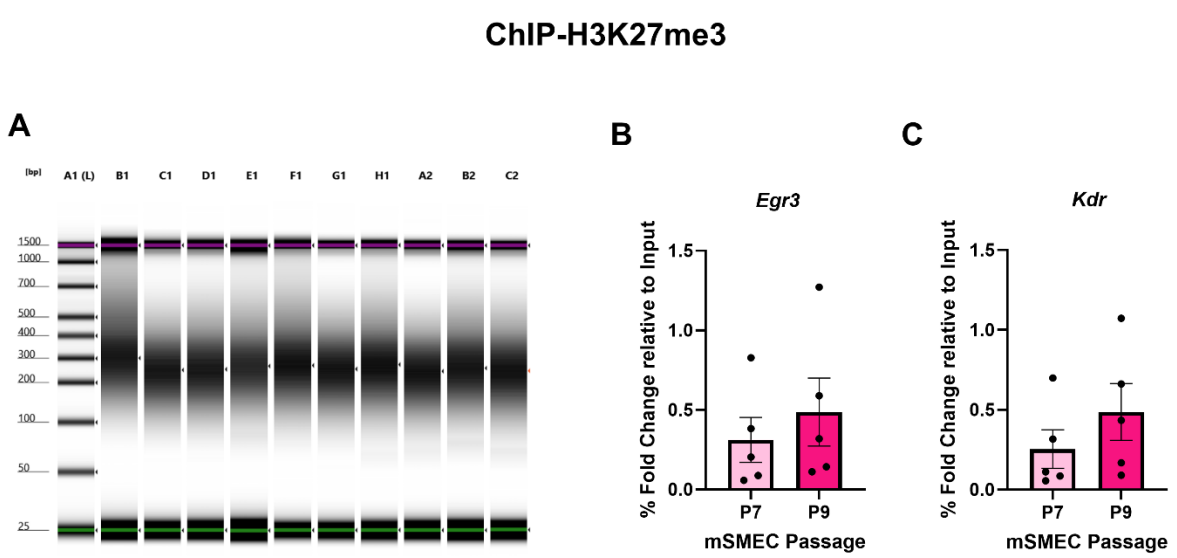

Lane	Sample Name	Peak bp	Average bp P7	Average bp P9
A1	Ladder	N/A	269.8	257
B1	mSMEC P7-1	302		
C1	mSMEC P7-2	252		
D1	mSMEC P7-3	255		
E1	mSMEC P7-4	269		
F1	mSMEC P7-5	271		
G1	mSMEC P9-1	256		
H1	mSMEC P9-2	274		
A2	mSMEC P9-3	247		
B2	mSMEC P9-4	260		
C2	mSMEC P9-5	248		

Figure 13. Slightly elevated levels of H3K27me^3 on promoters of both Egr3 and Kdr

A) Automated DNA gel electrophoresis (TapeStation 4200, Agilent Technologies) for chromatin extracts from P7 and P9 mSMECs with peak fragment sizes in base pairs (bp) with average bp listed by passage. These chromatin extracts were used to perform ChIP using an anti-H3K27me^3 antibody. Enrichment in H3K27me^3 marks on the promoter regions of *Egr3* **B**) and *Kdr* **C)** expressed as a fold of change to 5% INPUT. Welch's t-test assessed significant differences (n=5 per passage).

Discussion

The microvasculature of the skeletal muscle represents the vast majority of the vascular surface in mammalians (Wagenmakers et al., 2016). Alteration of the skeletal muscle microvasculature is a key factor in the loss of functionality in ageing individuals (Landers-Ramos & Prior, 2018). Yet, microvascular endothelial cells isolated from skeletal muscle are not the most used model to study loss of endothelial functions and angiogenic capacity. Indeed, HUVECs are most well-studied endothelial cells. There is a need for validating in-vitro models of skeletal muscle microvascular endothelial cells to study ageing. Our present work shows that passaging microvascular endothelial cells presents a significant limitation when aiming to study epigenetic processes known to be altered with ageing, such as mimicking senescence (Jothi & Kulka, 2024). Yet, passaging cells can replicate the reduction in VEGF-A signaling previously reported both in-vivo and in-vitro studies (Di et al., 2013; Ungvari et al., 2013).

Senescence, a common hallmark of ageing, was measured through mRNA levels of *p16* and *p21* and complimented by β-galactosidase staining. We observed that with passaging from P7 to P9 senescent markers *p16* and *p21* were significantly decreased. We also compared measures of *p16* and *p21* in mSMECs isolated from old mice (Aged mSMECs) to P7 and P9 mSMECs. Aged mSMECs expressed significantly higher levels of both *p16* and *p21* compared to P7 and P9 mSMECs, supporting senescence as a key characteristic of vascular ageing which is further supported by several studies (Avelar et al., 2020; Valieva et al., 2022; Minamino et al., 2002).

While it appears more appropriate to utilize cells isolated from old mice for studying age-related senescence, these cells have a low proliferation rate and cannot be expanded and maintained in culture long enough to yield sufficient sample size. Additionally, in attempting to grow both cell types in parallel for valid comparison, difficulties arose due to the difference in growth rates of the

cells isolated from young mice and old mice. One the other hand, passaging cells was very efficient in reducing the VEGF-A/VEGFR2 pathway sensitivity, as shown by the decrease in the *Egr3* response. Yet, this could also be an indication of de-differentiation, as VEGFR-2 is often used as a surface marker of primary endothelial cells (Kabrun et al., 1990). To be able to confirm this, more investigation will be required, by measuring others surface such as the Platelet endothelial cell adhesion molecule (PECAM) or the Von Willebrand Factor (VWF) (Goncharov et al., 2020). Despite not observing senescence, when passaging cells, we were able to have two distinct cell populations, one with low and one with high VEGFR-2 expression, representing a valuable model to clearly study VEGFR-2 and its downstream effectors in primary ECs.

In this work we report a significant decrease in VEGFR-2 at the mRNA level and at three different molecular weights at the protein level from passage 7 to 9. Directly after translation, VEGFR-2 protein has a molecular weight of 150 Kda (Lemieux et al., 2022; Takahashi & Shibuya, 1997) VEGFR-2 is highly glycosylated on its extracellular domain, shifting the molecular weight from 150 to 230 kDa as glycosylations are gained during maturation (Chandler et al., 2019). Glycosylation stabilizes VEGFR-2 at the surface of the endothelial cells and enhances VEGF-A binding (Chuang et al., 2015; Nacev et al., 2011; Takahashi & Shibuya, 1997). All forms of VEGFR-2 proteins decreased similarly with passaging. Passaging also decreased mRNA level of *VEGFR-2.* While the cause of VEGFR-2 protein expression decreases remains unclear, our results clearly show that passaging mSMECs negatively influences the expression of a mature form of VEGFR-2. This led us to question whether this reduces the capacity of VEGF-A to induce gene expression. We chose to look at *Egr3* and *Nr4a3*, two genes known to be quick and strong responders to VEGF-A (Kanki et al., 2022). The fact that P9 mSMECs had a lower capacity to increase mRNA levels of both genes than P7 mSMECs supports our thinking.

We performed short-term (2 hours) and long-term (48 hours) inhibition of EZH2, a key component of the PRC2 complex, using GSK343 to determine if EZH2 is required to maintain VEGF-A responsiveness. In late passages, greater levels of bivalently marked genes *Egr3* and *Nr4a3*, were observed after VEGF-A stimulation when cells were pre-treated with GSK343 for 2 hours. Long term treatment resulted not in an enhanced *Egr3* response as observed with 2 hours inhibition but an attenuated response. This further supports that H3K27me^3 marking is necessary for VEGF-A responsiveness of bivalent genes as previously reported (Chen et al., 2020). As seen in **Figure 12**, 2 hours inhibition results in minimal to no changes in H3K27me^3 but both the *Egr3* and *Nr4a3* response was enhanced with this treatment. We postulate that 2 hours inhibition may be sufficient to impair the capacity of EZH2 activity during VEGF-A stimulation while 48 hours inhibition results in a loss of bivalent sites due to the complete loss of H3K27me^3.

We then performed long-term EZH2 inhibition for 48 hours, which as previously stated completely depleted the epigenome of H3K27me^3, one of the two histone marks found on bivalently labelled gene promoters. Further evidence that this is unique to bivalent genes is that *VEGFR-2*, which has never been reported to be bivalent was completely unaffected by both short-term and long-term EZH2 inhibition. Our findings further support the importance of EZH2 in controlling VEGF-A responsiveness of bivalent genes (J. Chen et al., 2020; Kanki et al., 2022).

It was interesting to observe that baseline increases in *Nr4a3* in P9 mSMECs with GSK343 treatment for 2 hours could support a pro-angiogenic phenotype. Due to its function as a nuclear receptor capable of shifting endothelial cell gene expression to support proliferation and migration (Goyal & Goyal, 2019). Surprisingly, the increase in the *Nr4a3* response with GSK343 treatment was observed even without VEGF-A stimulation increasing the basal level. This begs the question whether this is a normalization of the EC response or an alteration. As previously mentioned, 2

hours treatment with GSK343 enhanced the *Egr3* response but only when combined with VEGF-A stimulation. This transcription factor is also known to regulate angiogenesis positively also migration, proliferation and tube formation (Suehiro et al., 2010). Due to enhancement seen in the response of both *Nr4a3* and *Egr3* with GSK343 treatment at P9, when 250 kDa VEGFR-2 surface receptor is almost completely lost, indicates these genes may be regulated independently of VEGFR-2. Further investigations are required to uncover the path in which VEGF-A is regulating these bivalent genes without the presence of VEGFR-2.

Lastly, due to consistent enhancement of the VEGF-A response of bivalent genes *Egr3* and *Nr4a3* when cells are pre-treated with 2 hours of EZH2 inhibitor GSK343 combined with the preliminary evidence of increases in the global abundance of H3K27me^3 we decided to conduct Chromatin Immunoprecipitation of H3K27me^3 on the promoters of *Egr3* and *Kdr*. We hypothesized that H3K27me^3 levels were increased in P9 compared to P7 mSMECs and that H3K27me^3 marking would be more prevalent on *Egr3* than *Kdr* due to its status as a bivalent gene. We observed that that H3K27me^3 expression was slightly elevated in P9 mSMECs compared to P7 on both the promoters of both *Egr3* and *Kdr,* though these findings were not significant. Perhaps, at P9 the cells are still in the preliminary stages of de-differentiation and therefore it is too early for differences in bivalent marking to be present.

Through this project we demonstrate that epigenetic modulation can be used as an approach to preserve the angiogenic capacity of ECs *in-vitro,* by enhancing responsiveness to VEGF-A, which may prove valuable in research settings. Our results bring to question whether VEGF-A responsive angiogenic relevant bivalent genes may be regulated independently of VEGFR-2.

Limitations

We have not measured VEGFR-2 phosphorylation levels which is crucial to truly test the activity of VEGFR-2 receptors and determine the level of interaction with VEGF-A (Shibuya, 2011). We also cannot truly confirm the level of bivalency between passages or between *Egr3* and *Kdr* as bivalent and non-bivalent genes, respectively, with just the H3K27me^3 ChIP. We would need to conduct a ChIP (H3K27me^3) followed by a consecutive re-ChIP (H3K4me^3) to verify whether there is a true state of bivalency.

Conclusion

Muscle mass is vital to overall health, but it is often reduced in the older population. It has been suggested that loss of small blood vessels (i.e. capillaries) might precede reductions in muscle mass. Aging alters the capacity to form new capillaries from existing vasculature through angiogenesis, as endothelial cells respond less efficiently to proangiogenic stimuli. Epigenetics emerges as a new research area to uncover how an ageing phenotype is acquired. The tri-methylation of Histone 3 on lysine 27 ($H3K27me^3$) is an epigenetic mark established by EZH2. This epigenetic mark was recently reported to control the endothelial response to VEGF-A. By studying how EZH2 regulates the pro-angiogenic pathway formed by VEGF-A and VEGFR-2, we aimed to bring new knowledge to elucidating the epigenetic mechanisms that influence the response of SMECs to a pro-angiogenic stimulus, in the context of aging.

Passaging young cells led to losses of VEGFR-2 protein and mRNA, minimal gain in $H3K27me^3$ and decreases in the upregulation of *Egr3* mRNA after VEGF-A stimulation. 2 hours of GSK343 pre-treatment had no impact on *VEGFR-2* mRNA, increased *Nr4a3* mRNA and restored the capacity of VEGF-A to increase *Egr3* mRNA at passage 9. In aged cells, p16 and p21 mRNA were higher than in young cells, independently of passaging.

Passaging mSMECs fails to mimic senescence, decreases SMEC sensitivity to VEGF-A and reduces VEGFR-2, suggesting de-differentiation is taking place. With passaging, EZH2 activity might reduce angiogenic capacity by decreasing basal level of *Nr4a3* and impairing *Egr3* sensitivity to VEGF-A, independently of any impact on VEGFR-2.

Supplemental Data

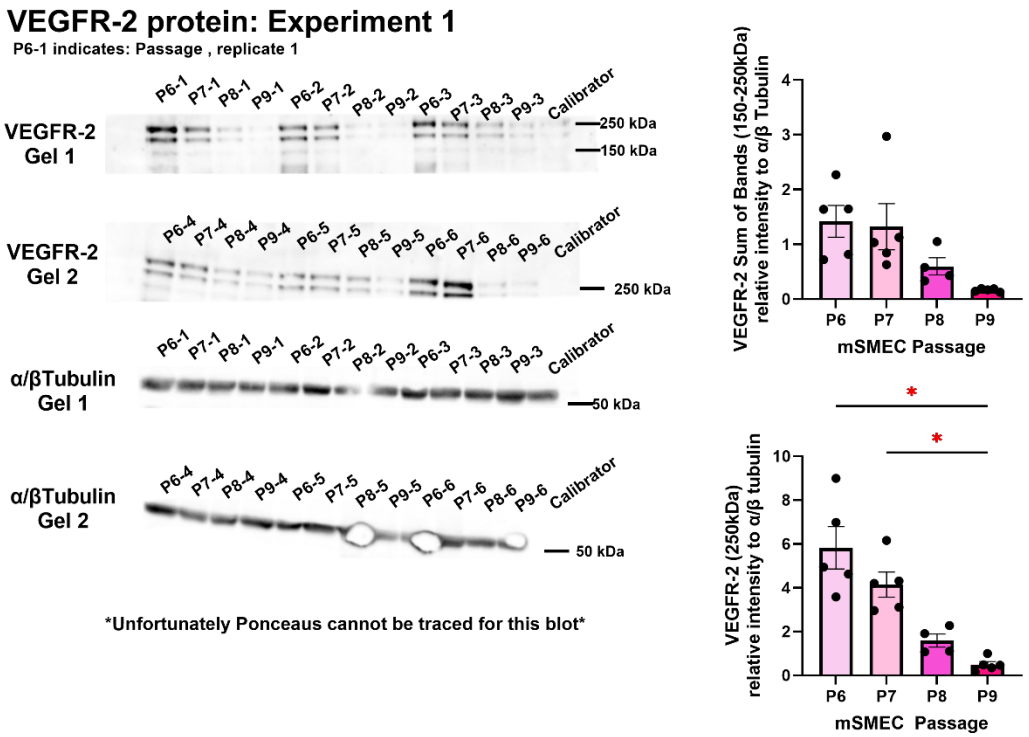

Supplemental Data-Figure 1: Initial western blot observing the effect of passaging on VEGFR-2 protein in mSMECs (corresponds to Figure 1)

Comprehensive immunoblot for VEGFR-2 expression of passages 6 to 9 mSMECs. α/β-Tubulin was used as the loading control. Ponceau S. staining is used qualitatively to visually confirm equal protein loading. Calibrator pool used for correction of individual gels. One-way ANOVA for quantitative analysis. VEGFR-2 bands 1-3 (150-250kDa). Data represented as means ± SEM (n=4/5 per group). *, indicates significant differences $P \leq 0.05$.

VEGFR-2 protein: Experiment 2

7C-1 indicates,Passage 7, replicate 1
G indicates 48hrs GSK treatment

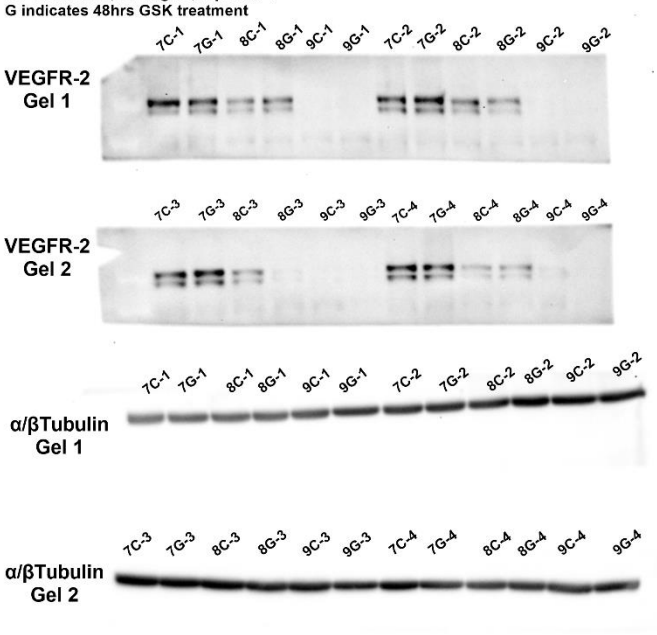

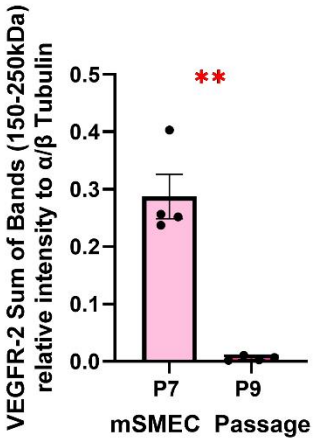

unfortunately cannot trace ponceaus for this blot

VEGFR-2 protein: Experiment 3

P7-1 indicates:Passage 7, replicate 1

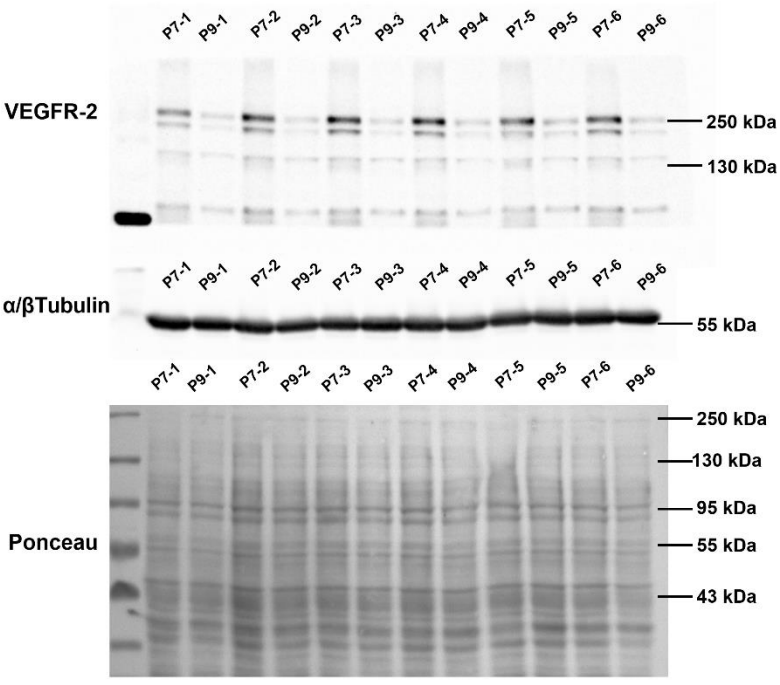

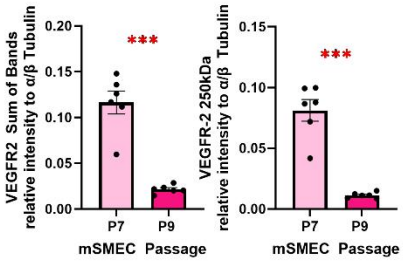

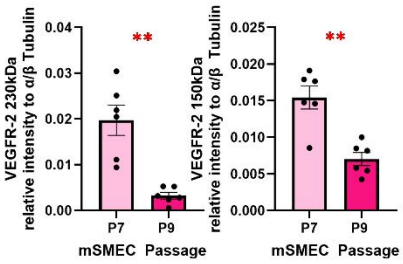

Supplemental Data-Figure 2: Additional western blots performed to compare VEGFR-2 protein levels across passages in mSMECs (P7 vs P9, experiment 2 and 3). Comprehensive immunoblots for VEGFR-2 expression of passages 7 to/and 9 mSMECs. α/β-Tubulin was used as the loading control. Ponceau S. staining is used qualitatively to visually confirm equal protein loading. Welch's t-test for quantitative analysis. VEGFR-2 bands 1-3 (150-250kDa). Data represented as means ± SEM (n=4/5 per group). **, indicates significant differences P≤0.01; ***indicates significant differences P≤0.001.

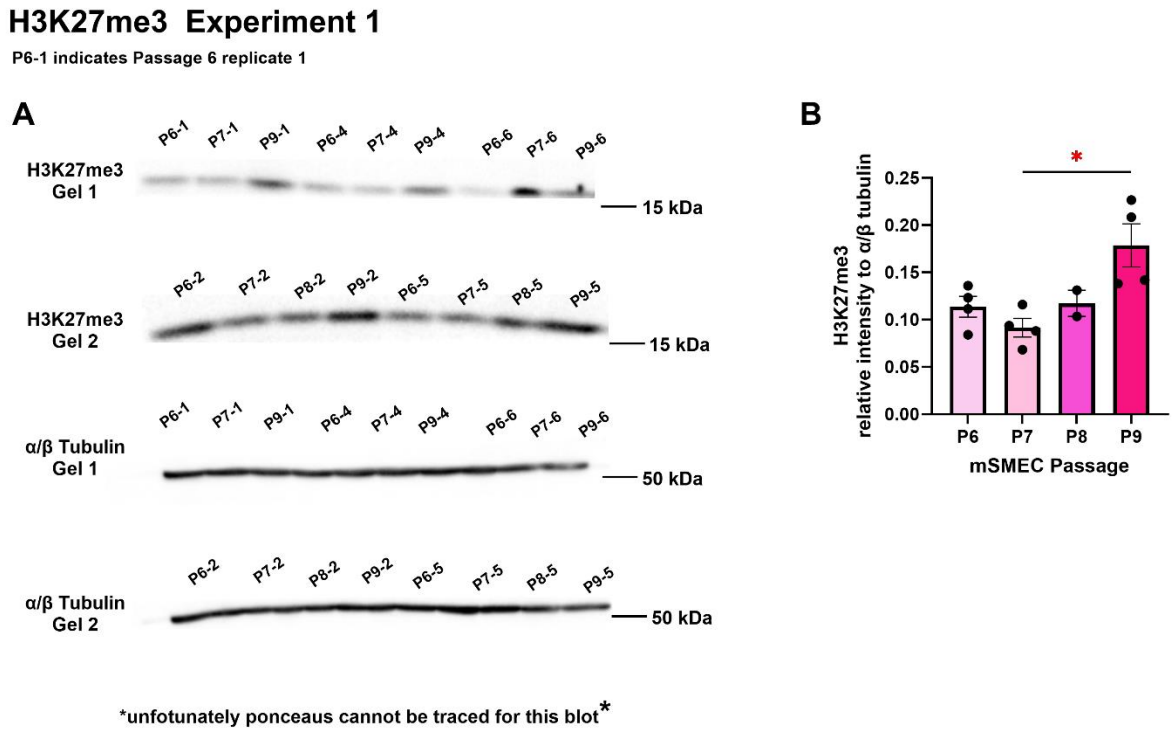

Supplemental Data-Figure 3: Initial western blot to observe effect of passaging on global abundance of H3K27me^3. **A)** Comprehensive immunoblot for H3K27me^3 expression of passages 6 to 9 mSMECs. α/β-Tubulin was used as the loading control. **B)** One-way ANOVA for quantitative analysis. Data represented as means ± SEM (n=2-4 per group). *, indicates significant differences P≤0.05;

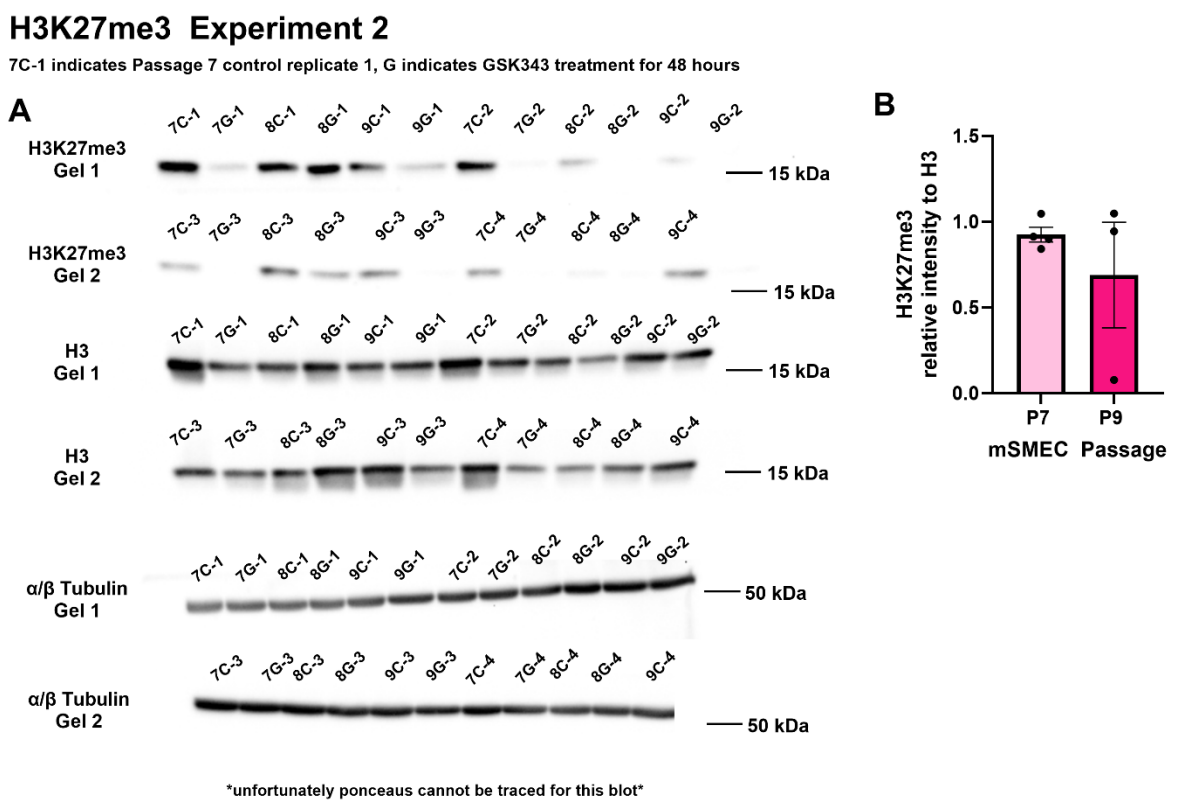

Supplemental Data-Figure 4: Second western blot conducted to compare global abundance of H3K27me^3 in P7 and P9 mSMECs. **A)** Comprehensive immunoblots for H3K27me^3 expression of passages 7 to 9 mSMECs. α/β-Tubulin was used as the loading control. **B)** Welch's t-test for quantitative analysis. Data represented as means ± SEM (n=3/4 per group).

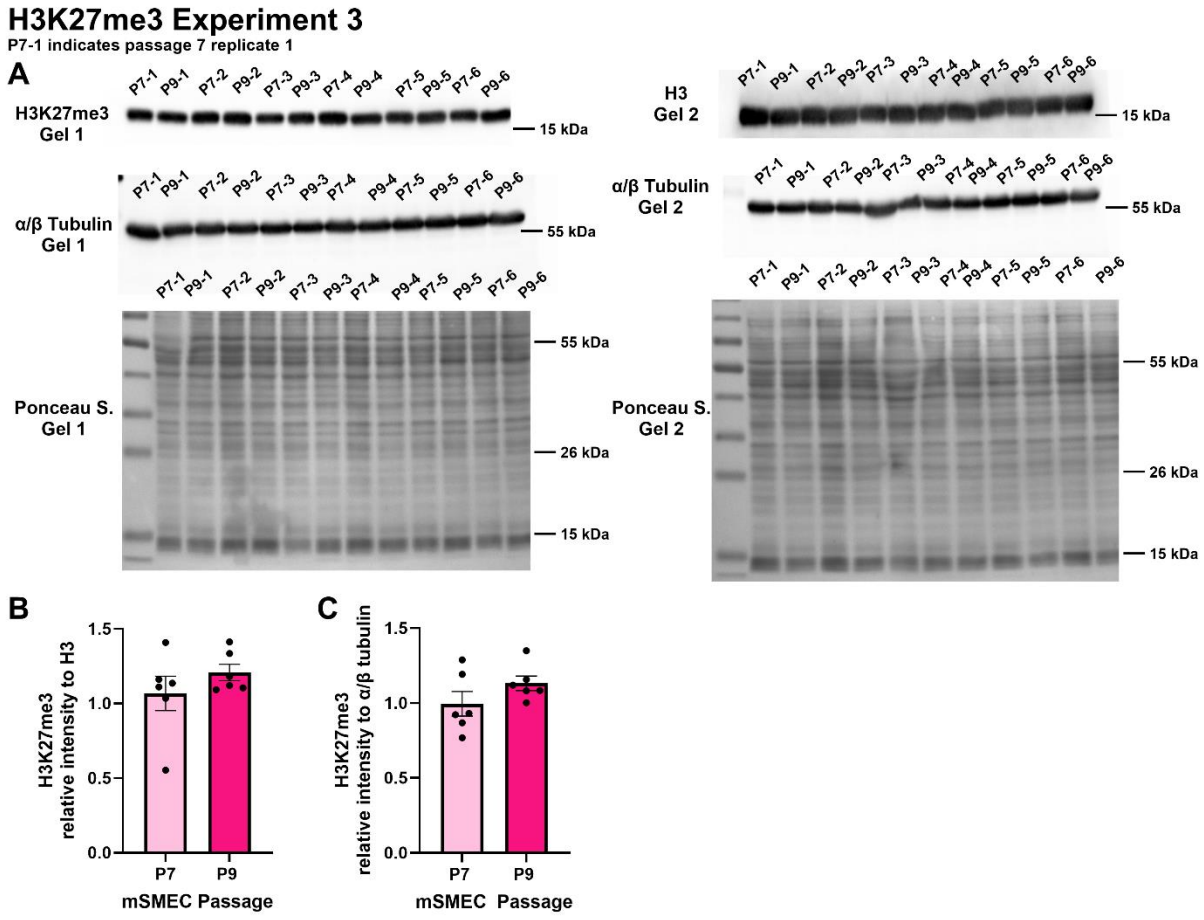

Supplemental Data-Figure 5: Third western blot conducted to compare global abundance of H3K27me3 in P7 and P9 mSMECs. **A)** Comprehensive immunoblots for H3K27me^3 expression of passages 7 and 9 mSMECs. α/β-Tubulin was used as the loading control. **B)** Welch's t-test for quantitative analysis of H3K27me3 relative to H3. **C)** Welch's t-test for quantitative analysis of H3K27me3 relative to α/β Tubulin. Data represented as means ± SEM (n=6 per group).

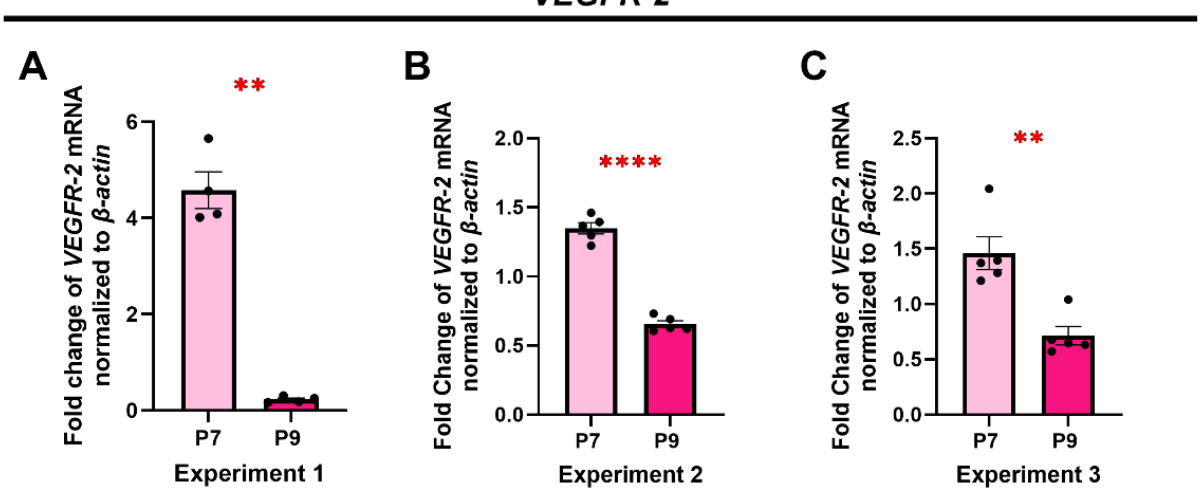

Supplemental Data-Figure 6: *VEGFR-2* (Kdr) mRNA in P7 vs P9 mSMECs, Experiment 1, 2, &3. All qPCR analyses performed to quantify *VEGFR-2* (Kdr) mRNA in SMECs at P7 and P9 showing results of all 3 experiments. Welch's t-test analysis of comparisons of P7 and P9 mSMECs **A)** Experiment 1, **B)** Experiment 2, **C)** Experiment 3. **, indicates significant differences P≤0.01 ****, indicates significant differences P≤0.0001. n=4/5 per passage.

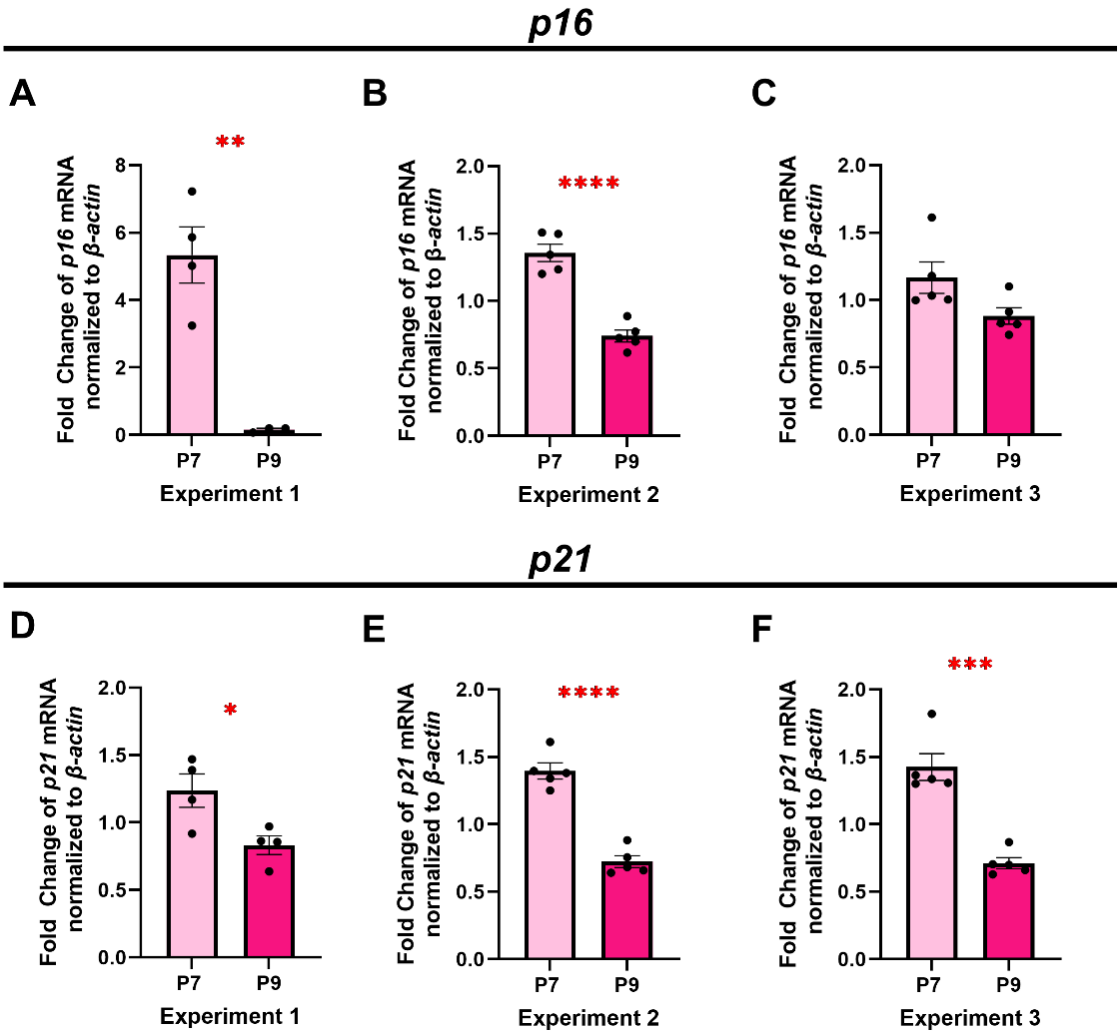

Supplemental Data-Figure 7: *p16* and *p21* mRNA in P7 vs P9 mSMECs, Experiment 1, 2, &3 All qPCR analyses performed to quantify *p16* and *p21* mRNA in SMECs at P7 and P9 showing results of all 3 experiments. Welch's t-test analysis of comparisons of P7 and P9 mSMECs **A)** *p16* Experiment 1 **B)** 2 **C)** 3 and **D)** *p21*Experiment 1, **E)** 2, **F)** 3. *, indicates significant differences P≤0.05; **, indicates significant differences P≤0.01; ***indicates significant differences P≤0.001; ****, indicates significant differences P≤0.0001. n= 4/5 per passage.

GSK343 2hrs Treatment: *Egr3*

P7 mSMECs

● -VEGF-A ▲ +VEGF-A

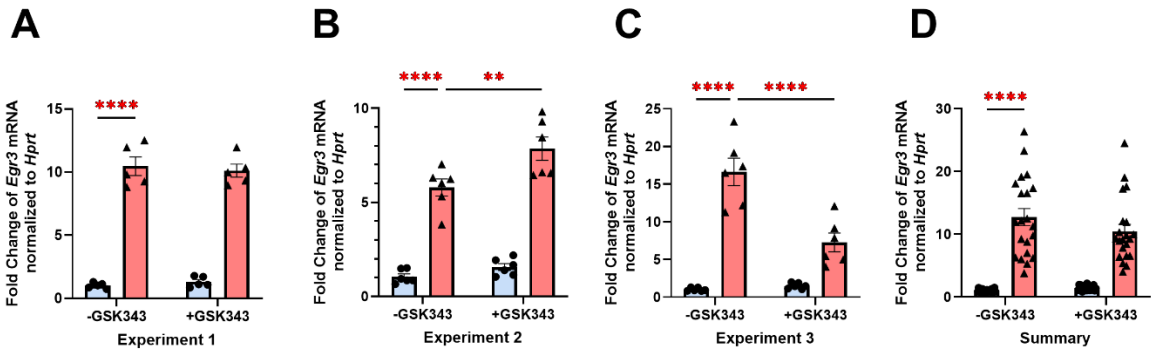

P9 mSMECs

● -VEGF-A ▲ +VEGF-A

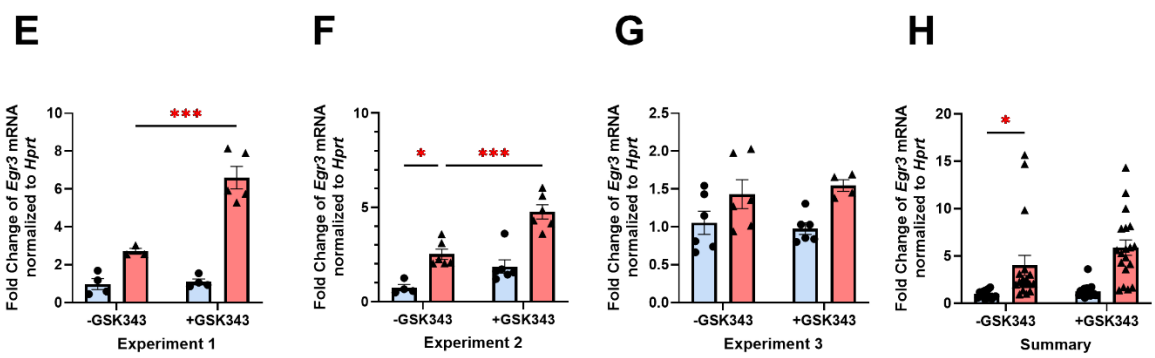

P7 vs P9 mSMECs

▲ +VEGF-A ◮ +VEGF-A +GSK343

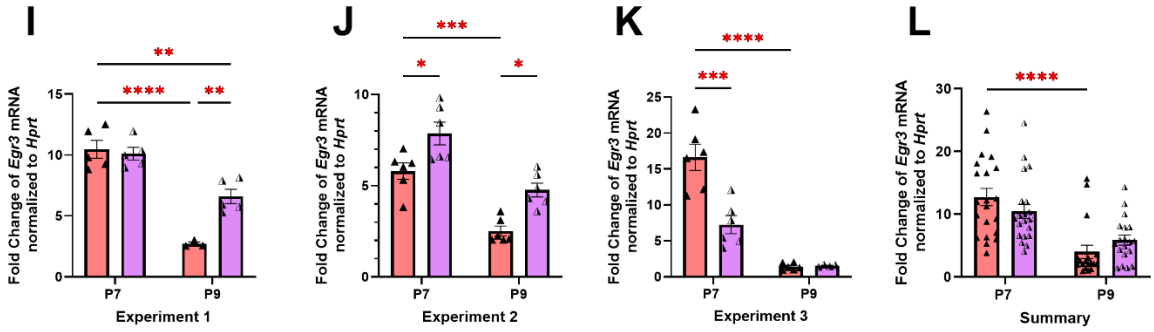

Supplemental Data-Figure 8: All qPCR analyses of the impact of short-term (2 hours) EZH2 inhibition by GSK343 on *Egr3* mRNA in response to VEGF-A stimulation. Experiment 1, 2 & 3. All qPCR analyses of the 3 experiments performed to assess the impact of short-term (2 hours) EZH2 inhibition by GSK343on *Egr3* mRNA in response to VEGF-A stimulation. Data shows results of individual experiments and summary/pooling of experiments. mSMECs at Passage 7 or 9 were starved for ~16hrs then treated with GSK343 (1μM, pre-treatment) for ~2 hrs followed by VEGF-A stimulation (100 ng/ml for 30 minutes). **A)** qPCR analysis shows fold change of *Egr3* mRNA in P7 mSMECs Experiment 1, **B)** 2, and **C)** 3 **D)** summary. **E)** qPCR analysis shows fold change of *Egr3* mRNA in P9 mSMECs Experiment 1, **F)** 2, and **G)** 3 **H)** summary. **I)** qPCR analysis shows fold change of *Egr3* mRNA comparing P7 and P9 mSMECs, VEGF-A alone and +GSK+VEGF treated groups only Experiment 1, **J)** 2, and **K)** 3 **L)** summary. Two-way ANOVAs used for quantitative analyses. *, indicates significant differences $P \leq 0.05$; **, indicates significant differences $P \leq 0.01$; ***indicates significant differences $P \leq 0.001$; ****, indicates significant differences $P \leq 0.0001$. n= 4-6 per group.

GSK343 2hrs Treatment: *Nr4a3*

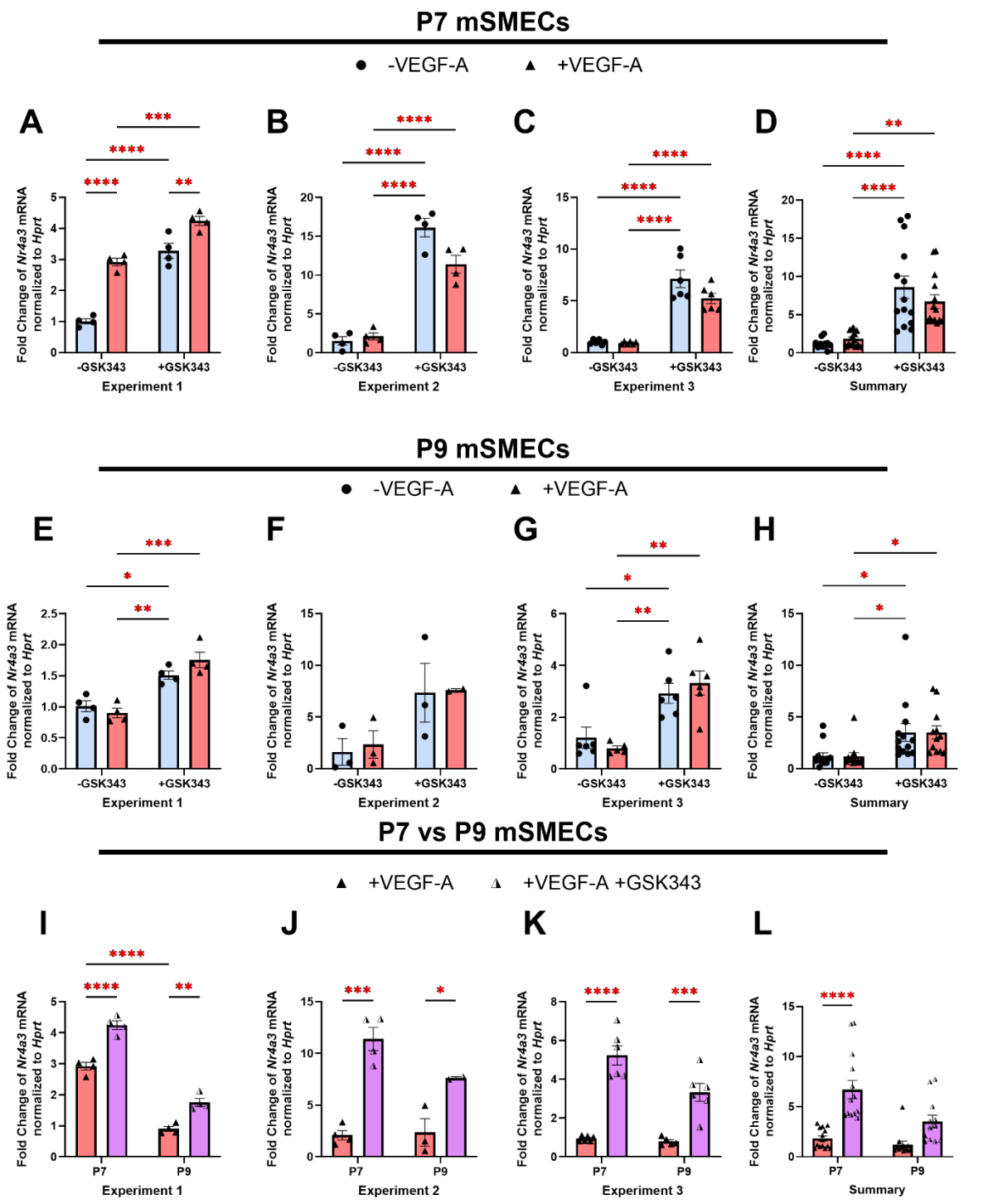

Supplemental Data-Figure 9: All qPCR analyses of the impact of short-term (2 hours) EZH2 inhibition by GSK343on *Nr4a3* mRNA in response to VEGF-A stimulation. Experiment 1, 2 & 3. All qPCR analyses of the 3 experiments performed to assess the impact of short-term (2 hours) EZH2 inhibition by GSK343on *Nr4a3* mRNA in response to VEGF-A stimulation. Data shows results of individual experiments and summary/pooling of experiments. mSMECs at Passage 7 or 9 were starved for ~16hrs then treated with GSK343 (1μM, pre-treatment) for ~2 hrs followed by VEGF-A stimulation (100 ng/ml for 30 minutes). **A)** qPCR analysis shows fold change of *Nr4a3* mRNA in P7 mSMECs Experiment 1, **B)** 2, and **C)** 3 **D)** summary. **E)** qPCR analysis shows fold change of *Nr4a3* mRNA in P9 mSMECs Experiment 1, **F)** 2, and **G)** 3 **H)** summary. **I)** qPCR analysis shows fold change of *Nr4a3* mRNA comparing P7 and P9 mSMECs, VEGF-A alone and +GSK+VEGF treated groups only Experiment 1, **J)** 2, and **K)** 3 **L)** summary. Two-way ANOVA used for quantitative analyses. *, indicates significant differences $P \leq 0.05$; **, indicates significant differences $P \leq 0.01$; ***indicates significant differences $P \leq 0.001$; ****, indicates significant differences $P \leq 0.0001$. n= 4-6 per group.

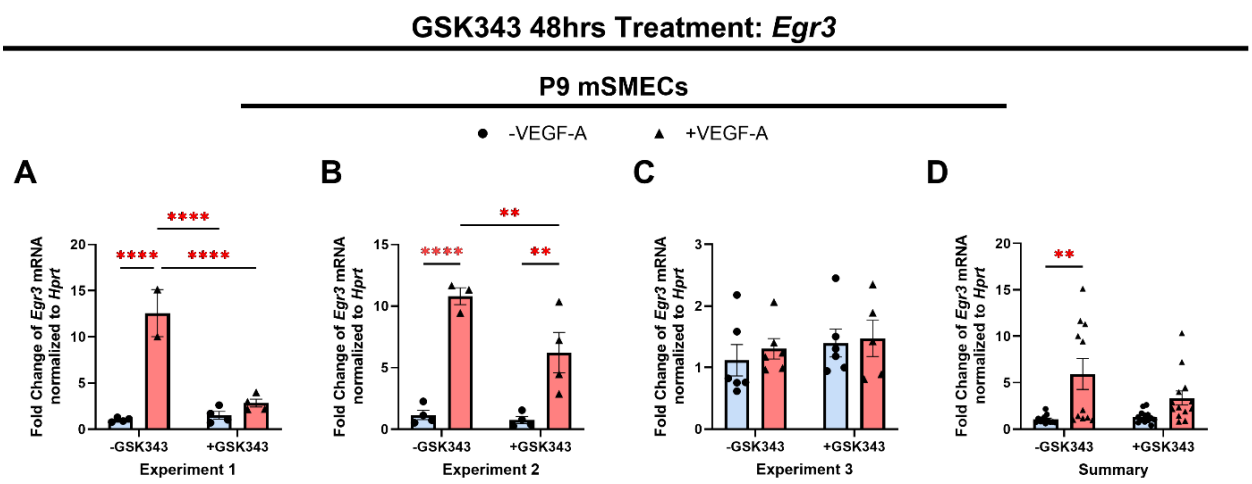

Supplemental Data-Figure 10: All qPCR analyses of the 3 experiments performed to assess the impact of long-term (48 hours) EZH2 inhibition by GSK343on *Egr3* mRNA in response to VEGF-A stimulation. Data shows results of individual experiments and summary/pooling of experiments. mSMECs at Passage 7 or 9 were starved for ~16hrs then treated with GSK343 (1μM, pre-treatment) for ~2 hrs followed by VEGF-A stimulation (100 ng/ml for 30 minutes). **A)** qPCR analysis shows fold change of *Egr3* mRNA in P7 mSMECs Experiment 1, **B)** 2, and **C)** 3 **D)** summary. Two-way ANOVA used for quantitative analyses. **, indicates significant differences P≤0.01; ****, indicates significant differences P≤0.0001. n= 2-5 per group.

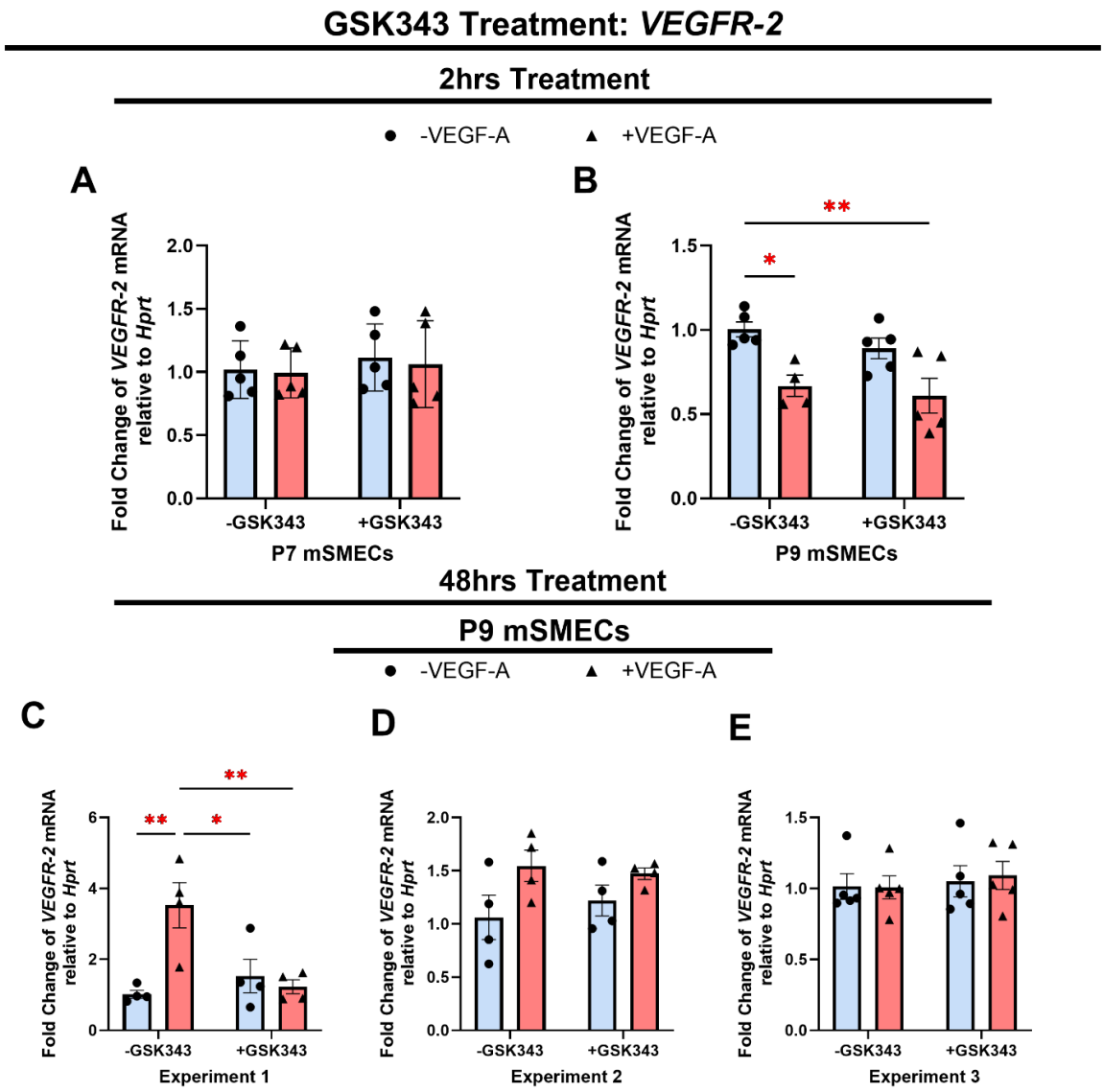
GSK343 Treatment: VEGFR-2
2hrs Treatment
-VEGF-A
+VEGF-A
A
Fold Change of VEGFR-2 mRNA relative to Hprt
-GSK343
+GSK343
P7 mSMECs
B
**
*
P9 mSMECs
48hrs Treatment
P9 mSMECs
C
D
E
Experiment 1
Experiment 2
Experiment 3

Supplemental Data-Figure 11: qPCR analyses of all experiments performed to assess the impact of short-term (2 hours) and long-term (48 hours) EZH2 inhibition by GSK343on *VEGFR-2* mRNA in response to VEGF-A stimulation. Data shows results of individual experiments. mSMECs at Passage 7 or 9 were starved for ~16hrs then treated with GSK343 (1μM, pre-treatment) for ~2 hrs or 48hrs followed by VEGF-A stimulation (100 ng/ml for 30 minutes). qPCR analysis shows fold change of *VEGFR-2* mRNA in **A)** P7 and **B)** P9 following VEGF stimulation with 2 hours of pre-treatment with GSK343. qPCR analysis shows fold change of *VEGFR-2* mRNA in P7 and P9 mSMECs following VEGF stimulation with 48hours of pre-treatment with GSK343 **C)** Experiment 1 **D)** 2, **E)** 3. Two-way ANOVA used for quantitative analyses. *, indicates significant differences $P \leq 0.05$; **, indicates significant differences $P \leq 0.01$. n= 4/5 per group.

Works Cited

Abe, M., & Sato, Y. (2001). cDNA microarray analysis of the gene expression profile of VEGF-activated human umbilical vien endothelial cells. *Angiogenesis*, *4*(4), 289–298. https://doi.org/10.1023/A:1016018617152

Adair, T. H., Gay, W. J., & Montani, J. P. (1990). Growth regulation of the vascular system: Evidence for a metabolic hypothesis. *American Journal of Physiology-Regulatory, Integrative and Comparative Physiology*, *259*(3), R393–R404. https://doi.org/10.1152/ajpregu.1990.259.3.R393

Adair, T. H., & Montani, J.-P. (2010). Overview of Angiogenesis. In *Angiogenesis*. Morgan & Claypool Life Sciences. https://www.ncbi.nlm.nih.gov/books/NBK53238/

Alegría-Torres, J. A., Baccarelli, A., & Bollati, V. (2011). Epigenetics and lifestyle. *Epigenomics*, *3*(3), 267–277. https://doi.org/10.2217/epi.11.22

Almohamad, M., Krall Kaye, E., Mofleh, D., & Spartano, N. L. (2022). The association of sedentary behaviour and physical activity with periodontal disease in NHANES 2011–2012. *Journal of Clinical Periodontology*, *49*(8), 758–767. https://doi.org/10.1111/jcpe.13669

Ameln, H., Gustafsson, T., Sundberg, C. J., Okamoto, K., Jansson, E., Poellinger, L., & Makino, Y. (2005). Physiological activation of hypoxia inducible factor-1 in human skeletal muscle. *The FASEB Journal*, *19*(8), 1009–1011. https://doi.org/10.1096/fj.04-2304fje

Andersen, P. (1975). Capillary Density in Skeletal Muscle of Man. *Acta Physiologica Scandinavica*, *95*(2), 203–205. https://doi.org/10.1111/j.1748-1716.1975.tb10043.x

Andersen, P., & Henriksson, J. (1977). Capillary supply of the quadriceps femoris muscle of man: Adaptive response to exercise. *The Journal of Physiology*, *270*(3), 677–690. https://doi.org/10.1113/jphysiol.1977.sp011975

Ang, S.-Y., Uebersohn, A., Spencer, C. I., Huang, Y., Lee, J.-E., Ge, K., & Bruneau, B. G. (2016). KMT2D regulates specific programs in heart development via histone H3 lysine 4 di-methylation. *Development*, *143*(5), 810–821. https://doi.org/10.1242/dev.132688

Angulo, J., El Assar, M., & Rodríguez-Mañas, L. (2016). Frailty and sarcopenia as the basis for the phenotypic manifestation of chronic diseases in older adults. *Molecular Aspects of Medicine*, *50*, 1–32. https://doi.org/10.1016/j.mam.2016.06.001

Arany, Z., Foo, S.-Y., Ma, Y., Ruas, J. L., Bommi-Reddy, A., Girnun, G., Cooper, M., Laznik, D., Chinsomboon, J., Rangwala, S. M., Baek, K. H., Rosenzweig, A., & Spiegelman, B. M. (2008). HIF-independent regulation of VEGF and angiogenesis by the transcriptional coactivator PGC-1α. *Nature*, *451*(7181), 1008–1012. https://doi.org/10.1038/nature06613

Arena, G., Riscal, R., Linares, L. K., & Le Cam, L. (2018). MDM2 controls gene expression independently of p53 in both normal and cancer cells. *Cell Death & Differentiation*, *25*(9), Article 9. https://doi.org/10.1038/s41418-018-0156-x

Avelar, R. A., Ortega, J. G., Tacutu, R., Tyler, E. J., Bennett, D., Binetti, P., Budovsky, A., Chatsirisupachai, K., Johnson, E., Murray, A., Shields, S., Tejada-Martinez, D., Thornton, D., Fraifeld, V. E., Bishop, C. L., & de Magalhães, J. P. (2020). A multidimensional systems biology analysis of cellular senescence in aging and disease. *Genome Biology*, *21*(1), 91. https://doi.org/10.1186/s13059-020-01990-9

Azuara, V., Perry, P., Sauer, S., Spivakov, M., Jørgensen, H. F., John, R. M., Gouti, M., Casanova, M., Warnes, G., Merkenschlager, M., & Fisher, A. G. (2006). Chromatin signatures of pluripotent cell lines. *Nature Cell Biology*, *8*(5), 532–538. https://doi.org/10.1038/ncb1403

Bannister, A. J., & Kouzarides, T. (2011). Regulation of chromatin by histone modifications. *Cell Research*, *21*(3), Article 3. https://doi.org/10.1038/cr.2011.22

Barnouin, Y., McPhee, J. S., Butler-Browne, G., Bosutti, A., De Vito, G., Jones, D. A., Narici, M., Behin, A., Hogrel, J.-Y., & Degens, H. (2017). Coupling between skeletal muscle fiber size and capillarization is maintained during healthy aging. *Journal of Cachexia, Sarcopenia and Muscle*, *8*(4), 647–659. https://doi.org/10.1002/jcsm.12194

Barrès, R., Yan, J., Egan, B., Treebak, J. T., Rasmussen, M., Fritz, T., Caidahl, K., Krook, A., O'Gorman, D. J., & Zierath, J. R. (2012). Acute Exercise Remodels Promoter Methylation in Human Skeletal Muscle. *Cell Metabolism*, *15*(3), 405–411. https://doi.org/10.1016/j.cmet.2012.01.001

Bernstein, B. E., Mikkelsen, T. S., Xie, X., Kamal, M., Huebert, D. J., Cuff, J., Fry, B., Meissner, A., Wernig, M., Plath, K., Jaenisch, R., Wagschal, A., Feil, R., Schreiber, S. L., & Lander, E. S. (2006). A bivalent chromatin structure marks key developmental genes in embryonic stem cells. *Cell*, *125*(2), 315–326. https://doi.org/10.1016/j.cell.2006.02.041

Bollati, V., Baccarelli, A., Sartori, S., Tarantini, L., Motta, V., Rota, F., & Costa, G. (2010). Epigenetic Effects of Shiftwork on Blood Dna Methylation. *Chronobiology International*, *27*(5), 1093–1104. https://doi.org/10.3109/07420528.2010.490065

Booth, L. N., & Brunet, A. (2016). The Aging Epigenome. *Molecular Cell*, *62*(5), 728–744. https://doi.org/10.1016/j.molcel.2016.05.013

Brookes, E., de Santiago, I., Hebenstreit, D., Morris, K. J., Carroll, T., Xie, S. Q., Stock, J. K., Heidemann, M., Eick, D., Nozaki, N., Kimura, H., Ragoussis, J., Teichmann, S. A., & Pombo, A. (2012). Polycomb Associates Genome-wide with a Specific RNA Polymerase II Variant, and Regulates Metabolic Genes in ESCs. *Cell Stem Cell*, *10*(2), 157–170. https://doi.org/10.1016/j.stem.2011.12.017

Burri, P. H., & Tarek, M. R. (1990). A novel mechanism of capillary growth in the rat pulmonary microcirculation. *The Anatomical Record*, *228*(1), 35–45. https://doi.org/10.1002/ar.1092280107

Canada, P. H. A. of. (2021, July 14). *Aging and chronic diseases: A profile of Canadian seniors* [Education and awareness]. https://www.canada.ca/en/public-health/services/publications/diseases-conditions/aging-chronic-diseases-profile-canadian-seniors-report.html

Canada, S. (2020, November 12). *Prevalence of Chronic Diseases and Risk Factors among Canadians aged 65 years and older* [Statistics].

https://www.canada.ca/en/services/health/publications/diseases-conditions/prevalence-chronic-disease-risk-factors-canadians-aged-65-years-older.html

Cencioni, C., Heid, J., Krepelova, A., Rasa, S. M. M., Kuenne, C., Guenther, S., Baumgart, M., Cellerino, A., Neri, F., Spallotta, F., & Gaetano, C. (2019). Aging Triggers H3K27 Trimethylation Hoarding in the Chromatin of Nothobranchius furzeri Skeletal Muscle. *Cells*, *8*(10), 1169. https://doi.org/10.3390/cells8101169

Chandler, K. B., Leon, D. R., Kuang, J., Meyer, R. D., Rahimi, N., & Costello, C. E. (2019). N-Glycosylation regulates ligand-dependent activation and signaling of vascular endothelial growth factor receptor 2 (VEGFR2). *The Journal of Biological Chemistry*, *294*(35), 13117–13130. https://doi.org/10.1074/jbc.RA119.008643

Chen, J., Fu, Y., Day, D. S., Sun, Y., Wang, S., Liang, X., Gu, F., Zhang, F., Stevens, S. M., Zhou, P., Li, K., Zhang, Y., Lin, R., Smith, L. E. H., Zhang, J., Sun, K., Melero-Martin, J. M., Han, Z., Park, P. J., … Pu, W. T. (2017). VEGF amplifies transcription through ETS1 acetylation to enable angiogenesis. *Nature Communications*, *8*(1), 383. https://doi.org/10.1038/s41467-017-00405-x

Chen, J., Liang, X., Zhang, S., Wang, S., Garcia, S. P., Yan, P., Yu, H., Li, Z., Liu, L., Zhang, F., Wei, W., Le, H., Zhang, Y., Yuan, G., Chen, S., Chen, Y., Sun, K., Pu, W. T., & Zhang, B. (2020). Two faces of bivalent domain regulate VEGFA responsiveness and angiogenesis. *Cell Death & Disease*, *11*(1), Article 1. https://doi.org/10.1038/s41419-020-2228-3

Chen, Y.-T., Zhu, F., Lin, W.-R., Ying, R.-B., Yang, Y.-P., & Zeng, L.-H. (2016). The novel EZH2 inhibitor, GSK126, suppresses cell migration and angiogenesis via down-regulating VEGF-A. *Cancer Chemotherapy and Pharmacology*, *77*(4), 757–765. https://doi.org/10.1007/s00280-016-2990-1

Chinsomboon, J., Ruas, J., Gupta, R. K., Thom, R., Shoag, J., Rowe, G. C., Sawada, N., Raghuram, S., & Arany, Z. (2009). The transcriptional coactivator PGC-1α mediates exercise-induced angiogenesis in skeletal muscle. *Proceedings of the National Academy of Sciences*, *106*(50), 21401–21406. https://doi.org/10.1073/pnas.0909131106

Chuang, I.-C., Yang, C.-M., Song, T.-Y., Yang, N.-C., & Hu, M.-L. (2015). The anti-angiogenic action of 2-deoxyglucose involves attenuation of VEGFR2 signaling and MMP-2 expression in HUVECs. *Life Sciences*, *139*(Complete), 52–61. https://doi.org/10.1016/j.lfs.2015.08.002

Cormie, P., Newton, R. U., Spry, N., Joseph, D., Taaffe, D. R., & Galvão, D. A. (2013). Safety and efficacy of resistance exercise in prostate cancer patients with bone metastases. *Prostate Cancer and Prostatic Diseases*, *16*(4), 328–335. https://doi.org/10.1038/pcan.2013.22

Cornelissen, V. A., Verheyden, B., Aubert, A. E., & Fagard, R. H. (2010). Effects of aerobic training intensity on resting, exercise and post-exercise blood pressure, heart rate and heart-rate variability. *Journal of Human Hypertension*, *24*(3), 175–182. https://doi.org/10.1038/jhh.2009.51

Correia de Sousa, M., Gjorgjieva, M., Dolicka, D., Sobolewski, C., & Foti, M. (2019). Deciphering miRNAs' Action through miRNA Editing. *International Journal of Molecular Sciences*, *20*(24), Article 24. https://doi.org/10.3390/ijms20246249

Cristofalo, V. J., & Pignolo, R. J. (1993). Replicative senescence of human fibroblast-like cells in culture. *Physiological Reviews*, *73*(3), 617–638. https://doi.org/10.1152/physrev.1993.73.3.617

Croley, A. N., Zwetsloot, K. A., Westerkamp, L. M., Ryan, N. A., Pendergast, A. M., Hickner, R. C., Pofahl, W. E., & Gavin, T. P. (2005). Lower capillarization, VEGF protein, and VEGF mRNA response to acute exercise in the vastus lateralis muscle of aged vs. Young women. *Journal of Applied Physiology (Bethesda, Md.: 1985)*, *99*(5), 1872–1879. https://doi.org/10.1152/japplphysiol.00498.2005

De Smet, F., Segura, I., De Bock, K., Hohensinner, P. J., & Carmeliet, P. (2009). Mechanisms of Vessel Branching. *Arteriosclerosis, Thrombosis, and Vascular Biology*, *29*(5), 639–649. https://doi.org/10.1161/ATVBAHA.109.185165

Di, Q., Cheng, Z., Kim, W., Liu, Z., Song, H., Li, X., Nan, Y., Wang, C., & Cheng, X. (2013). Impaired cross-activation of β3 integrin and VEGFR-2 on endothelial progenitor cells with aging decreases angiogenesis in response to hypoxia. *International Journal of Cardiology*, *168*(3), 2167–2176. https://doi.org/10.1016/j.ijcard.2013.01.240

Eelen, G., Treps, L., Li, X., & Carmeliet, P. (2020). Basic and Therapeutic Aspects of Angiogenesis Updated. *Circulation Research*, *127*(2), 310–329. https://doi.org/10.1161/CIRCRESAHA.120.316851

Endo, Y., Hwang, C. D., Zhang, Y., Olumi, S., Koh, D. J., Zhu, C., Neppl, R. L., Agarwal, S., & Sinha, I. (2023). VEGFA Promotes Skeletal Muscle Regeneration in Aging. *Advanced Biology*, *7*(10), 2200320. https://doi.org/10.1002/adbi.202200320

Frontera, W. R., & Ochala, J. (2015). Skeletal muscle: A brief review of structure and function. *Calcified Tissue International*, *96*(3), 183–195. https://doi.org/10.1007/s00223-014-9915-y

Fu, S.-P., He, S.-Y., Xu, B., Hu, C.-J., Lu, S.-F., Shen, W.-X., Huang, Y., Hong, H., Li, Q., Wang, N., Liu, X.-L., Liang, F., & Zhu, B.-M. (2014). Acupuncture Promotes Angiogenesis after Myocardial Ischemia through H3K9 Acetylation Regulation at VEGF Gene. *PLOS ONE*, *9*(4), e94604. https://doi.org/10.1371/journal.pone.0094604

Gavin, T. P., Ruster, R. S., Carrithers, J. A., Zwetsloot, K. A., Kraus, R. M., Evans, C. A., Knapp, D. J., Drew, J. L., McCartney, J. S., Garry, J. P., & Hickner, R. C. (2007). No difference in the skeletal muscle angiogenic response to aerobic exercise training between young and aged men. *The Journal of Physiology*, *585*(Pt 1), 231–239. https://doi.org/10.1113/jphysiol.2007.143198

Gavin, T. P., Spector, D. A., Wagner, H., Breen, E. C., & Wagner, P. D. (2000). Nitric oxide synthase inhibition attenuates the skeletal muscle VEGF mRNA response to exercise. *Journal of Applied Physiology*, *88*(4), 1192–1198. https://doi.org/10.1152/jappl.2000.88.4.1192

Georgiades, A., Sherwood, A., Gullette, E. C. D., Babyak, M. A., Hinderliter, A., Waugh, R., Tweedy, D., Craighead, L., Bloomer, R., & Blumenthal, J. A. (2000). Effects of Exercise and Weight Loss on Mental Stress–Induced Cardiovascular Responses in Individuals With High Blood Pressure. *Hypertension*, *36*(2), 171–176. https://doi.org/10.1161/01.HYP.36.2.171

Gianni-Barrera, R., Butschkau, A., Uccelli, A., Certelli, A., Valente, P., Bartolomeo, M., Groppa, E., Burger, M. G., Hlushchuk, R., Heberer, M., Schaefer, D. J., Gürke, L., Djonov, V., Vollmar, B., & Banfi, A. (2018). PDGF-BB regulates splitting angiogenesis in skeletal muscle by limiting

VEGF-induced endothelial proliferation. *Angiogenesis*, *21*(4), 883–900. https://doi.org/10.1007/s10456-018-9634-5

Gifre-Renom, L., Daems, M., Luttun, A., & Jones, E. A. V. (2022). Organ-Specific Endothelial Cell Differentiation and Impact of Microenvironmental Cues on Endothelial Heterogeneity. *International Journal of Molecular Sciences*, *23*(3), 1477. https://doi.org/10.3390/ijms23031477

Gladyshev, V. N., Kritchevsky, S. B., Clarke, S. G., Cuervo, A. M., Fiehn, O., de Magalhães, J. P., Mau, T., Maes, M., Moritz, R., Niedernhofer, L. J., Van Schaftingen, E., Tranah, G. J., Walsh, K., Yura, Y., Zhang, B., & Cummings, S. R. (2021). Molecular Damage in Aging. *Nature Aging*, *1*(12), 1096–1106. https://doi.org/10.1038/s43587-021-00150-3

Gliemann, L., Rytter, N., Yujia, L., Tamariz-Ellemann, A., Carter, H., & Hellsten, Y. (2021). A High Activity Level Is Required for Augmented Muscle Capillarization in Older Women. *Medicine & Science in Sports & Exercise*, *53*(5), 894. https://doi.org/10.1249/MSS.0000000000002566

Goncharov, N. V., Popova, P. I., Avdonin, P. P., Kudryavtsev, I. V., Serebryakova, M. K., Korf, E. A., & Avdonin, P. V. (2020). Markers of Endothelial Cells in Normal and Pathological Conditions. *Biochemistry (Moscow) Supplement. Series A, Membrane and Cell Biology*, *14*(3), 167–183. https://doi.org/10.1134/S1990747819030140

Gosain, A., & DiPietro, L. A. (2004). Aging and Wound Healing. *World Journal of Surgery*, *28*(3), 321–326. https://doi.org/10.1007/s00268-003-7397-6

Government of Canada, S. C. (2021, April 13). *Life expectancy and other elements of the complete life table, three-year estimates, Canada, all provinces except Prince Edward Island*. https://www150.statcan.gc.ca/t1/tbl1/en/tv.action?pid=1310011401

Goyal, D., & Goyal, R. (2019). Angiogenic Transformation in Human Brain Micro Endothelial Cells: Whole Genome DNA Methylation and Transcriptomic Analysis. *Frontiers in Physiology*, *10*, 1502. https://doi.org/10.3389/fphys.2019.01502

Haas, T. L., & Nwadozi, E. (2015). Regulation of skeletal muscle capillary growth in exercise and disease. *Applied Physiology, Nutrition, and Metabolism*, *40*(12), 1221–1232. https://doi.org/10.1139/apnm-2015-0336

Hawkins, R. D., Hon, G. C., Lee, L. K., Ngo, Q., Lister, R., Pelizzola, M., Edsall, L. E., Kuan, S., Luu, Y., Klugman, S., Antosiewicz-Bourget, J., Ye, Z., Espinoza, C., Agarwahl, S., Shen, L., Ruotti, V., Wang, W., Stewart, R., Thomson, J. A., … Ren, B. (2010). Distinct Epigenomic Landscapes of Pluripotent and Lineage-Committed Human Cells. *Cell Stem Cell*, *6*(5), 479–491. https://doi.org/10.1016/j.stem.2010.03.018

Hayflick, L. (1965). The limited in vitro lifetime of human diploid cell strains. *Experimental Cell Research*, *37*(3), 614–636. https://doi.org/10.1016/0014-4827(65)90211-9

Hellsten, Y., & Gliemann, L. (2024). Peripheral limitations for performance: Muscle capillarization. *Scandinavian Journal of Medicine & Science in Sports*, *34*(1), e14442. https://doi.org/10.1111/sms.14442

Henke, C. C., Cabri, J., Fricke, L., Pankow, W., Kandilakis, G., Feyer, P. C., & de Wit, M. (2014). Strength and endurance training in the treatment of lung cancer patients in stages IIIA/IIIB/IV. *Supportive Care in Cancer*, *22*(1), 95–101. https://doi.org/10.1007/s00520-013-1925-1

Høier, B., Olsen, K., Nyberg, M., Bangsbo, J., & Hellsten, Y. (2010). Contraction-induced secretion of VEGF from skeletal muscle cells is mediated by adenosine. *American Journal of Physiology-Heart and Circulatory Physiology*, *299*(3), H857–H862. https://doi.org/10.1152/ajpheart.00082.2010

Huo, Y.-B., Gao, X., Peng, Q., Nie, Q., & Bi, W. (2022). Dihydroartemisinin alleviates AngII-induced vascular smooth muscle cell proliferation and inflammatory response by blocking the FTO/NR4A3 axis. *Inflammation Research*, *71*(2), 243–253. https://doi.org/10.1007/s00011-021-01533-3

Hwang, C.-L., Yu, C.-J., Shih, J.-Y., Yang, P.-C., & Wu, Y.-T. (2012). Effects of exercise training on exercise capacity in patients with non-small cell lung cancer receiving targeted therapy. *Supportive Care in Cancer*, *20*(12), 3169–3177. https://doi.org/10.1007/s00520-012-1452-5

Jakobsson, L., Franco, C. A., Bentley, K., Collins, R. T., Ponsioen, B., Aspalter, I. M., Rosewell, I., Busse, M., Thurston, G., Medvinsky, A., Schulte-Merker, S., & Gerhardt, H. (2010). Endothelial cells dynamically compete for the tip cell position during angiogenic sprouting. *Nature Cell Biology*, *12*(10), 943–953. https://doi.org/10.1038/ncb2103

Jensen, L., Bangsbo, J., & Hellsten, Y. (2004). Effect of high intensity training on capillarization and presence of angiogenic factors in human skeletal muscle. *The Journal of Physiology*, *557*(Pt 2), 571. https://doi.org/10.1113/jphysiol.2003.057711

Jia, G., Aroor, A. R., Jia, C., & Sowers, J. R. (2019). Endothelial cell senescence in aging-related vascular dysfunction. *Biochimica et Biophysica Acta (BBA) - Molecular Basis of Disease*, *1865*(7), 1802–1809. https://doi.org/10.1016/j.bbadis.2018.08.008

Jothi, D., & Kulka, L. A. M. (2024). Strategies for modeling aging and age-related diseases. *Npj Aging*, *10*(1), 1–14. https://doi.org/10.1038/s41514-024-00161-5

Kabrun, N., Bühring, H.-J., Choi, K., Ullrich, A., Risau, W., & Keller, G. (1990). Flk-1 expression defines a population of early embryonic hematopoietic precursors. *Development*, *124*(10), 2039–2048. https://doi.org/10.1242/dev.124.10.2039

Kamba, T., Tam, B. Y. Y., Hashizume, H., Haskell, A., Sennino, B., Mancuso, M. R., Norberg, S. M., O'Brien, S. M., Davis, R. B., Gowen, L. C., Anderson, K. D., Thurston, G., Joho, S., Springer, M. L., Kuo, C. J., & McDonald, D. M. (2006). VEGF-dependent plasticity of fenestrated capillaries in the normal adult microvasculature. *American Journal of Physiology. Heart and Circulatory Physiology*, *290*(2), H560-576. https://doi.org/10.1152/ajpheart.00133.2005

Kanki, Y., Muramatsu, M., Miyamura, Y., Kikuchi, K., Higashijima, Y., Nakaki, R., Suehiro, J.-I., Sasaki, Y., Kubota, Y., Koseki, H., Morioka, H., Kodama, T., Nakao, M., Kurotaki, D., Aburatani, H., & Minami, T. (2022). Bivalent-histone-marked immediate-early gene regulation is vital for VEGF-

responsive angiogenesis. *Cell Reports*, *38*(6), 110332. https://doi.org/10.1016/j.celrep.2022.110332

Kanzleiter, T., Jähnert, M., Schulze, G., Selbig, J., Hallahan, N., Schwenk, R. W., & Schürmann, A. (2015). Exercise training alters DNA methylation patterns in genes related to muscle growth and differentiation in mice. *American Journal of Physiology-Endocrinology and Metabolism*, *308*(10), E912–E920. https://doi.org/10.1152/ajpendo.00289.2014

Kawano, F. (2021). Histone Modification: A Mechanism for Regulating Skeletal Muscle Characteristics and Adaptive Changes. *Applied Sciences*, *11*(9), Article 9. https://doi.org/10.3390/app11093905

Kerr, P., Tam, R., & Plane, F. (2011). Endothelium. In R. Fitridge & M. Thompson (Eds.), *Mechanisms of Vascular Disease: A Reference Book for Vascular Specialists*. University of Adelaide Press. http://www.ncbi.nlm.nih.gov/books/NBK534266/

Kitzman, D. W., Nicklas, B., Kraus, W. E., Lyles, M. F., Eggebeen, J., Morgan, T. M., & Haykowsky, M. (2014). Skeletal muscle abnormalities and exercise intolerance in older patients with heart failure and preserved ejection fraction. *American Journal of Physiology. Heart and Circulatory Physiology*, *306*(9), H1364-1370. https://doi.org/10.1152/ajpheart.00004.2014

Koeppel, M., Mathis, K., Schmitz, K. H., & Wiskemann, J. (2021). Muscle hypertrophy in cancer patients and survivors via strength training. A meta-analysis and meta-regression. *Critical Reviews in Oncology/Hematology*, *163*(Complete). https://doi.org/10.1016/j.critrevonc.2021.103371

Krüger-Genge, A., Blocki, A., Franke, R.-P., & Jung, F. (2019). Vascular Endothelial Cell Biology: An Update. *International Journal of Molecular Sciences*, *20*(18), 4411. https://doi.org/10.3390/ijms20184411

Krustrup, P., Randers, M. B., Andersen, L. J., Jackman, S. R., Bangsbo, J., & Hansen, P. R. (2013). Soccer Improves Fitness and Attenuates Cardiovascular Risk Factors in Hypertensive Men. *Medicine & Science in Sports & Exercise*, *45*(3), 553. https://doi.org/10.1249/MSS.0b013e3182777051

Kume, T. (2009). Novel insights into the differential functions of Notch ligands in vascular formation. *Journal of Angiogenesis Research*, *1*(1), 8. https://doi.org/10.1186/2040-2384-1-8

Landers-Ramos, R. Q., & Prior, S. J. (2018). The Microvasculature and Skeletal Muscle Health in Aging. *Exercise and Sport Sciences Reviews*, *46*(3), 172–179. https://doi.org/10.1249/JES.0000000000000151

Larionov, A., Hammer, C. M., Fiedler, K., & Filgueira, L. (2024). Dynamics of Endothelial Cell Diversity and Plasticity in Health and Disease. *Cells*, *13*(15), Article 15. https://doi.org/10.3390/cells13151276

Lear, S. A., Hu, W., Rangarajan, S., Gasevic, D., Leong, D., Iqbal, R., Casanova, A., Swaminathan, S., Anjana, R. M., Kumar, R., Rosengren, A., Wei, L., Yang, W., Chuangshi, W., Huaxing, L., Nair, S., Diaz, R., Swidon, H., Gupta, R., … Yusuf, S. (2017). The effect of physical activity on mortality and cardiovascular disease in 130 000 people from 17 high-income, middle-income, and low-income countries: The PURE study. *The Lancet*, *390*(10113), 2643–2654. https://doi.org/10.1016/S0140-6736(17)31634-3

Lee, S., Lee, J. W., & Lee, S.-K. (2012). UTX, a Histone H3-Lysine 27 Demethylase, Acts as a Critical Switch to Activate the Cardiac Developmental Program. *Developmental Cell*, *22*(1), 25–37. https://doi.org/10.1016/j.devcel.2011.11.009

Lemieux, P., Roudier, E., & Birot, O. (2022). Angiostatic freeze or angiogenic move? Acute cold stress prevents angiokine secretion from murine myotubes but primes primary endothelial cells for greater migratory capacity. *Frontiers in Physiology*, *13*, 975652. https://doi.org/10.3389/fphys.2022.975652

Li, R., Mi, X., Yang, S., Yang, Y., Zhang, S., Hui, R., Chen, Y., & Zhang, W. (2019). Long-term stimulation of angiotensin II induced endothelial senescence and dysfunction. *Experimental Gerontology*, *119*, 212–220. https://doi.org/10.1016/j.exger.2019.02.012

Lim, C., Shimizu, J., Kawano, F., Kim, H. J., & Kim, C. K. (2020). Adaptive responses of histone modifications to resistance exercise in human skeletal muscle. *PLOS ONE*, *15*(4), e0231321. https://doi.org/10.1371/journal.pone.0231321

Liu, H., Peng, L., So, J., Tsang, K. H., Chong, C. H., Mak, P. H. S., Chan, K. M., & Chan, S. Y. (2019). TSPYL2 Regulates the Expression of EZH2 Target Genes in Neurons. *Molecular Neurobiology*, *56*(4), 2640–2652. https://doi.org/10.1007/s12035-018-1238-y

Liu, L., Cheung, T. H., Charville, G. W., Hurgo, B. M. C., Leavitt, T., Shih, J., Brunet, A., & Rando, T. A. (2013). Chromatin Modifications as Determinants of Muscle Stem Cell Quiescence and Chronological Aging. *Cell Reports*, *4*(1), 189–204. https://doi.org/10.1016/j.celrep.2013.05.043

Liu, Y., Christensen, P. M., Hellsten, Y., & Gliemann, L. (2022). Effects of Exercise Training Intensity and Duration on Skeletal Muscle Capillarization in Healthy Subjects: A Meta-analysis. *Medicine & Science in Sports & Exercise*, *54*(10), 1714. https://doi.org/10.1249/MSS.0000000000002955

Lu, H., Yuan, P., Ma, X., Jiang, X., Liu, S., Ma, C., Philipsen, S., Zhang, Q., Yang, J., Xu, F., Zhang, C., Zhang, Y., & Zhang, W. (2023). Angiotensin-converting enzyme inhibitor promotes angiogenesis through Sp1/Sp3-mediated inhibition of notch signaling in male mice. *Nature Communications*, *14*(1), Article 1. https://doi.org/10.1038/s41467-023-36409-z

Lu, L., Li, L., Lü, X., Wu, X., Liu, D., & Liang, C. (2011). Inhibition of SIRT1 Increases EZH2 Protein Level and Enhances the Repression of EZH2 on Target Gene Expression. *Chinese Medical Sciences Journal*, *26*(2), 77–84. https://doi.org/10.1016/S1001-9294(11)60024-2

Maasar, M.-F., Turner, D. C., Gorski, P. P., Seaborne, R. A., Strauss, J. A., Shepherd, S. O., Cocks, M., Pillon, N. J., Zierath, J. R., Hulton, A. T., Drust, B., & Sharples, A. P. (2021). The Comparative Methylome and Transcriptome After Change of Direction Compared to Straight Line Running Exercise in Human Skeletal Muscle. *Frontiers in Physiology*, *12*, 619447. https://doi.org/10.3389/fphys.2021.619447

Maleszewska, M., Vanchin, B., Harmsen, M. C., & Krenning, G. (2016). The decrease in histone methyltransferase EZH2 in response to fluid shear stress alters endothelial gene expression and promotes quiescence. *Angiogenesis*, *19*, 9–24. https://doi.org/10.1007/s10456-015-9485-2

Margueron, R., & Reinberg, D. (2011). The Polycomb complex PRC2 and its mark in life. *Nature*, *469*(7330), 343–349. https://doi.org/10.1038/nature09784

Martínez-González, J., Cañes, L., Alonso, J., Ballester-Servera, C., Rodríguez-Sinovas, A., Corrales, I., & Rodríguez, C. (2021). NR4A3: A Key Nuclear Receptor in Vascular Biology, Cardiovascular Remodeling, and Beyond. *International Journal of Molecular Sciences*, *22*(21), 11371. https://doi.org/10.3390/ijms222111371

McGee, S. L., Fairlie, E., Garnham, A. P., & Hargreaves, M. (2009). Exercise-induced histone modifications in human skeletal muscle. *The Journal of Physiology*, *587*(24), 5951–5958. https://doi.org/10.1113/jphysiol.2009.181065

Melincovici, C. S., Bo, A. B., Mihu, C., Istrate, M., Moldovan, I.-M., Roman, A. L., & Mihu, C. M. (n.d.). *Vascular endothelial growth factor (VEGF) – key factor in normal and pathological angiogenesis*.

Merkwirth, C., Jovaisaite, V., Durieux, J., Matilainen, O., Jordan, S. D., Quiros, P. M., Steffen, K. K., Williams, E. G., Mouchiroud, L., Uhlein, S. N., Murillo, V., Wolff, S. C., Shaw, R. J., Auwerx, J., & Dillin, A. (2016). Two Conserved Histone Demethylases Regulate Mitochondrial Stress-Induced Longevity. *Cell*, *165*(5), 1209–1223. https://doi.org/10.1016/j.cell.2016.04.012

Minamino, T., Miyauchi, H., Yoshida, T., Ishida, Y., Yoshida, H., & Komuro, I. (2002). Endothelial Cell Senescence in Human Atherosclerosis. *Circulation*, *105*(13), 1541–1544. https://doi.org/10.1161/01.CIR.0000013836.85741.17

Minsky, N., & Oren, M. (2004). The RING Domain of Mdm2 Mediates Histone Ubiquitylation and Transcriptional Repression. *Molecular Cell*, *16*(4), 631–639. https://doi.org/10.1016/j.molcel.2004.10.016

Minteer, C., Morselli, M., Meer, M., Cao, J., Higgins-Chen, A., Lang, S., Pellegrini, M., Yan, Q., & Levine, M. (2021). *Cellular aging in vitro recapitulates multi-tissue epigenetic aging in vivo* (p. 2020.09.02.280073). bioRxiv. https://doi.org/10.1101/2020.09.02.280073

Morrison, O., & Thakur, J. (2021). Molecular Complexes at Euchromatin, Heterochromatin and Centromeric Chromatin. *International Journal of Molecular Sciences*, *22*(13), Article 13. https://doi.org/10.3390/ijms22136922

Mozhui, K., & Pandey, A. K. (2017). Conserved effect of aging on DNA methylation and association with EZH2 polycomb protein in mice and humans. *Mechanisms of Ageing and Development*, *162*, 27–37. https://doi.org/10.1016/j.mad.2017.02.006

Murrant, C. L., Lamb, I. R., & Novielli, N. M. (2017). Capillary endothelial cells as coordinators of skeletal muscle blood flow during active hyperemia. *Microcirculation*, *24*(3), e12348. https://doi.org/10.1111/micc.12348

Nacev, B. A., Grassi, P., Dell, A., Haslam, S. M., & Liu, J. O. (2011). The Antifungal Drug Itraconazole Inhibits Vascular Endothelial Growth Factor Receptor 2 (VEGFR2) Glycosylation, Trafficking, and Signaling in Endothelial Cells *. *Journal of Biological Chemistry*, *286*(51), 44045–44056. https://doi.org/10.1074/jbc.M111.278754

Niccoli, T., & Partridge, L. (2012). Ageing as a Risk Factor for Disease. *Current Biology*, *22*(17), R741–R752. https://doi.org/10.1016/j.cub.2012.07.024

Oeppen, J., & Vaupel, J. W. (2002). Broken Limits to Life Expectancy. *Science*, *296*(5570), 1029–1031. https://doi.org/10.1126/science.1069675

Oldervoll L. M., Loge J. H., Lydersen S., Paltiel H., Asp M. B., Nygaard U. V., Oredalen E., Frantzen T. L., Lesteberg I., Amundsen L., Hjermstad M. J., Haugen D. F., Paulsen Ø., & Kaasa S. (2011). Physical Exercise for Cancer Patients with Advanced Disease: A Randomized Controlled Trial. *The Oncologist*, *16*(11), 1649–1657. https://doi.org/10.1634/theoncologist.2011-0133

Olfert, I. M., Howlett, R. A., Wagner, P. D., & Breen, E. C. (2010). Myocyte vascular endothelial growth factor is required for exercise-induced skeletal muscle angiogenesis. *American Journal of Physiology-Regulatory, Integrative and Comparative Physiology*, *299*(4), R1059–R1067. https://doi.org/10.1152/ajpregu.00347.2010

Olsen, L. N., Hoier, B., Hansen, C. V., Leinum, M., Carter, H. H., Jorgensen, T. S., Bangsbo, J., & Hellsten, Y. (2020). Angiogenic potential is reduced in skeletal muscle of aged women. *The Journal of Physiology*, *598*(22), 5149–5164. https://doi.org/10.1113/JP280189

Park, S. H., Park, J. H., Song, P. S., Kim, D. K., Kim, K. H., Seol, S. H., Kim, H. K., Jang, H. J., Lee, J. G., Park, H. Y., Park, J., Shin, K. J., Kim, D. il, & Moon, Y. S. (2013). Sarcopenic obesity as an independent risk factor of hypertension. *Journal of the American Society of Hypertension*, *7*(6), 420–425. https://doi.org/10.1016/j.jash.2013.06.002

Paz, N. G. dela, Walshe, T. E., Leach, L. L., Saint-Geniez, M., & D'Amore, P. A. (2012). Role of shear-stress-induced VEGF expression in endothelial cell survival. *Journal of Cell Science*, *125*(4), 831. https://doi.org/10.1242/jcs.084301

Peixoto, P., Cartron, P.-F., Serandour, A. A., & Hervouet, E. (2020). From 1957 to Nowadays: A Brief History of Epigenetics. *International Journal of Molecular Sciences*, *21*(20), Article 20. https://doi.org/10.3390/ijms21207571

Pérez-Gutiérrez, L., & Ferrara, N. (2023). Biology and therapeutic targeting of vascular endothelial growth factor A. *Nature Reviews. Molecular Cell Biology*, *24*(11), 816–834. https://doi.org/10.1038/s41580-023-00631-w

Prickaerts, P., Adriaens, M. E., Beucken, T. van den, Koch, E., Dubois, L., Dahlmans, V. E. H., Gits, C., Evelo, C. T. A., Chan-Seng-Yue, M., Wouters, B. G., & Voncken, J. W. (2016). Hypoxia increases genome-wide bivalent epigenetic marking by specific gain of H3K27me3. *Epigenetics & Chromatin*, *9*, 46. https://doi.org/10.1186/s13072-016-0086-0

Prior, S. J., Ryan, A. S., Blumenthal, J. B., Watson, J. M., Katzel, L. I., & Goldberg, A. P. (2016). Sarcopenia Is Associated With Lower Skeletal Muscle Capillarization and Exercise Capacity in Older Adults. *The Journals of Gerontology: Series A*, *71*(8), 1096–1101. https://doi.org/10.1093/gerona/glw017

Reed, M. J., Corsa, A., Pendergrass, W., Penn, P., Sage, E. H., & Abrass, I. B. (1998). Neovascularization in aged mice: Delayed angiogenesis is coincident with decreased levels of transforming growth factor beta1 and type I collagen. *The American Journal of Pathology*, *152*(1), 113–123.

Reed, M. J., & Edelberg, J. M. (2004). Impaired angiogenesis in the aged. *Science of Aging Knowledge Environment: SAGE KE*, *2004*(7), pe7. https://doi.org/10.1126/sageke.2004.7.pe7

Rivard, A., Fabre, J.-E., Silver, M., Chen, D., Murohara, T., Kearney, M., Magner, M., Asahara, T., & Isner, J. M. (1999). Age-Dependent Impairment of Angiogenesis. *Circulation*, *99*(1), 111–120. https://doi.org/10.1161/01.CIR.99.1.111

Roberts, K. C., Rao, D. P., Bennett, T. L., Loukine, L., & Jayaraman, G. C. (2015). Prevalence and patterns of chronic disease multimorbidity and associated determinants in Canada. *Health Promotion and Chronic Disease Prevention in Canada*, *35*(6), 87–94. https://doi.org/10.24095/hpcdp.35.6.01

Ross, M., Kargl, C. K., Ferguson, R., Gavin, T. P., & Hellsten, Y. (2023). Exercise-induced skeletal muscle angiogenesis: Impact of age, sex, angiocrines and cellular mediators. *European Journal of Applied Physiology*, *123*(7), 1415–1432. https://doi.org/10.1007/s00421-022-05128-6

Roudier, E., Aiken, J., Slopack, D., Gouzi, F., Mercier, J., Haas, T. L., Gustafsson, T., Hayot, M., & Birot, O. (2013). Novel perspective: Exercise training stimulus triggers the expression of the oncoprotein human double minute-2 in human skeletal muscle. *Physiological Reports*, *1*(2). https://doi.org/10.1002/phy2.28

Roudier, E., Forn, P., Perry, M. E., & Birot, O. (2012). Murine double minute-2 expression is required for capillary maintenance and exercise-induced angiogenesis in skeletal muscle. *The FASEB Journal*, *26*(11), 4530–4539. https://doi.org/10.1096/fj.12-212720

Sadoun, E., & Reed, M. J. (2003). Impaired Angiogenesis in Aging Is Associated with Alterations in Vessel Density, Matrix Composition, Inflammatory Response, and Growth Factor Expression. *Journal of Histochemistry & Cytochemistry*, *51*(9), 1119–1130. https://doi.org/10.1177/002215540305100902

Sánchez-Sánchez, J. L., He, L., Morales, J. S., de Souto Barreto, P., Jiménez-Pavón, D., Carbonell-Baeza, A., Casas-Herrero, Á., Gallardo-Gómez, D., Lucia, A., del Pozo Cruz, B., & Valenzuela, P. L. (2024). Association of physical behaviours with sarcopenia in older adults: A systematic review and meta-analysis of observational studies. *The Lancet Healthy Longevity*, *5*(2), e108–e119. https://doi.org/10.1016/S2666-7568(23)00241-6

Schmid, V., Foulkes, S. J., Walesiak, D., Wang, J., Tomczak, C. R., Tucker, W. J., Angadi, S. S., Halle, M., & Haykowsky, M. J. (2024). Impact of whole-body and skeletal muscle composition on peak oxygen uptake in heart failure: A systematic review and meta-analysis. *European Heart Journal Open*, *4*(5), oeae082. https://doi.org/10.1093/ehjopen/oeae082

Shalaby, F., Rossant, J., Yamaguchi, T. P., Gertsenstein, M., Wu, X.-F., Breitman, M. L., & Schuh, A. C. (1995). Failure of blood-island formation and vasculogenesis in Flk-1-deficient mice. *Nature*, *376*(6535), 62–66. https://doi.org/10.1038/376062a0

Shibuya, M. (2011). Vascular Endothelial Growth Factor (VEGF) and Its Receptor (VEGFR) Signaling in Angiogenesis. *Genes & Cancer*, *2*(12), 1097–1105. https://doi.org/10.1177/1947601911423031

Shumaker, D. K., Dechat, T., Kohlmaier, A., Adam, S. A., Bozovsky, M. R., Erdos, M. R., Eriksson, M., Goldman, A. E., Khuon, S., Collins, F. S., Jenuwein, T., & Goldman, R. D. (2006). Mutant nuclear lamin A leads to progressive alterations of epigenetic control in premature aging. *Proceedings of the National Academy of Sciences*, *103*(23), 8703–8708. https://doi.org/10.1073/pnas.0602569103

Stamler, J. S., & Meissner, G. (2001). Physiology of nitric oxide in skeletal muscle. *Physiological Reviews*, *81*(1), 209–237. https://doi.org/10.1152/physrev.2001.81.1.209

Strahl, B. D., & Allis, C. D. (2000). The language of covalent histone modifications. *Nature*, *403*(6765), 41–45. https://doi.org/10.1038/47412

Suehiro, J., Hamakubo, T., Kodama, T., Aird, W. C., & Minami, T. (2010). Vascular endothelial growth factor activation of endothelial cells is mediated by early growth response-3. *Blood*, *115*(12), 2520–2532. https://doi.org/10.1182/blood-2009-07-233478

Sun, D., Luo, M., Jeong, M., Rodriguez, B., Xia, Z., Hannah, R., Wang, H., Le, T., Faull, K. F., Chen, R., Gu, H., Bock, C., Meissner, A., Göttgens, B., Darlington, G. J., Li, W., & Goodell, M. A. (2014). Epigenomic Profiling of Young and Aged HSCs Reveals Concerted Changes during Aging that Reinforce Self-Renewal. *Cell Stem Cell*, *14*(5), 673–688. https://doi.org/10.1016/j.stem.2014.03.002

Taha, M., AlNaam, Y. A., Al Maqati, T., Almusallam, L., Altalib, G., Alowfi, D., & Haider, N. (2022). Impact of muscle mass on blood glucose level. *Journal of Basic and Clinical Physiology and Pharmacology*, *33*(6), 779–787. https://doi.org/10.1515/jbcpp-2021-0316

Takahashi, T., & Shibuya, M. (1997). The 230 kDa mature form of KDR/Flk-1 (VEGF receptor-2) activates the PLC-gamma pathway and partially induces mitotic signals in NIH3T3 fibroblasts. *Oncogene*, *14*(17), 2079–2089. https://doi.org/10.1038/sj.onc.1201047

Tarantini, L., Bonzini, M., Apostoli, P., Pegoraro, V., Bollati, V., Marinelli, B., Cantone, L., Rizzo, G., Hou, L., Schwartz, J., Bertazzi, P. A., & Baccarelli, A. (2009). Effects of Particulate Matter on Genomic DNA Methylation Content and iNOS Promoter Methylation. *Environmental Health Perspectives*, *117*(2), 217–222. https://doi.org/10.1289/ehp.11898

Tsai, J.-C., Chang, W.-Y., Kao, C.-C., Lu, M.-S., Chen, Y.-J., & Chan, P. (2002). BENEFICIAL EFFECT ON BLOOD PRESSURE AND LIPID PROFILE BY PROGRAMMED EXERCISE TRAINING IN TAIWANESE PATIENTS WITH MILD HYPERTENSION. *Clinical and Experimental Hypertension*, *24*(4), 315–324. https://doi.org/10.1081/CEH-120004234

Ungvari, Z., Tucsek, Z., Sosnowska, D., Toth, P., Gautam, T., Podlutsky, A., Csiszar, A., Losonczy, G., Valcarcel-Ares, M. N., Sonntag, W. E., & Csiszar, A. (2013). Aging-Induced Dysregulation of Dicer1-Dependent MicroRNA Expression Impairs Angiogenic Capacity of Rat Cerebromicrovascular Endothelial Cells. *The Journals of Gerontology: Series A*, *68*(8), 877–891. https://doi.org/10.1093/gerona/gls242

Valieva, Y., Ivanova, E., Fayzullin, A., Kurkov, A., & Igrunkova, A. (2022). Senescence-Associated β-Galactosidase Detection in Pathology. *Diagnostics*, *12*(10), Article 10. https://doi.org/10.3390/diagnostics12102309

Wagenmakers, A. J. M., Strauss, J. A., Shepherd, S. O., Keske, M. A., & Cocks, M. (2016). Increased muscle blood supply and transendothelial nutrient and insulin transport induced by food intake and exercise: Effect of obesity and ageing. *The Journal of Physiology*, *594*(8), 2207–2222. https://doi.org/10.1113/jphysiol.2014.284513

White, M. J., Davies, C. T. M., & Brooksby, P. (1984). The Effects of Short-Term Voluntary Immobilization on the Contractile Properties of the Human Triceps Surae. *Quarterly Journal of Experimental Physiology*, *69*(4), 685–691. https://doi.org/10.1113/expphysiol.1984.sp002860

Wienken, M., Dickmanns, A., Nemajerova, A., Kramer, D., Najafova, Z., Weiss, M., Karpiuk, O., Kassem, M., Zhang, Y., Lozano, G., Johnsen, S. A., Moll, U. M., Zhang, X., & Dobbelstein, M. (2016). MDM2 Associates with Polycomb Repressor Complex 2 and Enhances Stemness-Promoting Chromatin Modifications Independent of p53. *Molecular Cell*, *61*(1), 68–83. https://doi.org/10.1016/j.molcel.2015.12.008

Wienken, M., Moll, U. M., & Dobbelstein, M. (2017). Mdm2 as a chromatin modifier. *Journal of Molecular Cell Biology*, *9*(1), 74–80. https://doi.org/10.1093/jmcb/mjw046

Yamaura, H., & Matsuzawa, T. (1980). Decrease in capillary growth during aging. *Experimental Gerontology*, *15*(2), 145–150. https://doi.org/10.1016/0531-5565(80)90086-8

Yang, N., Occean, J. R., Melters, D. P., Shi, C., Wang, L., Stransky, S., Doyle, M. E., Cui, C.-Y., Delannoy, M., Fan, J., Slama, E., Egan, J. M., De, S., Cunningham, S. C., Cabo, R. de, Sidoli, S., Dalal, Y., & Sen, P. (2023). A hyper-quiescent chromatin state formed during aging is reversed by regeneration. *Molecular Cell*, *83*(10), 1659-1676.e11. https://doi.org/10.1016/j.molcel.2023.04.005

Yi, S., Lin, K., Jiang, T., Shao, W., Huang, C., Jiang, B., Li, Q., & Lin, D. (2020). NMR-based metabonomic analysis of HUVEC cells during replicative senescence. *Aging (Albany NY)*, *12*(4), 3626–3646. https://doi.org/10.18632/aging.102834

Zeng, H., Qin, L., Zhao, D., Tan, X., Manseau, E. J., Van Hoang, M., Senger, D. R., Brown, L. F., Nagy, J. A., & Dvorak, H. F. (2006). Orphan nuclear receptor TR3/Nur77 regulates VEGF-A-induced angiogenesis through its transcriptional activity. *The Journal of Experimental Medicine*, *203*(3), 719–729. https://doi.org/10.1084/jem.20051523

Zhao, W., Qiao, L., Yan, S., Nie, Q., & Zhang, L. (2021). Mathematical modeling of histone modifications reveals the formation mechanism and function of bivalent chromatin. *iScience*, *24*(7), 102732. https://doi.org/10.1016/j.isci.2021.102732

Zhou, S., Gu, L., He, J., Zhang, H., & Zhou, M. (2011). MDM2 regulates vascular endothelial growth factor mRNA stabilization in hypoxia. *Molecular and Cellular Biology*, *31*(24), 4928–4937. https://doi.org/10.1128/MCB.06085-11